ROADMAP • OPEN ACCESS

Roadmap on wavefront shaping and deep imaging in complex media

To cite this article: Sylvain Gigan *et al* 2022 *J. Phys. Photonics* **4** 042501

View the article online for updates and enhancements.

Journal of Physics: Photonics

ROADMAP

Roadmap on wavefront shaping and deep imaging in complex media

Sylvain Gigan[4,*] , Ori Katz[19,*] , Hilton B de Aguiar[4] , Esben Ravn Andresen[13], Alexandre Aubry[8],
Jacopo Bertolotti[9], Emmanuel Bossy[5] , Dorian Bouchet[5] , Joshua Brake[31], Sophie Brasselet[6],
Yaron Bromberg[28], Hui Cao[23] , Thomas Chaigne[6], Zhongtao Cheng[32], Wonshik Choi[7], Tomáš Čižmár[10,22],
Meng Cui[35], Vincent R Curtis[15], Hugo Defienne[29] , Matthias Hofer[6], Ryoichi Horisaki[21],
Roarke Horstmeyer[33], Na Ji[2], Aaron K LaViolette[1], Jerome Mertz[3], Christophe Moser[11], Allard P Mosk[26] ,
Nicolas C Pégard[15,17,18], Rafael Piestun[30], Sebastien Popoff[8], David B Phillips[9], Demetri Psaltis[12],
Babak Rahmani[11], Hervé Rigneault[6], Stefan Rotter[27] , Lei Tian[3,14] , Ivo M Vellekoop[20], Laura Waller[16],
Lihong Wang[32,34] , Timothy Weber[3], Sheng Xiao[3], Chris Xu[1] , Alexey Yamilov[24] , Changhuei Yang[34]
and Hasan Yılmaz[25]

1   School of Applied and Engineering Physics, Cornell University, Ithaca, NY, 14853, United States of America
2   University of California Berkeley, Berkeley, CA, United States of America
3   Department of Biomedical Engineering, Boston University, Boston, MA, United States of America
4   Laboratoire Kastler Brossel, ENS-Université PSL, CNRS, Sorbonne Université, Collège de France, 24 rue Lhomond, 75005 Paris, France
5   University Grenoble Alpes, CNRS, LIPhy, 38000 Grenoble, France
6   Aix Marseille University, CNRS, Centrale Marseille, Institut Fresnel, F-13013 Marseille, France
7   Institute for Basic Science, Department of Physics, Korea University, Seoul, Republic of Korea
8   Institut Langevin, ESPCI, PSL University, CNRS, Paris, France
9   School of Physics & Astronomy, University of Exeter, Exeter, EX4 4QL, United Kingdom
10   Leibniz Institute of Photonic Technology, Albert-Einstein-Straße 9, 07745 Jena, Germany
11   Laboratory of Applied Photonics Devices, School of Engineering, Ecole Polytechnique Fédérale de Lausanne, 1015 Lausanne, Switzerland
12   Laboratory of Optics, School of Engineering, Ecole Polytechnique Fédérale de Lausanne, 1015 Lausanne, Switzerland
13   Université de Lille, CNRS UMR 8523—PhLAM—Laboratoire de Physique des Lasers, Atomes et Molécules, F-59000 Lille, France
14   Department of Electrical and Computer Engineering, Boston University, Boston, MA 02215, United States of America
15   Department of Applied Physical Sciences, UNC Chapel Hill, Chapel Hill, NC, United States of America
16   Department of Electrical Engineering and Computer Sciences, UC Berkeley, Berkeley, CA, United States of America
17   Department of Biomedical Engineering, UNC Chapel Hill, Chapel Hill, NC, United States of America
18   UNC Neuroscience Centre, UNC Chapel Hill, Chapel Hill, NC, United States of America
19   Department of Applied Physics, Hebrew University of Jerusalem, Jerusalem, Israel
20   Department of Science and Technology, University of Twente, Enschede, The Netherlands
21   The University of Tokyo, Japan
22   Institute of Scientific Instruments of the Czech Academy of Sciences, Královopolská 147, 612 64 Brno, Czech Republic
23   Department of Applied Physics, Yale University, New Haven, CT, 06520, United States of America
24   Department of Physics, Missouri University of Science and Technology, Rolla, MO, 65409, United States of America
25   Institute of Materials Science and Nanotechnology, National Nanotechnology Research Center (UNAM), Bilkent University, Ankara, 06800, Turkey
26   Debye Institute for Nanomaterials Science, Utrecht University, Utrecht, The Netherlands
27   Institute for Theoretical Physics, TU Wien, Vienna, Austria
28   Racah Institute of Physics, The Hebrew University of Jerusalem, Jerusalem, Israel
29   School of Physics and Astronomy, University of Glasgow, Glasgow, United Kingdom
30   University of Colorado Boulder, Boulder, CO, United States of America
31   Department of Engineering, Harvey Mudd College, Claremont, CA 91711, United States of America
32   Caltech Optical Imaging Laboratory, Andrew and Peggy Cherng Department of Medical Engineering, California Institute of Technology, Pasadena, CA 91106, United States of America
33   Department of Biomedical Engineering, Duke University, Durham, NC 27708, United States of America
34   Department of Electrical Engineering, California Institute of Technology, Pasadena, CA 91106, United States of America
35   Electrical and Computer Engineering and Biology Department, Purdue University, West Lafayette, IN, United States of America
*   Authors to whom any correspondence should be addressed.

E-mail: sylvain.gigan@lkb.ens.fr and orik@mail.huji.ac.il

Abstract

The last decade has seen the development of a wide set of tools, such as wavefront shaping, computational or fundamental methods, that allow us to understand and control light propagation in a complex medium, such as biological tissues or multimode fibers. A vibrant and diverse community is now working in this field, which has revolutionized the prospect of diffraction-limited imaging at depth in tissues. This roadmap highlights several key aspects of this fast developing field, and some of the challenges and opportunities ahead.

Contents

Introduction

SylvainGigan[1] *and Ori Katz*[2]
[1] Laboratoire Kastler Brossel, ENS-Université PSL, CNRS, Sorbonne Université, Collège de France, 24 rue Lhomond, 75005 Paris, France
[2] Department of Applied Physics, Hebrew University of Jerusalem, Jerusalem, Israel

Wavefront shaping in complex media, the high-resolution manipulation of light waves in order to control light in disordered environments, is a relatively young field. Its commonly accepted inception can be traced back to 2007 when Vellekoop and Mosk demonstrated that, via an iterative optimization algorithm, a diffraction-limited focus could be obtained through a visually opaque strongly scattering medium by phase control of thousands of optical modes [1]. However, while being a relatively young field, it builds on decades of experimental works performed in several established fields, from adaptive optics (AO) for astronomy, through holography, phase conjugation, time reversal of ultrasound waves, to RADAR imaging. It also builds on decades of fundamental insight from mesoscopic physics. Although the exact boundary between AO and wavefront shaping is still rather fuzzy, one possible way to define the crossover is whenever low-order mode corrections (in the Zernike basis) are not sufficient anymore, corresponding to at least a few scattering mean free paths. However, wavefront shaping is essentially nothing more than AO in an extreme regime of wave perturbation.

Deep imaging in complex environments is a hugely important challenge, from noninvasive biomedical investigations to seeing through fog. However, due to the highly scattering nature of many real-world samples, direct imaging in complex samples, such as biological tissues, is conventionally limited to shallow depths of a few hundred microns. While other imaging modalities, such as ultrasound, magnetic resonance imaging (MRI), and x-rays, can penetrate deeper into biological tissue, they are inferior to optical microscopy in terms of resolution (limited by the wavelength of light), variety of contrast mechanisms (e.g. chemical sensitivity, and functional information), or their non-ionizing nature. Wavefront shaping offers a unique possibility: to achieve optical resolution focusing and imaging, without being limited by the exponential decay of ballistic photons with depth. It is relatively safe to say that, to obtain micrometer or submicrometer resolution images deep in complex media, retrieving information from scattered light (either through physical wavefront control or through computation) is the only way to go.

One of the main reasons for the fast recent progress in the field of wavefront shaping is the great technological advances in both digital modulators and detectors. Spatial light modulators (SLMs) based on a variety of technologies, from liquid crystals through micro-electro-mechanical systems to acousto-optic modulators, now allow one to ramp up the number of controlled modes and speed. The progress in cameras and detector technologies has also had a great impact in the field due to several now widely available devices from multi-megapixel fast cameras, through ultrasensitive electron-multiplying CCDs (EMCCDs) and sCMOS detector technologies, to single-photon detector arrays.

The great advancements in modulators and detectors come hand in hand with the now available computational power, data bandwidth and memory, which are required to digitally transfer and process the huge amounts of scattered light information. The field also naturally strongly benefits from the current advancements in signal processing and AI revolution, with the emergence of deep learning (DL). In some instances, these advancements in signal processing and machine learning algorithms allow one to simplify or even shortcut the stringent requirements of wavefront shaping, both in terms of number of measurements and even in the need for a wavefront shaping device.

Simultaneously, the field continuously revisits and makes use of theoretical concepts from mesoscopic physics to improve imaging and light delivery deep inside visually opaque samples. A first example is the transmission matrix, initially a theoretician concept, which became a versatile tool for imaging once it was demonstrated that it could be effectively recorded. Another notable example for imaging is the optical 'memory effect,' a correlation of multiply scattered waves predicted in the 1980s. It was proposed for imaging (and other tasks) as early as the 1990s in a visionary work by Freund [2]. However, it is only in the last decade that its practical potential has been realized and put into practice thanks to wavefront shaping. Very recently, fundamental concepts such as open channels, or time-delay eigenstates, have been increasingly studied in the context of imaging and light control in complex media.

The applications of wavefront shaping now span well beyond simple focusing and imaging inside complex media: it has been employed to allow looking around corners, for energy delivery through opaque samples, for trapping and optical manipulation, near-field imaging, plasmonics, spectroscopy, and ultrafast pulse shaping; virtually all aspects of photonics have been explored in combination with wavefront shaping. One specifically important extension of wavefront shaping is its application for light control through long

multimode and multicore fibers, which has emerged as an extremely fruitful path. In particular, it allows the development of miniature lensless endoscopes for deep imaging, now a very active subfield.

In terms of imaging modalities, wavefront shaping has been experimentally demonstrated in essentially every widespread optical modality (most often in proof of principle experiments): these include confocal imaging, multiphoton imaging, photoacoustics, acousto-optics, phase contrast, optical coherence tomography, fluorescence imaging, structured illumination, temporal and spectral control, Raman, and other spectroscopic techniques. Interestingly, optical super-resolution techniques, such as STED, PALM, and STORM, still remain to date largely unexplored in the scattering regime, although significant progress in aberrating specimens using AO has been reported [3].

By and large, the field is now relatively mature, but remains very active and shows no sign of slowing down in terms of innovation; one can cite very recent progress such as fluorescence-based incoherent transmission matrices, applying DL approaches to image reconstruction, and the emergence of novel ultrafast SLMs, to cite just a few salient results. It also focuses more and more on applications in real-world samples rather than basic proof of principle demonstrations.

In this roadmap we highlight, from multiple and different perspectives, many of these recent advances as well as the challenges and opportunities that the field may offer in the years to come.

1. Three-dimensionally resolved fluorescence microscopy in deep-scattering biological tissue

Aaron K LaViolette and Chris Xu

School of Applied and Engineering Physics, Cornell University, Ithaca, NY, 14853, United States of America

Status

One-photon (1P) confocal, two-photon (2P) and three-photon (3P) microscopy provide three-dimensionally resolved, high-spatial-resolution fluorescence imaging in scattering biological tissues. 1P confocal microscopy is typically only applicable within shallow imaging depths, while 2P microscopy (2PM) and eventually 3P microscopy (3PM) are preferred as the imaging depth increases. Such a photon 'upmanship' [4] for deep tissue fluorescence imaging can be understood by considering the effective attenuation coefficient (α_e) of the tissues for ballistic photons, the maximum allowable power, multiphoton cross sections, out-of-focus background fluorescence generation, and availability of fluorophores.

α_e is a function of excitation wavelength and is the sum of the scattering coefficient (α_s) and absorption coefficient (α_a), i.e. $\alpha_e = \alpha_s + \alpha_a$. For *in vivo* imaging, the absorption of brain tissue is dominated by blood and water. Figure 1 shows the calculated and experimentally measured α_e for mouse brain tissue *in vivo* [5–11]. Because the excitation power at the focus, $P(z)$, decreases exponentially as a function of imaging depth z, $P(z) = P_0 \exp(-\alpha_e z)$, where P_0 is the power at the brain surface; the value of α_e is the most important consideration for deep imaging. Therefore, the preferred excitation wavelengths for deep tissue imaging reside within the long wavelength windows around 1300, 1700, and 2200 nm.
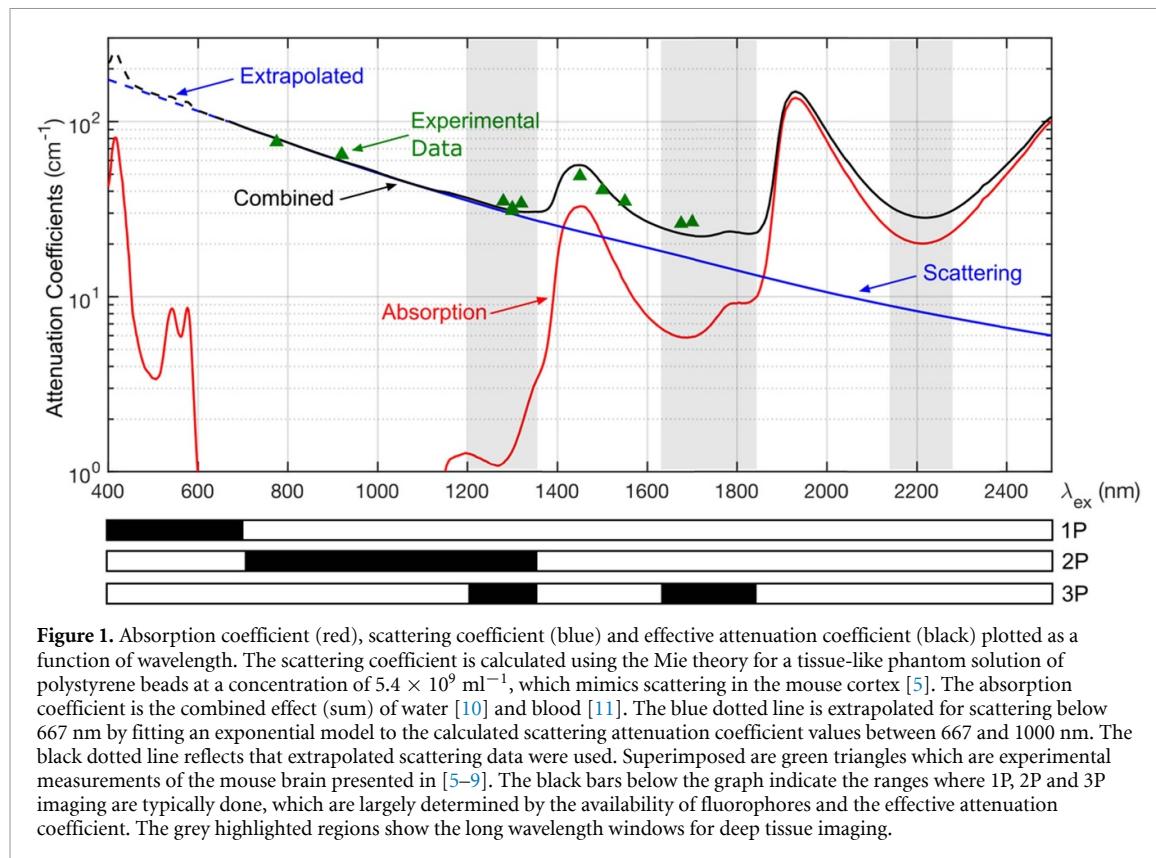
While α_e is the most important consideration for penetration depth, tissue absorption determines the maximum permissible power for imaging (i.e. the maximum value of P_0) [7]. For the three spectral windows with the lowest α_e, the absorption increases at the longer wavelength (figure 1). Although the values of α_e around 1300 and 2200 nm are comparable, the 1300 nm window is preferred because of the higher allowable power due to the lower tissue absorption, while the low α_e around 1700 nm indicates that the 1700 nm window is the best for the deepest imaging.

Most existing fluorophores require excitation wavelengths within the visible to near infrared (NIR) range, which limits 1P confocal imaging to excitations between about 350 and 700 nm, where α_e is large. Thus, 1P confocal microscopy is generally best in shallow regions. While 2P and 3P excitation makes the low attenuation spectral windows compatible with existing fluorophores, only red or NIR fluorophores can be excited in the 1300 nm window by 2P excitation, excluding the most commonly used green and yellow fluorophores for deep tissue 2PM. 3P imaging can be performed within the 1300 nm spectral window for blue, green, and yellow fluorophores, and the 1700 nm spectral window for red and NIR fluorophores. The spectral 'gap' for 3P imaging is due to the large water absorption between 1400 and 1600 nm. The 2200 nm window, in addition to the high tissue absorption, is too long for nearly all existing fluorophores even with 3P excitation.

In addition to the practical considerations listed above, the imaging depth of three-dimensionally resolved imaging is fundamentally limited by out-of-focus background fluorescence [12]. In general, a higher-order nonlinear excitation will result in a higher excitation confinement and less out-of-focus background, resulting in a higher signal-to-background ratio (SBR). However, higher-order nonlinear excitation is less efficient due to the small multiphoton excitation cross sections. Therefore, the improvement in SBR comes at the expense of the signal strength. The trade-off between SBR and signal strength indicates that there is a depth for the fluorophore under consideration beyond which 3P imaging outperforms 2P imaging [7]. This depth can be quantified based on a metric grounded in detection theory (e.g. for the detection of calcium-transients with the *d'* metric [7, 13] or binary objects with the binary detection factor metric [14]).

Current and future challenges

The penetration depths of 1P confocal and 2P imaging are limited by the SBR (i.e. the depth limit). Neglecting the Stokes shift and the pinhole size, 1P confocal imaging has nearly the same point-spread function as 2PM. Therefore, the depth limit determined by the SBR is similar for 1P confocal and 2P imaging when the excitation wavelength is the same. Both theoretical and experimental studies show that the depth limit for 1P confocal and 2P imaging is between 1.5 and 2 mm, when imaging mouse brain vasculature, in the long wavelength windows of 1300 and 1700 nm [15–18]. The biggest challenge facing deep tissue long wavelength 1P confocal microscopy is the lack of IR dyes with excitation wavelengths >1200 nm. In addition, low-cost, low-noise, high-gain, high-quantum-efficiency detectors in the 1300 and 1700 nm windows must be developed. For long wavelength 2PM, the availability and performance of deep red and NIR functional indicators are major limitations for practical applications.

Figure 1. Absorption coefficient (red), scattering coefficient (blue) and effective attenuation coefficient (black) plotted as a function of wavelength. The scattering coefficient is calculated using the Mie theory for a tissue-like phantom solution of polystyrene beads at a concentration of 5.4×10^9 ml^{-1}, which mimics scattering in the mouse cortex [5]. The absorption coefficient is the combined effect (sum) of water [10] and blood [11]. The blue dotted line is extrapolated for scattering below 667 nm by fitting an exponential model to the calculated scattering attenuation coefficient values between 667 and 1000 nm. The black dotted line reflects that extrapolated scattering data were used. Superimposed are green triangles which are experimental measurements of the mouse brain presented in [5–9]. The black bars below the graph indicate the ranges where 1P, 2P and 3P imaging are typically done, which are largely determined by the availability of fluorophores and the effective attenuation coefficient. The grey highlighted regions show the long wavelength windows for deep tissue imaging.

3P excitation best matches existing dyes with the low tissue attenuation windows, and 3P imaging depths of >1 mm and >2 mm have been demonstrated, respectively, for green/yellow fluorophores using 1300 nm excitation [19, 20] and red fluorophores using 1700 nm excitation [21]. The higher-order nonlinear excitation has also enabled 3PM to image deep in densely labeled samples or through a highly scattering layer (e.g. the mouse skull or corpus callosum [22]) where the imaging depth of long wavelength 2PM is severely limited by the SBR. Theoretical analysis and experimental studies on tissue phantoms show that 3PM has the potential to image much deeper than has been achieved so far. Indeed, the predicted maximum penetration depth limited by the SBR is about 3–4 mm for 3PM when imaging mouse brain vasculature, which is nearly twice the deepest imaging today [23]. The biggest challenge in pushing the imaging depth of 3PM is the small 3P cross section. Together with the maximum allowable power, small 3P cross sections limit the 3P signal strength and currently set the practical imaging depth limit.

Advances in science and technology to meet challenges
The depth limits of long wavelength 1P confocal and 2P imaging have already been reached in the mouse brain. However, further improvements are required to transform them into valuable practical tools for biological research. For deep tissue 1P confocal microscopy, the biggest advancement would be creating a plethora of fluorophores, fluorescent proteins, and functional indicators with excitation wavelengths >1200 nm. However, significant effort has been devoted to finding long wavelength fluorophores for *in vivo* imaging in the last 10–20 years, which has proven to be challenging, particularly for fluorophores excited with wavelengths >800 nm. Quantum dots (QDs), including carbon dots, are probably the most promising path so far but making QDs into robust functional indicators may yet prove difficult. Additionally, the recent development of superconducting nanowire detectors (SNDs) is promising for 1P confocal imaging at 1300 and 1700 nm [18]. While still expensive, advancements in materials and manufacturing for SNDs could reduce the cost and make these detectors affordable for biological imaging. Noticeable progress has been made in deep red or NIR fluorescent proteins and functional indicators for 2PM around 1300 nm. Further improvement in their performance will greatly improve the practical utility of long wavelength deep tissue 2PM and could make long wavelength 2PM of deep red or NIR fluorophores an alternative to 3PM of green fluorophores for many applications.

The depth limit of 3PM has not been reached in any *in vivo* biological samples and increasing the imaging depth of 3PM will require improving the signal strength. Fluorophores with enhanced multiphoton cross sections can increase the imaging depth of 2PM and 3PM and lower the cost of the excitation source.

While past attempts to explore the molecular structures of fluorophores have largely failed to create new ones with extraordinarily large 2P or 3P cross sections for *in vivo* imaging, exploring resonance enhanced 3P excitation appears to be promising. Indeed, already approximately ten times enhanced 3P cross sections have been demonstrated [24]. Additionally, adaptive optics (AO), which is a well-established technique for improving the spatial resolution and increasing the signal generation for *in vivo* brain imaging [25, 26], may be considered. AO has been shown to have a larger impact in 3PM than in 2PM due to the higher-order nonlinear excitation and deeper imaging depth [27], where a 5–10 times signal strength increase can be achieved for deep 3PM [28]. One of the AO challenges is the lack of a fast and direct wavefront sensing method in deep scattering tissue.

For both 2PM and 3PM, a promising way forward is the development of high-pulse-energy, low-repetition-rate femtosecond lasers for deep imaging such as optical parametric chirped pulse amplifiers. This is because the pulse energy required by the laser increases exponentially as a function of imaging depth, and so the repetition rate of the laser must be reduced exponentially due to the limit on the maximum allowable power. The ideal laser for deep tissue imaging should provide constant output average power and a user-defined, tunable repetition rate. While lasers with high pulse energy and tunable repetition rate have become available for 2PM and 3PM in the last five years, such sources cannot yet maintain a constant output power as the repetition rate is tuned. Furthermore, by illuminating the regions of interest only, pulse-on-demand systems (e.g. the adaptive excitation source [29]) can increase the signal strength without increasing the average excitation power in the sample or requiring higher average laser output. Such adaptive lasers can improve the performance of deep tissue 2PM (e.g. imaging speed) and are likely to prove essential for reaching the depth limit for 3PM.

Concluding remarks

This roadmap aims to elucidate the challenges for high-spatial-resolution, deep tissue, three-dimensionally resolved fluorescence microscopy. The compatibility of the long wavelength windows and the availability of fluorophores, together with the trade-off between the SBR and the signal strength, form the basis for the current choices of 1P confocal microscopy, 2PM, and 3PM and the depth limit of each imaging modality. High-spatial-resolution fluorescence imaging in deep scattering tissue is challenging because the 'difficulty' grows exponentially as a function of imaging depth. While long wavelength multiphoton microscopy can image at >2 mm in the mouse brain, the imaging depth is still less than a quarter of that of an adult mouse brain *in vivo*. Future advancements in fluorophores, detectors, and lasers can perhaps push the imaging depth of three-dimensionally resolved fluorescence microscopy by another factor of two (e.g. 3–4 mm when imaging the mouse brain vasculature). Breakthrough innovations are needed to image much deeper than long wavelength multiphoton microscopy.

Acknowledgment

2. Adaptive optical multiphoton fluorescence microscopy

Na Ji

University of California Berkeley, United States of America

Status

Adaptive optics (AO) was originally developed to combat atmospheric aberrations that degrade the image quality of astronomical objects. Here, wavefront distortion is measured directly using devices such as a Shack–Hartmann wavefront sensor. With increasing applications of optical microscopy in imaging of complex tissues, AO methods have been developed for microscopy to correct sample-induced aberrations in order to maintain optimal imaging performance [25]. Biological aberrations are distinct from their astronomical counterparts in that there is little to no temporal variation in the aberration profile but the samples are often optically opaque. Together, these characteristics have motivated the development of indirect wavefront sensing methods whose performance is not affected by light scattering.

Both direct and indirect wavefront sensing have been applied to multiphoton fluorescence microscopy (MPFM). The most popular and powerful method for imaging opaque samples is to measure the tissue-induced aberrations in the excitation light and then cancel them out by pre-shaping the excitation wavefront using a deformable mirror or spatial light modulator (SLM). To reduce scattering in direct wavefront sensing, far red and near infrared (NIR) fluorophores were employed [30, 31]. Indirect wavefront sensing methods use serial evaluations of image metrics (e.g. brightness, spatial resolution, contrast, point spread function) while manipulating the excitation light to deduce the wavefront profile [32–36]. When implemented properly, both types of methods are capable of forming a diffraction-limited focus deep in tissue to excite fluorescence at diffraction-limited spatial resolution.

In the opaque mouse brain, AO has enabled MPFM to visualize subcellular structures such as dendrites and dendritic spines hundreds of micrometers below the brain surface (figure 2). It has also enabled biological discovery: using an AO-enabled two-photon fluorescence microscope, we characterized the input from the visual thalamus in the mouse visual cortex and discovered previously unknown orientation selectivity of their synapses [37]. The rich repertoire of AO technologies and extensive demonstrations of their capabilities have firmly established AO to be essential for high-resolution MPFM investigations of complex tissues at depth.

Current and future challenges

Because fluorophores emitting in the visible spectrum are most commonly used to probe biological processes, the requirement of introducing additional fluorophores with far red and NIR emission for direct wavefront sensing complicates sample preparation. The easiest way to introduce these far red/NIR fluorophores into brain tissues is by injecting them (typically chemical dyes) into the blood [31]. However, this approach may lead to corrections with smaller isoplanatic patches due to the high curvature of blood vessels and is not applicable to tissues devoid of vasculature. Indirect wavefront sensing methods can work with fluorophores in the visible spectrum, but the depth at which they can be applied in opaque tissues remains limited by scattering of the excitation light and the brightness of the fluorophores.

Currently, AO has largely remained the domain of physicists rather than biologists. One challenge, therefore, is how to maximize their impact on biological fields where optical microscopy is routinely applied to enable discovery. AO systems developed for telescopes in large observatories have in-house staff that ensure their optimal performance, allowing external users to benefit from the high resolution without requiring them to have optical expertise. However, there are no microscopy facilities that operate on a similarly large scale, with most biology laboratories having their own microscopes or relying on core facilities at their institutions. Integrating AO modules into existing commercial microscopes is hindered for both software- and hardware-related reasons. Many AO methods require access to software that controls the microscope, acquires data, and processes images, which, as provided by microscope manufacturers, are almost always proprietary and closed source. Typical commercial MPFMs are also designed without careful consideration of optical conjugation. For example, the galvos for 2D scanning of the excitation focus are usually not conjugated to each other. In this case, if the excitation light is shaped by a wavefront corrector (e.g. an SLM or deformable mirror) before the galvos, the corrective pattern would be in constant motion at the objective back pupil plane during scanning, reducing the effective area for AO correction. Placing the wavefront corrector in between the galvos and the objective would solve the motion problem, but requires physical access that is often unavailable. Finally, in commercial systems, the microscope objective is often placed with its back focal plane substantially offset from the plane conjugated to the wavefront sensing
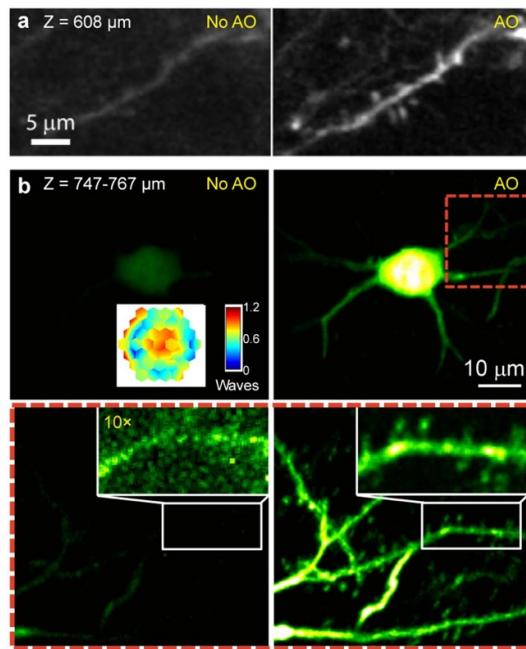
Figure 2. AO improves image quality of multiphoton fluorescence microscopy in the live mouse brain. (a) Two-photon fluorescence images of dendrites and dendritic spines before and after AO using direct wavefront sensing [31]. (b) Three-photon fluorescence images of a neuron, its dendrites, and dendritic spines before and after AO using indirect wavefront sensing [37].

device, which can lead to similar performance degradation. Given the lack of commercially available adaptive optical microscopes, implementation of AO in laboratories that pursue biological inquiry has been limited to a few groups straddling optics and biology.

Advances in science and technology to meet challenges

Because longer wavelength light is less scattered by tissue, using excitation light of longer wavelengths (three- versus two-photon, e.g. 1.3 μm versus 0.9 μm excitation for green fluorophores) can increase the imaging depth in tissue (see previous section). At such large imaging depths, AO remains essential in achieving high spatial resolution. Because tissues often absorb more at these longer wavelengths, by increasing the focal intensity, AO enables the reduction of average excitation power and reduces heating-induced tissue damage.

Effort has also been put into developing far-red and NIR fluorescence proteins, which target cell types, biomolecules, and biological processes with much higher specificity than chemical dyes. For example, recently a NIR protein was developed to sense intracellular calcium concentration [38]. Although still inferior to visible fluorescent proteins in terms of brightness and photostability, continued efforts in engineering better NIR proteins could eventually allow them to provide both structural and functional information, as well as act as guidestars for direct wavefront sensing, substantially reducing the demand for sample preparation.

Due to the lack of commercially available microscopy systems, to maximize the impact of AO technologies, it is essential to reduce the complexity of their implementation both in terms of hardware and software. Direct wavefront sensing requires a sensor and a modulator of the wavefront, both of which need to be carefully calibrated and aligned. Therefore, for labs to integrate AO into their existing microscopes, indirect wavefront sensing techniques that utilize a single wavefront modulator can be more easily incorporated into the microscopy beam path. A standalone software module that can be operated independently of the microscope control program has also been developed [36], which should further lower the threshold of entry for biological laboratories.

Concluding remarks

By canceling out tissue-induced aberrations and recovering a diffraction-limited focus for multiphoton excitation, AO methods utilizing both direct and indirect wavefront sensing have led to drastic improvement of image quality of MPFM in complex tissues. Although their applications have yet to go much beyond demonstrations of physical principles, efforts have been made to improve the accessibility of these methods

to non-experts. Together with the continued push to develop brighter fluorophores with longer wavelengths, AO will become an essential component of cutting-edge MPFMs in pushing the imaging depth for biological investigations at high spatial resolution.

Acknowledgment

3. Optical wavefront engineering for intravital fluorescence microscopy

Meng Cui
Electrical and Computer Engineering and Biology Department, Purdue University, United States of America

Status
Cellular resolution imaging in live biological systems holds great significance in biology and medicine [39]. Thanks to the rapid advance of genetic fluorescence function indicators, various cellular activities can be captured by optical measurement. However, a major challenge in applying optical measurement in live animals is the limited imaging depth as a result of the inhomogeneous refractive index of biological tissue [40–42]. Achieving *in vivo* large volume high-throughput 3D imaging remains a challenge in most animal models. Wavefront engineering has been explored to improve the performance of deep tissue imaging. First, tissue-induced light scattering and aberration is a reversible process. Proper engineering of the optical wavefront can correct optical aberrations and even suppress light scattering, which can improve the imaging spatial resolution and signal-to-noise ratio (SNR) [40–42]. Second, wavefront engineering can be employed to achieve 3D volumetric imaging [39]. Various devices can be employed to generate a defocusing wavefront which leads to axial control of the imaging plane. Third, wavefront engineering can be coupled with miniature invasive imaging probes to access extremely large depths [43]. Miniature imaging devices often have inherent aberration, which greatly reduces their imaging performance including resolution, field of view (FoV), and imaging throughput. Wavefront engineering can help assist miniature probe imaging to improve the overall imaging performance. Further advances in all three directions are expected to enable new observations and knowledge in biomedical research.

Current and future challenges
Cellular resolution functional imaging has been widely employed in biomedical research (figure 3). In immunology, intravital imaging has been used to track the motility and interactions of immune cells, which provides key information about the function and dynamics of various cell types [39]. In neuroscience, *in vivo* measurements are performed over a wide range of spatiotemporal scales. To study the neuronal plasticity related to development, learning, and memory, one needs to observe subtle morphological changes of neuronal structures at a sub-micrometer spatial resolution over days or weeks. To capture the neuronal activity during behavior, fluorescence images based on calcium or voltage indicators need to be recorded at a 10–1000 Hz frame rate with cellular or subcellular resolution. Spatial resolution, 3D signal confinement, and SNR are highly important for these measurements, which demand high-quality focus deep in biological tissue. Although the index of refraction of biological tissue is similar to that of water, the index of cellular components is slightly higher, which causes spatially varying wavefront distortion. Moreover, the movement of cellular structure and the trafficking of blood cells also cause temporal variation. To fully compensate for the wavefront distortion, we need to provide dynamic correction which also varies over space and time. As the cellular dynamics are inherently three-dimensional, we also need to capture the dynamics in 3D. For applications on awake animals, the motion of the animal also causes image instability. As a result, slow recording will suffer from motion artifacts. With high-speed 3D recording techniques, we can eliminate such artifacts through post-measurement image registration. To access very deep regions (e.g. several millimeters or more), miniature invasive imaging probes are commonly employed. However, the design and the dimension limit of these miniature lenses cause inevitable aberrations, which are also field-position-dependent. Routine applications often suffer from reduced resolution, SNR, FoV, and throughput. Advanced wavefront correction is needed to enable high-quality large volume imaging through these miniature imaging devices.

Advances in science and technology to meet challenges
To provide *in vivo* wavefront measurement, sensor-based and sensorless methods have both been developed. For multiphoton excitation, the excitation and emission wavelengths are far apart. The short wavelength emission suffers from much more severe aberration and scattering. Therefore, sensorless methods that modulate the excitation wavefront profiles are often preferred [40]. High-speed methods can achieve microsecond-level measurement time per spatial mode [44]. To correct for highly complex wavefront distortion, the iterative multi-photon adaptive compensation technique (IMPACT) has been developed [40], which leverages the iterative feedback and the inherent nonlinearity in multi-photon imaging to force the focus to converge to a diffraction-limited spot inside highly scattering biological tissue. In addition to high-resolution imaging inside the thick brain and lymph node tissue, IMPACT also enables high-resolution noninvasive transcranial imaging through intact mouse skulls [45]. For high-throughput large FoV imaging, the imaging system needs to provide simultaneous spatially varying aberration correction. Multi-pupil
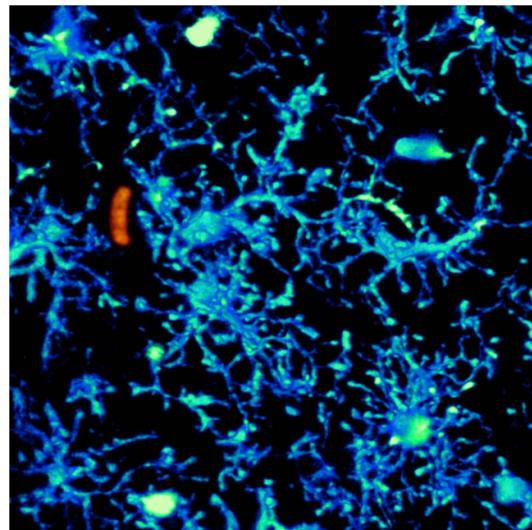
Figure 3. High-speed 3D volumetric imaging of a mouse brain. Cyan, microglia; orange, blood cell.

adaptive optics has been developed to achieve high-speed, high-resolution imaging [46]. Moreover, defocusing control can be applied to the desired region to achieve non-planar imaging such that the features of interest can be shifted to the same 2D recording plane for simultaneous fast recording. Toward fast 3D volumetric imaging, an optical phase-locked ultrasound lens has been explored to provide a microsecond-scale defocusing wavefront control [39]. Such capabilities can convert existing 2D raster scanning microscopes for fast 3D volumetric recording. An important technique for 3D laser scanning imaging is the remote focusing method [47], which relays a defocusing wavefront through a pair of objective lenses to the desired focal plane to rapidly shift the laser focus. The perfect operation of remote focusing demands perfect telecentric objective and relay lenses. However, perfect telecentricity is not the design goal of common objective lenses and is hardly achievable. To improve the imaging performance, an image plane adaptive correction method has been developed which can greatly extend the working range of remote focusing systems [48]. For imaging beyond several millimeters, miniature invasive probes are often used. The inherent aberration limits the resolution and accessible tissue volume. Recently, the clear optically matched panoramic access channel technique (COMPACT) has been developed, which provides two to three orders of magnitude increase in tissue access volume [43]. Combined with aberration correction, COMPACT can yield high-quality images over massive tissue volumes.

Concluding remarks

The ultimate goal of *in vivo* imaging is to noninvasively image deep inside live biological systems. Currently, the majority of the development is still to correct for the static slowly varying low-order aberrations. Although these developments lead to better resolution and SNR, the imaging depth advance is still moderate. Significant imaging depth increase can only happen if the wavefront correction can handle the high-order spatially varying dynamic wavefront distortion in live animals. Currently, none of the established methods is close to achieving this goal. Major innovations that can offer real-time high-speed wavefront measurement and correction are needed to break the current limit. An important aspect of tool development is the broad and routine adoption by the users, which requires the developed technique to be highly robust and easy to use. Without such capabilities, the development will likely have negligible impacts.

Acknowledgments

4. High-speed wavefront shaping

Rafael Piestun
University of Colorado Boulder, United States of America

Status

Spatially modulating light at high speed is critical for the success of multiple optical techniques and applications. Early use of spatial light modulators (SLMs) in 3D holographic displays, optical signal processing, and pattern recognition was hampered by the lack of adequate SLMs at the time. From initial liquid crystal displays with low space-bandwidth product and poor phase modulation to photorefractives, a plethora of modulation techniques would require decades to mature to the level required for current deep imaging needs. Adaptive optics (AO) became practical early on through the use of mechanically deformable mirrors which, despite having a relatively small number of actuators, adapt effectively to the task of compensating for optical aberrations.

Most biological applications of wavefront shaping (WFS) require fast wavefront modulation, regardless of the specific technique used to calculate the compensating wavefront. In techniques that use iterative optimization, optical systems utilize feedback over multiple iterations to attain a wavefront that satisfies a target performance. Alternatively, in transmission matrix (TM) calculations, a large set of wavefronts needs to be projected and the respective outputs measured, ideally before the medium changes again. Similarly, in direct digital phase conjugation, the spatial modulation is calculated directly from direct measurements of the wavefront but latencies and dynamic changes of the medium are still an issue. Fast spatial modulation is critical in high-speed scanning through or inside a complex medium regardless of how the SLM pattern is obtained, including techniques based on digital phase conjugation, TM, or iterative optimization.

In live biological tissue, typical decorrelation timescales are of the order of milliseconds. However, the need for fast modulation techniques goes beyond biology, being a requirement in dynamic imaging, sensing and focusing, with implications in optical communications as well as quantum and nonlinearity control.

Recent demonstrations using micro-electro-mechanical systems (MEMSs) and acousto-optics have shown a path from the early modulation rates in the 10s of Hz to 100s of kHz. These experiments help motivate the development of larger and better SLM arrays, as well as the investigation into novel physical modulation mechanisms. In effect, current SLM constraints imply that speed is typically achieved at the expense of a lower number of degrees of freedom or a reduction in efficiency, if not both.

This section reviews recent progress in achieving high-speed WFS, requiring the adoption of new modulation mechanisms, as well as optical, electronic, and computation optimization.

Current and future challenges

A general WFS problem, as depicted in figure 4, seeks to image through or inside a complex medium. These are defined as highly inhomogeneous media that generate multiple scattering events for any light propagating in their interior, hence scrambling the information to a degree that has been traditionally approached via statistical methods. This is the result of having a huge number of scatterers, with unknown locations and optical properties. Additionally, complicating the problem even further, these scatterers and the whole medium are dynamically changing.
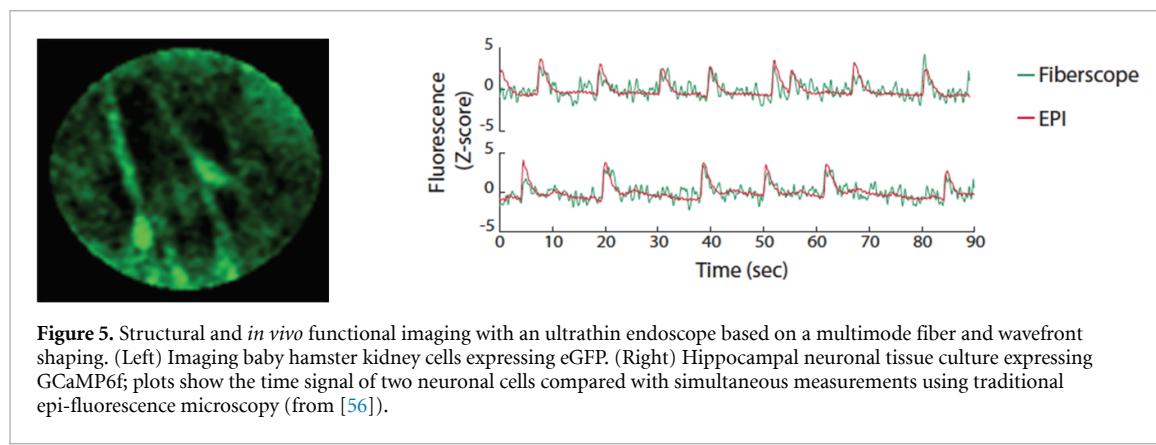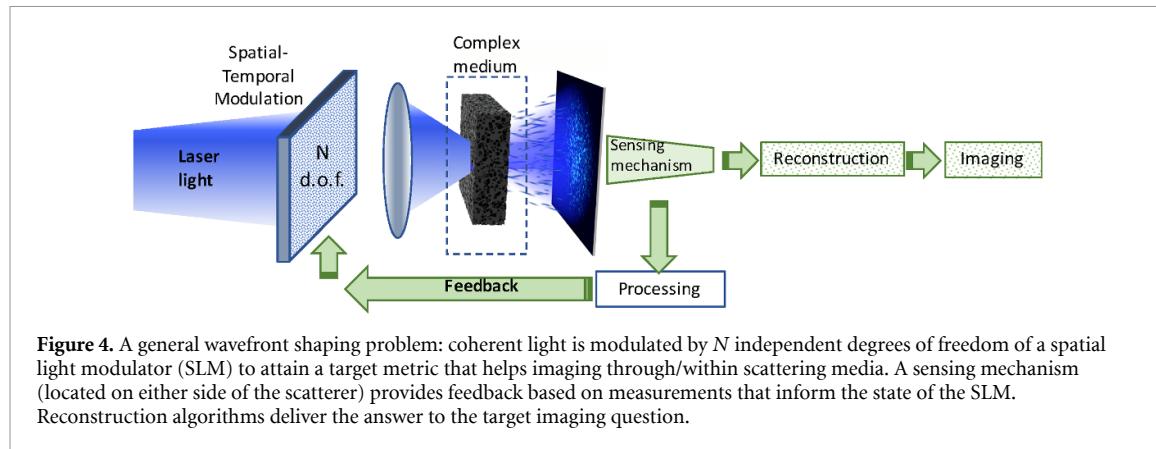
The use of coherent laser light provides high-intensity sources that somehow mitigate the need to consider chromatic dispersion while enabling sensitive phase measurements. Notwithstanding, multispectral or short pulse generalizations have been considered.

Measurements are provided via a sensing mechanism such as photodetectors collecting excited fluorescence or acoustic transducers detecting photoacoustic signals. These measurements are used to inform and update the SLM state, typically multiple times as the complex medium changes or as part of a sequence of measurements to characterize the medium. The process continues with a series of measurements followed by a matched reconstruction algorithm to attain the target imaging task.

The principle of phase conjugation for the correction of distortions by inhomogeneous objects was recognized shortly after the invention of holography [49]. Nowadays, the concepts of holography, optical, digital, or computer-generated, provide a useful framework for understanding and devising techniques for imaging through highly inhomogeneous media.

The traditional optical holographic process is slow for most dynamic imaging situations. The advent of fast detector arrays, interfacing electronics, SLMs, and computers in combination with a new understanding of complex media and insights into computational imaging have opened opportunities for previously unthinkable imaging performance.

The ideal SLM, in particular, has a large number of pixels, number of phase levels, phase stroke, and diffraction efficiency, while simultaneously achieving fast response time, switching frequency and low

Figure 4. A general wavefront shaping problem: coherent light is modulated by *N* independent degrees of freedom of a spatial light modulator (SLM) to attain a target metric that helps imaging through/within scattering media. A sensing mechanism (located on either side of the scatterer) provides feedback based on measurements that inform the state of the SLM. Reconstruction algorithms deliver the answer to the target imaging question.

Figure 5. Structural and *in vivo* functional imaging with an ultrathin endoscope based on a multimode fiber and wavefront shaping. (Left) Imaging baby hamster kidney cells expressing eGFP. (Right) Hippocampal neuronal tissue culture expressing GCaMP6f; plots show the time signal of two neuronal cells compared with simultaneous measurements using traditional epi-fluorescence microscopy (from [56]).

latency. While progress in SLM technologies has been significant, the currently available spatial and temporal space bandwidths are far from what is needed when compared to the degrees of freedom of most complex media. Hence, managing tradeoffs is critical to advancing imaging applications.

Advances in science and technology to meet challenges

One approach to overcome current limitations is to use fast SLMs with a lower number of pixels and/or a lower number of states (e.g. binary), while compensating using holographic encoding. For instance, it is possible to use a binary-amplitude SLM such as the deformable mirror device in conjunction with computer generated holography concepts to achieve millisecond-scale TM measurements [50, 51]. The electronic implementation via dedicated hardware is critical to reduce latencies due to communication and computation [51].

Another possibility is to use the dimensionality transformation enabled by scattering media to take advantage of existing fast 1D modulators [52]. In effect, the actual arrangement of the input modes is almost irrelevant as long as the coupling to the output modes is strong enough. In this case, the scattering medium converts the light from each pixel of the 1D SLM into a 2D speckle pattern. Adjusting the phase of each pixel provides a means to exert control of the output light distribution in two or even three dimensions. Hence, 1D modulation (at 100s of kHz) provides opportunities to control light about three orders of magnitude faster than with liquid crystal SLMs [52].

A little-explored area is the control of nonlinear phenomena using WFS [53]. Nonlinear WFS imaging techniques, such as multi-photon excitation, Raman scattering, or second-harmonic generation, provide new means to interrogate different materials. High-speed modulation could also benefit emerging hybrid imaging modalities [54, 55].

Functional imaging of the brain, an imaging grand challenge, could help understand the neural pathways that trigger human brain function. The use of WFS in multimode fibers has enabled the thinnest endoscopes to functionally image the activity of live neurons [56]. Real-time imaging is critical to follow the neuron action potential patterns (figure 5), accessing the brain with cellular resolution at depths where non-invasive techniques cannot reach.

Emerging techniques also include the use of acousto-optic devices to control the phase via programmable RF signals that encode beams in the medium. This is followed by measurement of the phases of the scattered

beams with a fast single-pixel detector. The acousto-optic deflector phase conjugates the beams and creates a spatio-temporal focus possibly scanned at high speed [57].

Concluding remarks

Progress in high-speed WFS is accelerating to such an extent that a description of all advances exceeds the scope of this article. While some ideas might take years to become practical, others are already having an impact by managing tradeoffs such as speed vs degrees of freedom or speed vs system complexity. It should be emphasized that most existing SLMs were not developed targeting WFS, so naturally, some of the current technological limitations (e.g. number of active elements in MEMS devices) are not fundamental in nature. Novel concepts are still needed, for instance with the adoption of tools such as machine learning or novel physical mechanisms for modulation. An intriguing development to watch is based on the use of the so-called active metasurfaces [58]. An outgrowth of subwavelength diffractive optics, they implement planar nano-structured arrays whose optical response can be dynamically tuned. The control is achieved by different physical mechanisms and material systems, including mechanical deformation, phase-change media, free-carrier density modulation, thermo-optic and electro-optics effects.

Acknowledgments

5. Imaging in complex media by scattered back-illumination

Jerome Mertz, Timothy Weber and Sheng Xiao
Department of Biomedical Engineering, Boston University, United States of America

Status

When imaging in complex media one must first be clear on what exactly one is interested in imaging. For example, in fluorescence imaging, one is interested in the spatial distribution of fluorescent markers. Complexity of the medium in this case can introduce aberrations that degrade image contrast and resolution. On the other hand, when performing label-free imaging, contrast generally arises from scattering, enabling structures of interest to be distinguished by their size. For example, one might wish to image small, point-like scatterers embedded in an aberrating medium of spatially varying refractive index (RI). Alternatively, one might be interested in reconstructing the RI variations themselves, whereupon point-like scatterers only undermine image quality by introducing multiple scattering. This last case can be of particular interest since a retrieval of the RI distribution can enable the application of adaptive optics (AO) to improve image quality.

However, obtaining a 3D image of the RI distribution in a complex medium is no easy task, particularly if the medium is so thick that it can only be accessed from one side. The difficulty comes from the fact that only sharp structures in the medium, such as point-like reflectors or interfaces, provide sufficiently high spatial frequencies to scatter light in the backward direction so that it can be detected. More slowly varying structures scatter light only in the forward direction, making them invisible to conventional epi-detection devices. Such is the case with optical coherence tomography (OCT), which can only reveal sharp sample structures, producing highly granular images. The retrieval of slowly varying structures must be inferred indirectly in this case, for example by considering their effects on the image granularity and solving an inverse problem to simultaneously reconstruct both high- and low-frequency structure [59, 60]. An alternative simpler approach, which is the subject of this roadmap, is to exploit the multiple scattering from deeper layers within the sample and use this to back-illuminate regions of interest in shallower layers. In this manner, contrast becomes based on light transmission rather than reflection, providing access to low-frequency sample structure. Such is the principle of oblique back-illumination microscopy (OBM) [61], depicted in figure 6, along with its scanning analog based on oblique back-detection (formally equivalent by virtue of Helmholtz reciprocity [62]). OBM has recently been shown to enable quantitative RI reconstruction in 3D [63].
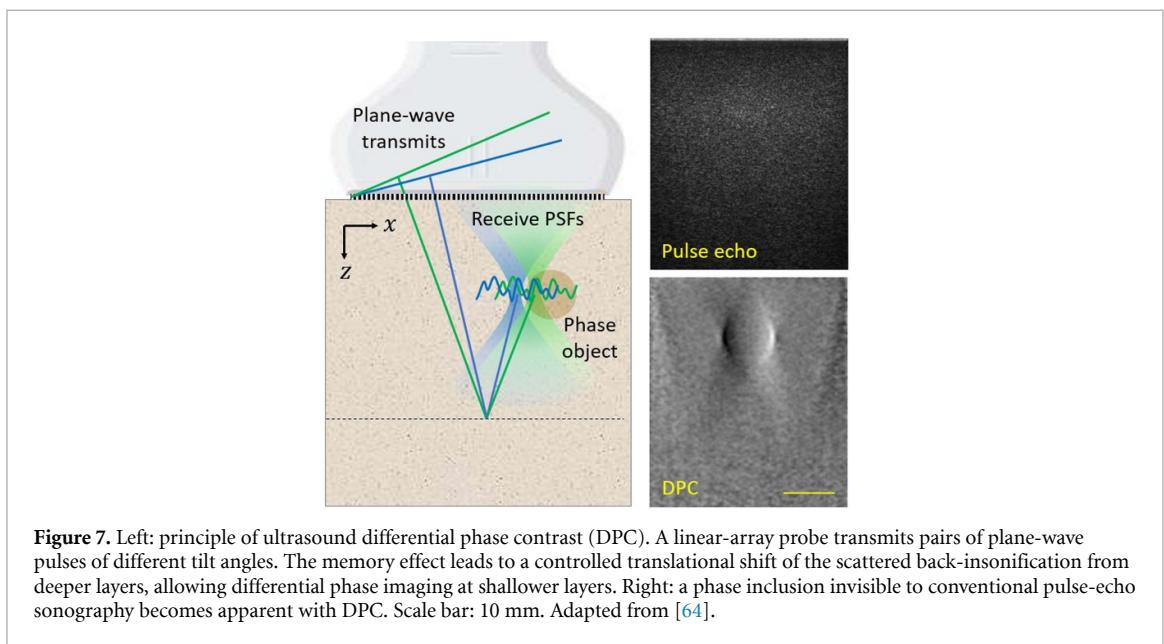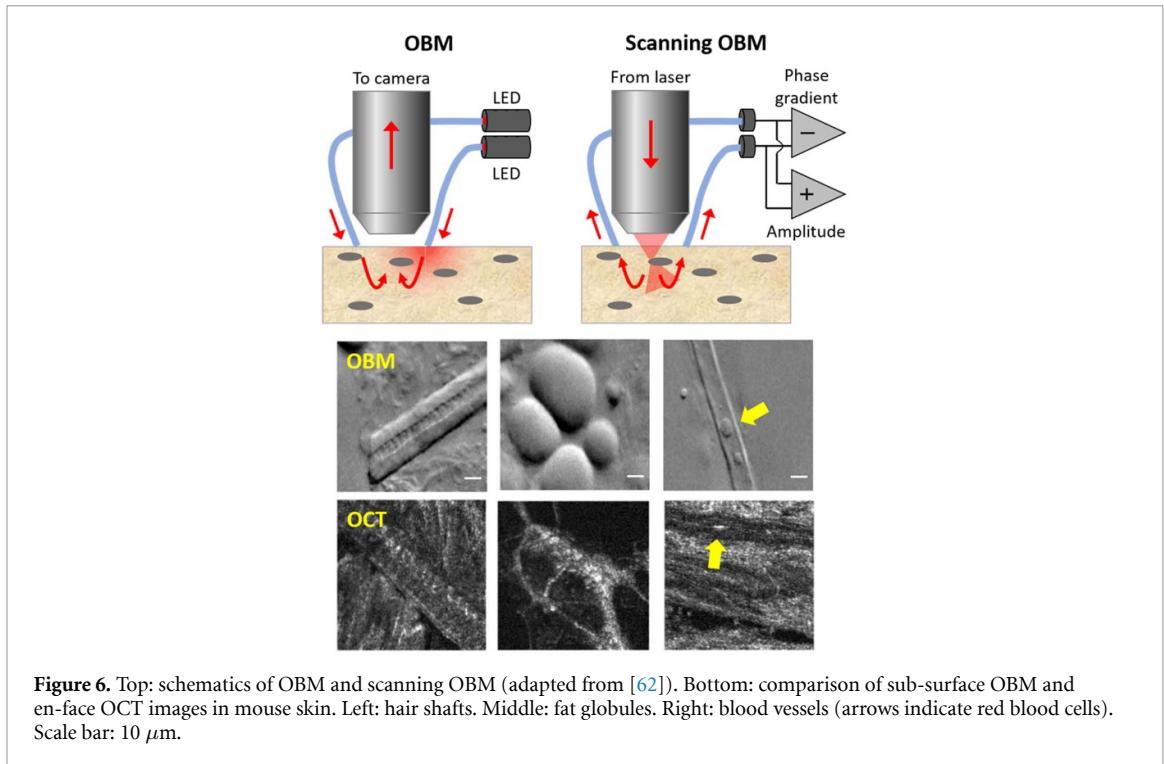
Current and future challenges

OBM is simple to implement, basically as an add-on to any conventional microscope; however, it does suffer from drawbacks. For one, while it allows imaging within arbitrarily thick, complex samples (indeed, complexity is required to obtain backscattering in the first place), it does not provide particularly deep imaging. For example, it does not attain the same penetration depths as OCT, despite the fact that both modalities are based on scattering. One reason for this is that OCT makes use of coherent illumination which, in turn, allows the possibility of interferometric time gating (or coherence gating) to reject background and improve contrast. Another reason is that OCT is based on ballistic light illumination and detection, which is easy to control (e.g. by spatial filtering). In contrast, OBM relies on diffuse backscattering, which is much more difficult to control.

Nevertheless, diffuse backscattering is not impossible to control. In particular, a remarkable phenomenon called the memory effect [2] prescribes that diffuse light obeys ballistic transmission or reflection laws even in thick complex media, but only within a very narrow angular range dependent on basic media properties (thickness in transmission, transport scattering length in reflection; see section 13). A hint as to how the memory effect can be exploited to improve OBM comes from the field of acoustical imaging [64], as shown in figure 7. Here, diffuse back-insonification, even though it is spatially incoherent, is controlled by the memory effect to enable essentially a coherent version of OBM based on measurements of differential phase rather than differential intensity. Because the back-insonification is in the transmission direction, it can reveal weak structures within the medium that are completely invisible to standard ultrasound imaging based on pulse-echo sonography (the acoustic equivalent of OCT). In addition, what can be loosely thought of as an acoustic version of scanning OBM has also been demonstrated, though with a more involved inversion-based image reconstruction algorithm where the memory effect is more implicit [65].

Advances in science and technology to meet challenges

A feature of acoustic imaging compared to optical imaging is that the wave frequencies involved are orders of magnitude smaller (typically ∼8). As such, actuators are readily available that allow the coherent reception of acoustic waves where both amplitude and phase can be directly resolved, leading to the possibility of

Figure 6. Top: schematics of OBM and scanning OBM (adapted from [62]). Bottom: comparison of sub-surface OBM and en-face OCT images in mouse skin. Left: hair shafts. Middle: fat globules. Right: blood vessels (arrows indicate red blood cells). Scale bar: 10 μm.

Figure 7. Left: principle of ultrasound differential phase contrast (DPC). A linear-array probe transmits pairs of plane-wave pulses of different tilt angles. The memory effect leads to a controlled translational shift of the scattered back-insonification from deeper layers, allowing differential phase imaging at shallower layers. Right: a phase inclusion invisible to conventional pulse-echo sonography becomes apparent with DPC. Scale bar: 10 mm. Adapted from [64].

sub-cycle time gating. The same cannot be said of optical detectors, which are currently too slow to directly resolve the optical phase. This becomes important in applications involving the memory effect, since the range of this effect is known to increase when time gating becomes more refined [66]. It is for this reason that the memory effect can be easily exploited with acoustic OBM, enabling coherent differential phase detection, while it cannot with optical OBM, which to date has only been demonstrated with incoherent differential intensity detection.

Time-resolved imaging is, of course, possible and routinely performed with light, but attaining better than picosecond time resolution requires some kind of trick typically involving interferometry. For example, ultrafast pulsed lasers are readily available, enabling sub-picosecond time gating by interference with a pulsed reference wave. This principle is exploited in time-domain OCT. Alternatively, broadband spatially coherent sources are also readily available that allow the Fourier synthesis of a time gate, as exploited in frequency-domain OCT (and also in [66]). The application of such tricks to optical OBM may be envisaged, though perhaps more conceivably in its scanning configuration which involves only single-element detectors.

However, the problem of engineering appropriate reference waves still remains. Much more straightforward would be a method of time gating that does not require interferometry, perhaps making use of a Kerr gate or, better still, by direct detection with an ultrafast detector. Advances in single-photon avalanche detectors, either in single element or in array form, may lead the way here. Indeed, the development of higher-speed devices enabling the direct coherent detection of light is one of the key technological advances that the optical imaging community is eagerly awaiting.

Concluding remarks

The purpose of this section is to highlight the possibility of indirectly rather than directly imaging structures within complex media by way of scattered back-illumination, leading to the possibility of transmission-based imaging with its attendant benefits, and allowing structures to be revealed that would normally be invisible. Scattered back-illumination can be controlled to a surprising degree of precision by way of the memory effect (at least in acoustics). Remarkably, this memory effect is far more general than utilized here [67], extending beyond spatial degrees of freedom to even polarization and spectral degrees. Such a generality opens the door to far richer contrast modalities than simple phase imaging as shown here, and promises to span a wide range of applications including biomedical, imaging around corners, lidar, sonar, seismology, and many more.

Acknowledgment

6. Guidestar-assisted wavefront shaping

Joshua Brake[1,5], *Zhongtao Cheng*[2,5], *Roarke Horstmeyer*[3], *Lihong Wang*[2,4] *and Changhuei Yang*[4]

[1] Department of Engineering, Harvey Mudd College, Claremont, CA 91711, United States of America
[2] Caltech Optical Imaging Laboratory, Andrew and Peggy Cherng Department of Medical Engineering, California Institute of Technology, Pasadena, CA 91106, United States of America
[3] Department of Biomedical Engineering, Duke University, Durham, NC 27708, United States of America
[4] Department of Electrical Engineering, California Institute of Technology, Pasadena, CA 91106, United States of America
[5] Joshua Brake and Zhongtao Cheng contributed equally to this work.

Status

Focusing light efficiently into complex scattering media is significant for many applications, including optical imaging, manipulation, therapy, and stimulation. However, scattering media randomize the wavefront of an incident optical field, preventing the light from being easily focused as it would in free space. To overcome this challenge, guidestar-assisted wavefront shaping methods are being actively developed. The general principle of guidestar-assisted wavefront shaping is illustrated in figure 8(a). The guidestar, which is typically located at the desired focus spot inside a scattering medium, interacts with the scattered photons and encodes its location in the scattered light. The measurement system detects the exiting scattered light and identifies the components that originate from the guidestar's location. The system then determines a wavefront modulation map to present on a spatial light modulator (SLM) to tailor the wavefront of the incident laser. Various information from the guidestar can be used, such as the scattered wavefront itself (figure 8(b)) [68], wavefront variation induced by the guidestar (figure 8(c)) [69], the scattering point spread function (figure 8(d)) [35], or the total signal intensity from the guidestar (figure 8(e)). According to the specific measured quantity, the wavefront modulation map is updated iteratively to maximize the desired optical pattern (e.g. a focal spot) inside the scattering media, or directly determined by phase conjugation, to refocus light to the guidestar location.

One example of a popular guidestar mechanism is to generate new photons with a different frequency. Examples of this class of guidestar include nanoparticles which generate a nonlinear second−harmonic signal [70], focused ultrasound which generates frequency-shifted photons using the acousto-optic effect [68, 71], and fluorescent materials [35, 72]. Among these examples, focused ultrasound provides a noninvasive and freely addressable approach for focusing light into scattering media (figure 8(b)), which is more promising for general wavefront shaping applications. A related guidestar is the photoacoustic guidestar (figure 8(e)), which is detailed in section 7. A guidestar can also encode its location information by inducing wavefront variation, which is termed a dynamic guidestar. Dynamic guidestars can be physical, such as magnetic particles [73, 74] and microbubbles [75], or virtual, such as the adapted perturbation in samples [69] or perturbations induced by an ultrasound field [76]. Through detecting and conjugating the differential field of collected scattered light in two different states of a dynamic guidestar, an optical focus can be realized at the position where the wavefront variation originates inside the scattering medium (i.e. the dynamic guidestar location) (figure 8(c)). Since fluorescence is an important contrast mechanism in optical imaging, the fluorescence-based guidestar has intrinsic advantages for adoption in fluorescence microscopy. This type of approach has been previously demonstrated for adaptive optics correction with standard one-photon fluorescence [77] as well as two-photon (2P) excitation microscopy. As 2P excitation-based detection facilitates clear image formation deeper within tissue than standard fluorescence, the intrinsic guidestar approach has been integrated into several 2P systems as a promising means to extend imaging depths to 400 μm or more within biological tissue [78]. Existing approaches include an iterative SLM update technique [40] (iterative multi-photon adaptive compensation technique), a scanning-based approach for point-spread function estimation [35] (focus scanning holographic aberration probing, figure 8(d)), and a holographic phase stepping approach for rapid correction [79] (dynamic adaptive scattering compensation holography). Such techniques provide a promising means to jointly focus and rapidly scan out images at improved tissue depths with minimal additional hardware and in a noninvasive manner.

Current and future challenges

The major areas of development that can improve guidestar-assisted wavefront shaping fall into two main categories: (a) improvement of system latency to enable focusing deeper in dynamic scattering media and (b) development of new guidestar mechanisms to improve focusing performance and enable increased adoption. Solving these challenges will enable wavefront shaping to advance beyond experiments with carefully controlled and designed samples to more practical applications throughout biomedicine.
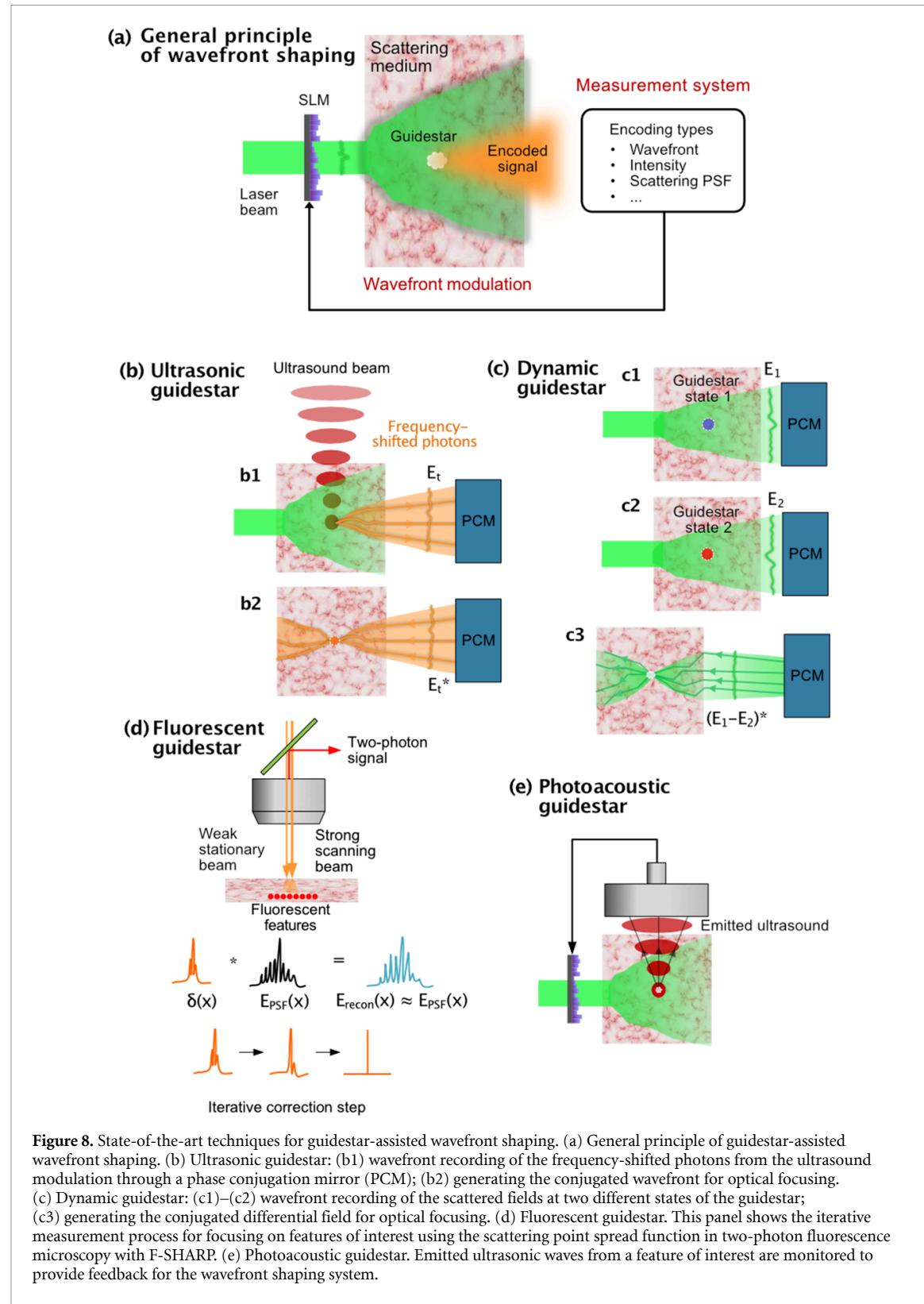
Figure 8. State-of-the-art techniques for guidestar-assisted wavefront shaping. (a) General principle of guidestar-assisted wavefront shaping. (b) Ultrasonic guidestar: (b1) wavefront recording of the frequency-shifted photons from the ultrasound modulation through a phase conjugation mirror (PCM); (b2) generating the conjugated wavefront for optical focusing. (c) Dynamic guidestar: (c1)–(c2) wavefront recording of the scattered fields at two different states of the guidestar; (c3) generating the conjugated differential field for optical focusing. (d) Fluorescent guidestar. This panel shows the iterative measurement process for focusing on features of interest using the scattering point spread function in two-photon fluorescence microscopy with F-SHARP. (e) Photoacoustic guidestar. Emitted ultrasonic waves from a feature of interest are monitored to provide feedback for the wavefront shaping system.

The latency between recording and playback in a wavefront shaping system is one of the most critical specifications for practical biomedical applications. The wavefront that focuses light to a desired location is valid only for a limited time due to biological motion such as blood flow. This timescale can be as long as several seconds in acute brain slices *in vitro* [80], but the decorrelation time at the same depth within *in vivo* specimens drops by three orders of magnitude to around 1 ms. Such fast decorrelation requires that the latency of a wavefront shaping system be on a timescale of milliseconds or less, which is challenging for most

current techniques. In addition, for effective wavefront shaping into thicker samples, the control of additional degrees of freedom (i.e. additional pixels in the wavefront shaping device) is desirable, which places additional demands on system latency that must be considered.

The second main challenge is related to the guidestar mechanisms themselves. While many different guidestar mechanisms (such as those discussed previously) have been developed, they each have specific applications for which they are best suited. For example, one of the main advantages of the ultrasonic guidestar is that it is freely addressable and can be easily moved to target a desired focal location. However, it has a low modulation efficiency (defined as the percentage of light interacting with the guidestar location and subsequently 'tagged' with a different frequency), it is difficult to use in a reflection geometry due to its non-isotropic tagging behavior, and it is impacted by acoustic absorption, especially at higher ultrasound frequencies which are optimal for achieving high-resolution foci. As this one example indicates, further development of additional guidestar techniques or improvements to existing guidestars is necessary to achieve the goals of a freely addressable, high-resolution, efficient guidestar which is compatible with a reflection geometry and can access depths up to the optical absorption limit.

Advances in science and technology to meet challenges

Addressing the challenges of lower latency wavefront shaping systems and better guidestars requires a combination of technological development and the invention of new ways to leverage intrinsic or extrinsic signals within a sample for focusing.

Improving the latency of a wavefront shaping system can be accomplished by developing faster techniques and technologies for the various stages of the recording and playback process. The primary areas for improvement are (a) SLM response, (b) data transfer, (c) phase map calculation, and (d) guidestar integration.

The most widely used SLM technology is based on liquid crystal (LC) technology, which can be configured to control either the amplitude or phase of the wavefront. Digital micromirror devices are another popular technology that are several orders of magnitude faster than LC-based SLMs, but in their simplest configuration offer only binary amplitude control of a wavefront. While other novel SLM technologies based on acousto-optics or liquid light valves exist and offer even faster modulation, these methods are normally limited in terms of the number of modes they can control. Thus, they are limited in terms of their practical capabilities. State-of-the-art wavefront shaping systems leverage fast SLMs (e.g. digital micromirror devices) and optimized electronics (e.g. field programmable gate arrays FPGAs) to maximize the system throughput and minimize the latency between recording and playback.

When controlling many modes simultaneously, the data transfer requirements also quickly become non-trivial. A typical scientific CMOS camera contains 5×10^6 16 bit pixels, meaning that a single raw frame is on the order of 10 MB. Even using the fastest commercially available data links, maximum frame rates typically top out at 100 frames per second. The amount of data also impacts the time required to calculate the appropriate phase mask for playback. Using a phase shifting approach requires a few addition operations and a division per pixel, whereas more complicated measurement schemes such as those based on off-axis interferometers may require more involved computations such as Fourier transforms. Fortunately, many of these calculations can be highly optimized and parallelized using specialized hardware such as graphics processing units or custom digital hardware on FPGAs. Besides advances in hardware, computational methods are also emerging for facilitating wavefront shaping via reduced data acquisition, such as single-shot ultrasound-assisted optical focusing [81].

A promising approach toward improving the system latency is an integrated sensor and wavefront shaping architecture that combines the functionality of an image sensor and an SLM into a single device with some basic computation capabilities provided in each pixel [82]. In this device, each pixel can capture and compute its playback phase in parallel, thus eliminating the need to transfer data. Using a micromirror-based architecture for the wavefront-shaping elements will provide low-latency shaping capabilities. Furthermore, this architecture can solve the alignment challenges of time-reversal-based wavefront shaping systems by co-locating the sensing and shaping elements.

To deal with the low signal-to-noise ratio of the ultrasonic guidestar, multiple iterative measurements of the phase map can be made to improve the focus peak-to-background ratio. However, each of these iterations requires a recording and playback cycle and thus can significantly increase the effective wavefront shaping system latency. Other guidestars, such as magnetic particles that can provide higher wavefront modulation efficiency, are better in this respect since they can provide higher signal-to-noise ratios at the same focusing depth. In summary, each guidestar technology comes with its own tradeoffs and benefits, and balancing these tradeoffs for a particular application is critical.

Concluding remarks

Guidestar-assisted wavefront shaping is an attractive technique for deep imaging and efficient delivery of light energy beyond the diffusion limit. Although the system latency and guidestar mechanism of current wavefront shaping technologies are still the main limiting factors for more practical biomedical applications, advances in science and technology are showing great potential to gradually resolve or alleviate these limitations. The rapid evolution of semiconductor and LC technologies for optical sensors and modulators will enable high-speed and high-resolution wavefront sensing and control in the future. Meanwhile, advanced computational methods are being actively developed for more efficient information extraction to accelerate wavefront shaping. The continued development of these techniques offers the potential for guidestar-assisted wavefront shaping to expand the optical imaging capabilities of scientists both in the laboratory and clinic.

7. Imaging at depth with linear feedback

Hilton B de Aguiar and Sylvain Gigan
Laboratoire Kastler Brossel, ENS-Université PSL, CNRS, Sorbonne Université, Collège de France, 24 rue
Lhomond, 75005 Paris, France

Status

High-resolution noninvasive imaging at depth is currently performed mostly by wavefront shaping to compensate for scattering, be it by optimization, phase conjugation, or transmission matrices approaches [83] (see also sections 8–10). To be noninvasive, these methods require a 'guidestar' mechanism. Besides acoustic-based methods, all require a nonlinear feedback mechanism, for instance second−harmonic signal, or multiphoton fluorescence in order to converge to a single-grain focus, typically diffraction-limited [84] (see also section 5). Even acoustic methods benefit from nonlinearities, allowing to improve the resolution close to the optical diffraction limit. Linear feedback is conventionally considered not to be feasible because of the impossibility to converge to a focus from an extended object. In parallel, algorithmic tools have been introduced and become very popular for retrieving hidden fluorescent objects thanks to the memory effect. Nevertheless, they remain limited in size and complexity of the object. However, linear contrasts, such as fluorescence and Raman, are extremely important in biomedical imaging: they are the easiest and cheapest to implement, are extremely widespread in life sciences and medicine, and, particularly for fluorescence, provide an unprecedented level of signal (compared to its nonlinear counterpart). Reaching deep imaging using such linear incoherent feedback is therefore an important goal for the field.

In this section, we want to cover a few computational strategies, allowing retrieving objects with linear incoherent contrast, such as fluorescence and spontaneous Raman scattering.

Current and future challenges

Deep imaging has mostly been done exploiting nonlinear feedback for wavefront shaping experiments. Soon after the seminal work from Mosk's group, it was realized that a feedback signal for single-grain focusing within the scattering medium was far from simple. Hence, the field has drastically focused on nonlinear signals as a feedback mechanism due to its ability to converge to a single focus in wavefront shaping experiments, as seen for instance very recently [85]. However, nonlinear processes are less popular in science and engineering due to the cost associated with the hardware (mostly the laser source).
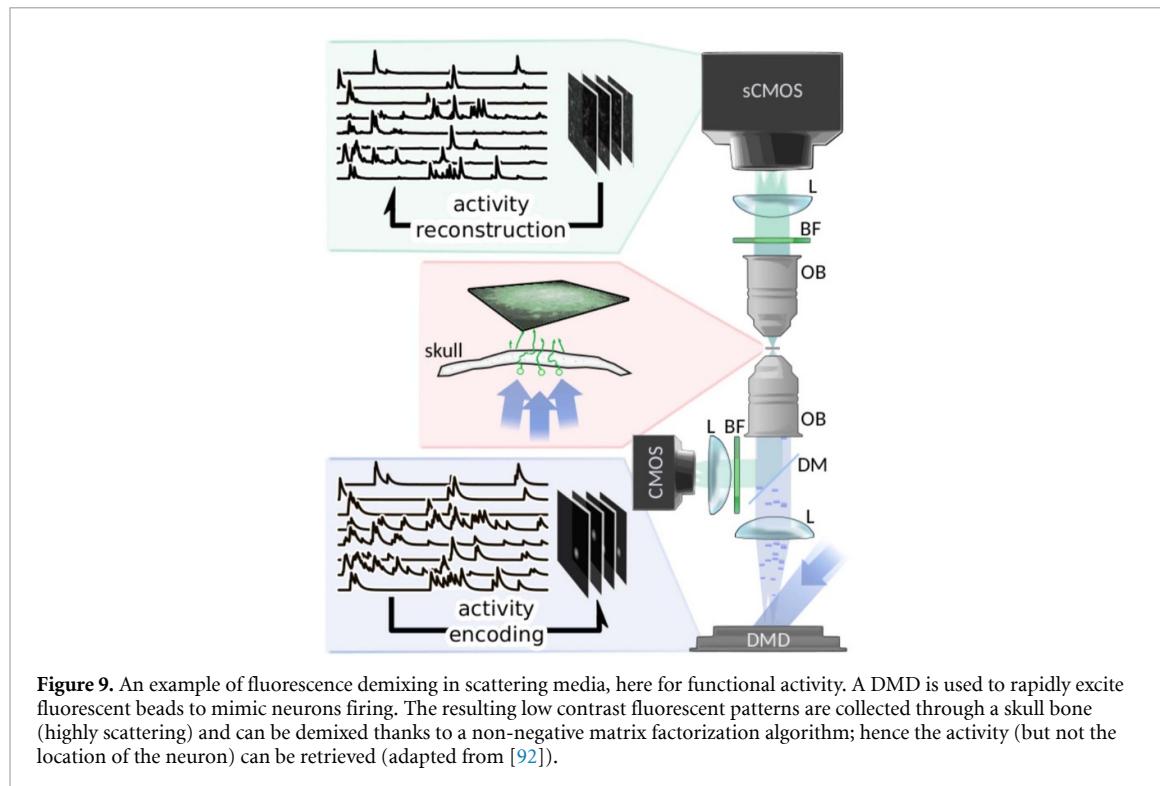
With the emergence of the Big Data era, computational microscopy has brought new directions to the wavefront shaping toolbox. In particular, computational tools exploit other properties of scattering—that may allow for unique single-grain focusing in wavefront shaping experiments or retrieve an image without resorting to wavefront shaping—using linear optical processes as readout, in particular fluorescence. A first set of computational tools has recently been put forward using variance-based methods using linear fluorescence and Raman signals [86–88]: variance calculations can be seen as a 'nonlinear metric,' therefore allowing for focusing convergence in wavefront shaping experiments. However, imaging is only possible with focus-scanning techniques, and hence is time consuming. More recently [89] has solved this issue by combining wavefront shaping with computational modeling and algorithm tools allowing for imaging without focus-scanning methodologies. Indeed, most recent results have shown that costly wavefront shapers are actually not needed: reading out linear fluorescence excited by a set of speckle excitation, combined with computational microscopy tools, allows for image recovery at depth [90]. Along the same lines, one may achieve super-resolution capabilities within scattering media by exploiting computational tools without resorting to wavefront shaping hardware [91]. These examples highlight the wealth of information that the incoherent properties of linear fluorescence allow for deep imaging.

While conventional wisdom forces us to think that actual imaging is necessary, the randomness embedded in the speckle allows for imageless retrieval of precious information at depth. For instance, in [92] demixing algorithms were used to retrieve the temporal activity of neurons (fluctuations of fluorescence), without the need to modulate the illumination (figure 9).

Advances in science and technology to meet challenges

These recent outcomes exploiting computational tools highlight a fertile field ahead. Several of these successful demonstrations rely on the fact that fluorescence is an incoherent effect and often sparse. While these aspects are embedded in many off-the-shelf algorithms, going beyond the incoherent assumption and low sparsity object in computational tools are certainly new challenges to tackle.

As we have learned [83], correlations in multiple scattering help in convergence in the image retrieval process. Up to now, mostly spatial correlations have been used (i.e. spatial memory effect). Other correlation

Figure 9. An example of fluorescence demixing in scattering media, here for functional activity. A DMD is used to rapidly excite fluorescent beads to mimic neurons firing. The resulting low contrast fluorescent patterns are collected through a skull bone (highly scattering) and can be demixed thanks to a non-negative matrix factorization algorithm; hence the activity (but not the location of the neuron) can be retrieved (adapted from [92]).

properties are known, such as spectral (see below) and polarization [93], and could also be exploited in future computational tools.

Despite the fact that fluorescence is the major incoherent contrast mechanism in wavefront shaping methods, there is still much to be done with Raman scattering, another popular contrast method with molecular selectivity. Unlike fluorescence, the main challenge in Raman scattering is its weak signals that deteriorate the performance of any method. Nevertheless, there is richness in the Raman spectrum that is still to be unveiled as only very recently the spectral information embedded in the Raman signal has been exploited. To date, only one report has shown noninvasive focusing using highly sparse samples (therefore focusing convergence is guaranteed) [94], highlighting the need to develop tools for deep Raman imaging, although recent work has shown that variance-based computational methods allow for 'chemical' focusing using wavefront shaping [88]. Finally, speckles have been used to enable super-resolution in Raman-based processes [95], opening another research venue for exploiting computational tools in deep imaging.

Concluding remarks

To conclude, linear feedback mechanisms have originally been seen as a no-go for single-grain focusing in wavefront shaping experiments. Nevertheless, they have recently been re-analyzed, with advances in computational tools showing that there is still a lot to be exploited from these well-established and popular microscopy contrasts, therefore opening important perspectives for deep imaging. Beyond the incoherent contrasts discussed here, coherent mechanisms (in particular Raman) would also open important new applications. The computational tools developed so far have been shown to be very useful, but modern machine learning tools, in particular physics-informed neural networks (see sections 11 and 16), may also prove extremely powerful and versatile.

Acknowledgments

8. Photoacoustic-guided optical wavefront shaping

Emmanuel Bossy[1] *and Thomas Chaigne*[2]
[1] University Grenoble Alpes, CNRS, LIPhy, 38000 Grenoble, France
[2] Aix Marseille University, CNRS, Centrale Marseille, Institut Fresnel, F-13013 Marseille, France

Status

In an ongoing effort to develop optical imaging techniques that can reach large depths into scattering biological tissue, photoacoustic imaging stands out due to its unique capabilities. Relying on the emission of an ultrasonic wave upon the absorption of a pulsed illumination, this modality can be used in a variety of optical excitation and acoustic detection schemes. Depending on the acoustic frequency content of the detected signal, the geometry of the detector and the optical illumination system, various regimes can be explored, with a typical depth to resolution ratio of about 200.

The imaging resolution depends on the depth and scattering regime, and one can distinguish two main categories: below a few scattering mean free paths, it is possible to focus the optical illumination beam, and thus to achieve optical resolution. Beyond this limit, the illumination light is multiply scattered and diffuse, and, without scattering compensation, the resolution is set by the acoustic detection bandwidth, higher frequencies providing a better resolution. The depth–resolution tradeoff is then ultimately set by the increasing attenuation of ultrasound with frequency (typically $\sim$1 dB cm^{-1} MHz^{-1} for biological tissue) and the maximum optical energy that biological tissue can receive without damage. Typically, photoacoustic imaging of biological tissue can provide maps of light absorption with a resolution of about 100 μm at a depth of around 2 cm.

Because the amount of light absorption depends on both the light intensity and the absorption coefficient, photoacoustics has been proposed about a decade ago as a guidestar mechanism for wavefront shaping, as it enables to probe the light intensity impinging on an optically absorbing structure lying deep inside soft tissue. Various schemes involving optimization procedures or the measurement of a so-called photoacoustic transmission matrix have been proposed [54, 96–104]. Any of these methods basically comes down to the following: when a diffuse coherent light field (a speckle pattern) impinges on an optically absorbing object imaged using a photoacoustic system, a modulation of the speckle pattern translates into a modulation of the photoacoustic signal. This photoacoustic signal can serve as a feedback signal to implement optical wavefront shaping methods, in particular to focus light through scattering media. The size of the optical focus is generally dictated by the ultrasound resolution [96, 105], but focusing down to the optical diffraction limit has also been demonstrated [54, 101, 104] (see figure 1).

Comparing this modality to other guidestar mechanisms mentioned in section 6, photoacoustic imaging enables us to probe endogenous optical absorption throughout large volumes, even when tissue can only be accessed from one surface (so-called reflection geometry in optics). Various guidestar locations can therefore be selected without the need to introduce labeling molecules, or scanning a beam or a detector.

Current and future challenges

To date, focusing through a scattering medium with photoacoustic feedback has been demonstrated only in a quite biologically irrelevant experimental configuration: all previous experiments required speckle illumination with large enough speckle grains, obtained via free space propagation between a scattering medium and the absorbing target (see figure 11(a)). This configuration provides an enhanced relative modulation of the photoacoustic feedback signal, as the feedback region contains only a limited number of speckle grains. The larger the number of speckle grains inside the photoacoustic feedback region, the lower the relative modulation. Currently, the modulation of photoacoustic signals from optical absorbers embedded inside a multiply scattering medium, i.e. illuminated with diffraction-limited optical speckle patterns, has never been measured, and remains a hurdle toward photoacoustic-guided wavefront shaping at depth. This is due to the extremely weak amplitude modulation as compared to the mean photoacoustic signal, inherently caused by the mismatch between the ultrasound resolution and the optical resolution, as illustrated in figures 11(d) and (e). In other words, the current fundamental limitation in performing photoacoustic-guided wavefront shaping at depth in tissue is fundamentally a limitation of signal-to-noise and dynamic range considerations. Increasing the ultrasound detection bandwidth to increase the ultrasound resolution may increase the relative amplitude modulation on the one hand, but the subsequent increase in the ultrasound attenuation will decrease the signal-to-noise ratio (SNR) on the other hand.

Very importantly, *focusing* through or inside a complex medium via wavefront shaping does not mean *imaging*, as in this context imaging usually requires the ability to scan a focused spot. Currently, there has never been any realistic demonstration of imaging based on photoacoustic-guided optical focusing: imaging was only demonstrated by scanning an object behind a *fixed* diffuser and *fixed* focal spot (see [54] for
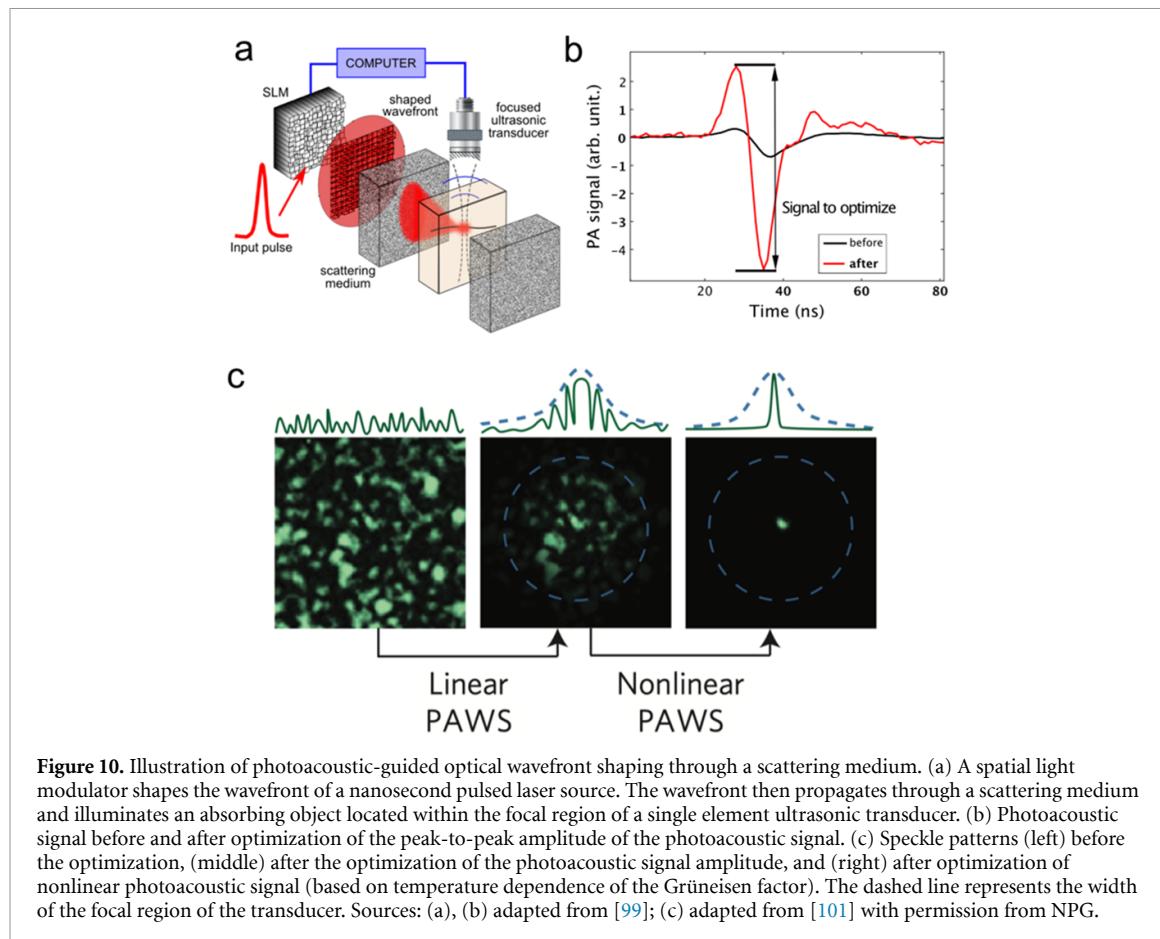
Figure 10. Illustration of photoacoustic-guided optical wavefront shaping through a scattering medium. (a) A spatial light modulator shapes the wavefront of a nanosecond pulsed laser source. The wavefront then propagates through a scattering medium and illuminates an absorbing object located within the focal region of a single element ultrasonic transducer. (b) Photoacoustic signal before and after optimization of the peak-to-peak amplitude of the photoacoustic signal. (c) Speckle patterns (left) before the optimization, (middle) after the optimization of the photoacoustic signal amplitude, and (right) after optimization of nonlinear photoacoustic signal (based on temperature dependence of the Grüneisen factor). The dashed line represents the width of the focal region of the transducer. Sources: (a), (b) adapted from [99]; (c) adapted from [101] with permission from NPG.

instance), whereas imaging a complex medium requires scanning a focal spot through scattering media, at best fixed, but in most practical scenarios dynamically varying within milliseconds. The optical memory effect through scattering media provides a means to scan a focal spot through or inside a scattering medium (see section 14 by Professor Ori Katz), but it is limited to very shallow depths, while photoacoustic imaging aims at depths beyond several millimeters.

We note that performing photoacoustic-guided wavefront shaping at depth *in vivo* also has the same limitations common to all optical wavefront shaping techniques (see section by Professor Changhuei Yang and Professor Lihong Wang), i.e. the need to measure and control an enormous number of modes within times shorter than decorrelation times induced from various motion (flow, breathing, Brownian motion) in living tissue.

Advances in science and technology to meet challenges

As discussed above, advancing photoacoustic-assisted optical imaging requires both performing wavefront shaping extremely fast and detecting very weak photoacoustic signals and associated modulations. Because the average power density that a tissue can safely withstand is limited, going fast with high-repetition-rate lasers turns into weak photoacoustic signals per pulse. At the end, SNR and dynamic range are always the fundamental limitations of photoacoustic sensing, whether to perform photoacoustic imaging or to guide optical wavefront shaping. Because the amount of light is limited by tissue safety limits rather than by laser sources, the only possible direction to meet the requirements of photoacoustic-assisted optical imaging seems to be the development of ultra-sensitive and large-bandwidth acoustic detectors. Very recent technological breakthroughs in this domain, with the advent of transducers having sensitivities enhanced by orders of magnitude as compared to conventional piezoelectric sensing or optical sensing, are very promising and could address the challenges of photoacoustic-assisted optical wavefront shaping and imaging [106].

While we have discussed the use of the photoacoustic effect as a feedback mechanism for wavefront shaping, wavefront shaping has also been proposed as a way to improve photoacoustic imaging [107]. Controlling light propagation through tissue can help minimizing the intensity attenuation caused by multiple scattering and improve the SNR of photoacoustic detection while maintaining the same total power delivered to the tissue, therefore increasing the resolution (by extending the exploitable acoustic bandwidth) and/or the imaging depth of photoacoustic imaging. We also note that optical wavefront shaping is also
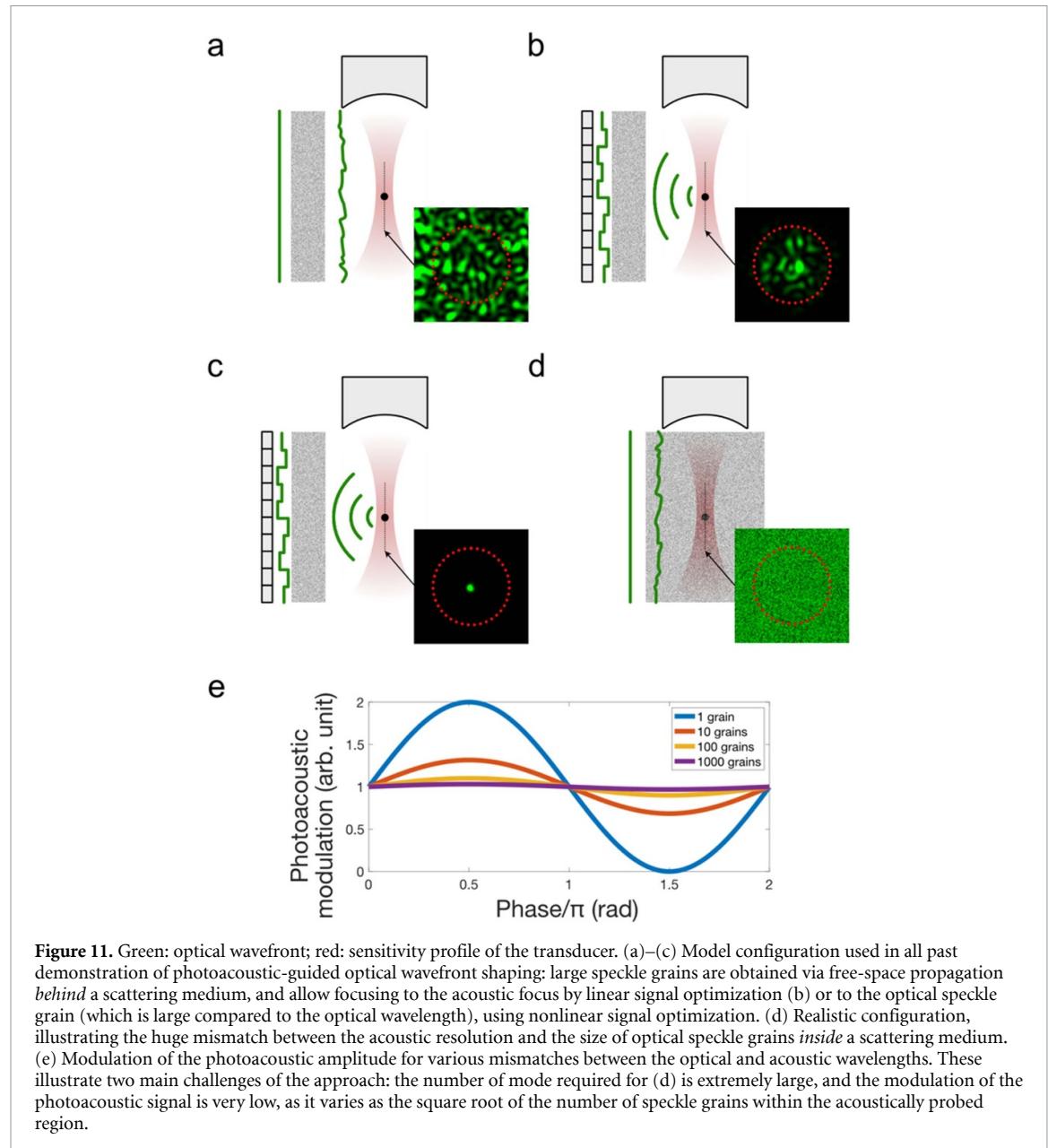
Figure 11. Green: optical wavefront; red: sensitivity profile of the transducer. (a)–(c) Model configuration used in all past demonstration of photoacoustic-guided optical wavefront shaping: large speckle grains are obtained via free-space propagation *behind* a scattering medium, and allow focusing to the acoustic focus by linear signal optimization (b) or to the optical speckle grain (which is large compared to the optical wavelength), using nonlinear signal optimization. (d) Realistic configuration, illustrating the huge mismatch between the acoustic resolution and the size of optical speckle grains *inside* a scattering medium. (e) Modulation of the photoacoustic amplitude for various mismatches between the optical and acoustic wavelengths. These illustrate two main challenges of the approach: the number of mode required for (d) is extremely large, and the modulation of the photoacoustic signal is very low, as it varies as the square root of the number of speckle grains within the acoustically probed region.

exploited for photoacoustic imaging in the context of minimally invasive photoacoustic endomicroscopy through multimode fibers [108].

All these applications require nanosecond laser sources with coherence lengths of several centimeters, with high repetition rates (>1 kHz), tunable wavelength, short pulse duration (∼1 ns), and reasonable power (∼1 W). Sources meeting these requirements in full are yet to be developed.

Concluding remarks

Several proof-of-concept experiments have showcased how photoacoustics and optical wavefront shaping can be exploited synergistically, either to assist optical wavefront shaping or to improve photoacoustic imaging. However, the relevance of the proposed approaches for practical applications remains to be demonstrated. Novel ultrasensitive ultrasound detectors can hopefully push this field a significant step forward in the near future.

Acknowledgment

9. Deep optical imaging based on a reflection matrix

Wonshik Choi
Institute for Basic Science, Department of Physics, Korea University, Republic of Korea

Status

Optical imaging is the action of probing a sample with a light wave and finding object information from the wave momentum change induced by a target object of interest. One of the most widely used imaging configurations in biology and medicine is a confocal detection scheme, which is to scan a focused beam and collect backscattered waves at a point conjugate to the illumination spot. This detection scheme, which is in fact equivalent to tracking the momentum change, works reasonably well up to a shallow depth where the returning wave forms a sharp focus. However, the increase in imaging depth gives rise to sample-induced aberrations distorting the point-spread-function (PSF) and multiple scattering noise. Distinguishing the distorted PSF from multiple scattering noise is an ill-posed problem in confocal imaging due to insufficient data acquisition.

Reflection matrix approach has come to the rescue [109–112]. Unlike confocal detection, it records electric field maps of backscattered waves arriving at non-confocal points as well as those at confocal points. In other words, both the obscured PSFs and multiple scattering noise are recorded in full (figure 12). Essentially, the reflection matrix constructed by a set of these electric field maps deterministically characterizes the input–output response of the sample to the best possible degree. A unique algorithm termed closed-loop accumulation of single scattering (CLASS) was developed to process the reflection matrix to separate the distorted PSF from multiple scattering noise without the need for guide stars. Furthermore, it enables us to find out the one-way wavefront aberrations from the round trip aberrations where input and output distortions are convolved [113]. With the addition of time-gated detection for rejecting a majority of multiple scattering noise, the depth limit to which the obscured PSFs can be corrected has been pushed close to ten times the scattering mean free path in tissue. The degree of wave distortion that the reflection matrix approach can deal with is much higher than the conventional adaptive optics (AO) approaches relying on limited resources. For instance, an ideal diffraction limit could be recovered by imaging underneath an intact mouse skull presenting an extreme form of aberrations [114]. All these exceptional capabilities come from the recording the full input–output response, which in turn slows down the image acquisition and processing. While this limits its applicability in the short term, proper addressing of these issues is likely to make the reflection matrix approach an essential tool for life sciences and medicine.
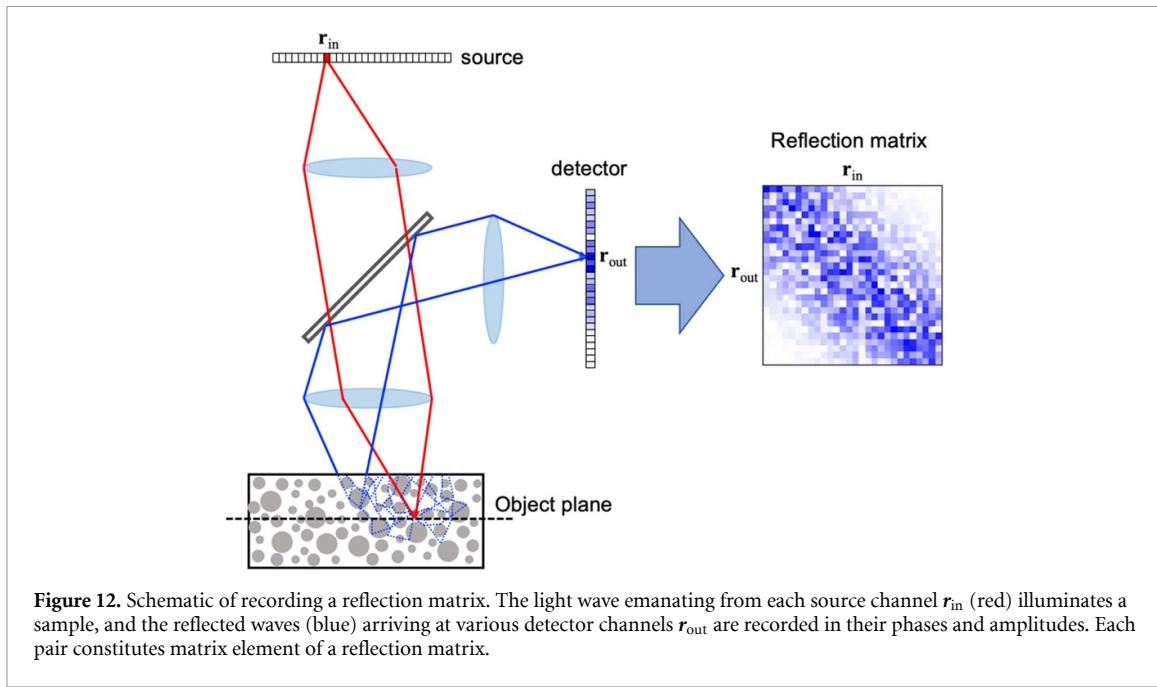
Current and future challenges

Data acquisition and image processing speed

Recording of a reflection matrix is intrinsically slower than confocal detection as it requires wide-field interferometric imaging for various illumination modes as opposed to single-point detection. It used to take a few minutes to record a single matrix in the early studies [110, 113], but ingenious experimental configurations employing scanning mirrors made it possible to reduce the matrix recording time well below 1 s [114, 115]. This allows *in vivo* imaging of nervous systems in small animals such as zebrafish and through-skull imaging of a living mouse. However, the covered field of view is still too narrow for comprehensive biological studies. Strategies for optimal downsampling will be necessary depending on the types of samples. New approaches to handling the matrix, such as forming a time-reversal matrix [116], can be adopted to allow sparse sampling without sacrificing too much of performance. Another challenge arises from the processing time for a recorded reflection matrix containing tens of millions of elements. Rapid advances in graphics processing unit technology in terms of processing speed and memory capacity along with the optimization of the algorithms will put real-time reconstruction and visualization forward.

Outreach to other imaging modalities

In the context of AO, a reflection matrix approach can be considered a software-based AO as it can computationally reconstruct aberration-free images from the recorded matrix itself. However, it can also serve as a wavefront sensing AO as the measured aberration map can be transferred to a wavefront shaping device to physically correct the wavefront distortion. In comparison with other wavefront sensing AOs, the key benefit is its capability to retrieve tissue aberration maps without resorting to guide stars. In fact, the image reconstruction algorithm enables us to use the target object itself, or any type of target including structures generating speckle-like reflections, as effective guide stars. By applying the aberration correction map to a spatial light modulator in the excitation beam path of multi-photon fluorescence microscopy, through-skull imaging of dendritic spines was realized with near-diffraction-limited resolution (figure 13) [114]. This strategy can be extended to other fluorescence imaging modalities such as single-molecule

Figure 12. Schematic of recording a reflection matrix. The light wave emanating from each source channel r_{in} (red) illuminates a sample, and the reflected waves (blue) arriving at various detector channels r_{out} are recorded in their phases and amplitudes. Each pair constitutes matrix element of a reflection matrix.

localization microscopy, coherent Raman microscopy, STED microscopy and so on to extend their working depths. To expedite this outreach, shortening the data acquisition and processing time will be crucial again. Outreach to lensless fiber endoscopes is another interesting possibility. Phase retardations due to fiber bending and twisting require the calibration of the fiber transmission matrix (TM), precluding the realization of flexible endoscopes. The fiber TM can be retrieved from the reflection matrix in the case of a fiber-bundle endoscope [117], which leads to a calibration-free flexible endoscopic microscope. Further investigation may extend this approach to endoscopes using a single multimode optical fiber.

Advances in science and technology to meet challenges
Can we increase the imaging depth further? The immediate approach is to follow a recent trend and employ light sources with wavelengths of 1.3 mm and 1.7 mm. Although there are additional difficulties in implementing matrix recording systems at these wavelengths in comparison with multi-photon imaging due to the requirement for wide-field interferometric imaging, they will surely be addressed in the short term.

Can there be more fundamental and yet practically useful advances? Achievable imaging depth will ultimately be determined by how much of multiple scattering is to be used for image reconstruction [112]. The currently used CLASS algorithm identifies ballistic waves in the reflection matrix that do not alter their propagation directions in the scattering medium surrounding a target object and finds their one-way phase retardations causing the distortion of shift-invariant PSFs. In this respect, it only exploits ballistic waves, not the multiply scattered waves. How can we extend this algorithm such that multiple scattering can be incorporated into the image reconstruction? One possible strategy is to extend its capability to deal with local aberrations. As shown in the through-skull imaging (figure 13), the reflection matrix can be processed to find wavefront distortion in each subregion whose size is as small as $10 \times 10 \ \mu m^2$. This means that multiple scattering is responsible for translationally variant PSFs at the length scale of $10 \ \mu m$ was identified and used for image reconstruction. The question remains how to extend this concept to extremely short-range local aberrations. Another potential strategy is to solve high-order inverse scattering problems based on various types of forward scattering models incorporating multiple scattering. The problem is severely underdetermined, and it will be challenging to selectively train multiply scattered waves that interact with the object of interest while excluding the majority of those from the bulk scattering medium. Novel computational tools including deep neural networks may help to expedite the progress.

Concluding remarks
Reflection matrix approach has made it possible to extract translationally invariant or slowly varying distorted PSFs in the epi-detection geometry in the presence of strong multiple scattering noise. A full characterization of the input–output response of a sample along with a unique algorithm provides a robust solution to this problem that used to be ill-posed in a confocal detection scheme. Technical advances in matrix recording and processing speeds have realized *in vivo* biological studies and expedited their dissemination to other powerful imaging modalities. Extracting short-range translationally variant PSFs
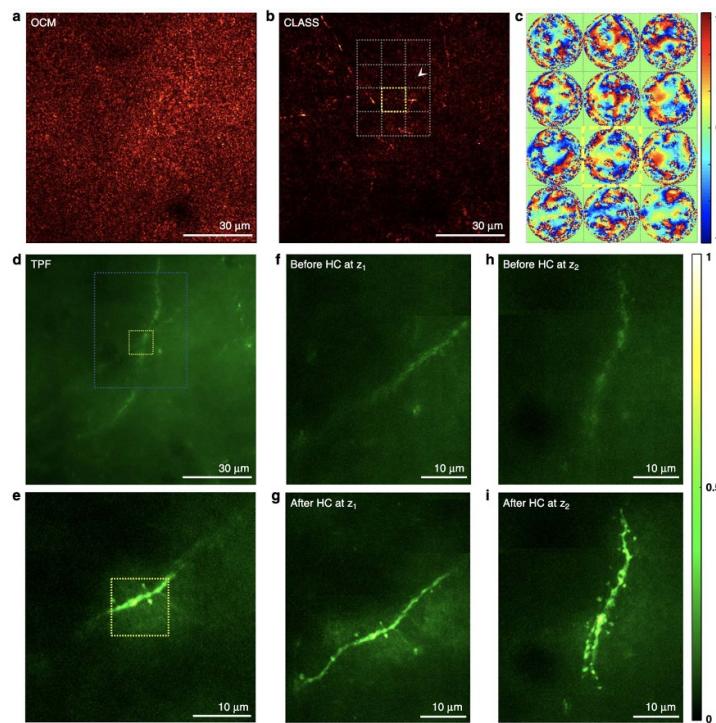
Figure 13. Exemplary application of reflection matrix microscopy for label-free imaging and two-photon fluorescence (TPF) imaging through intact skull. (a) Conventional OCM image under an intact mouse skull before aberration correction. The thickness of the skull was about 85 μm, and the focal plane was set to a depth of 125 μm from the upper surface of the skull. (b) Aberration-corrected image by the reflection matrix microscopy. About 15×15 subregions were individually processed to find local aberrations. (c) Aberration maps of subregions at 125 μm depth indicated by the gray dotted boxes in (b). The size of the subregion is 10×10 μm^2, and each phase map contains 9880 angular modes. Color bar, phase in radians. (d) TPF images at the same position as (a) before hardware aberration correction. (e) TPF image after physical aberration correction for the subregion indicated by the yellow box in (b). Yellow boxes in (d) and (e) correspond to the same yellow box area in (b). (f) and (g) TPF images at the depth of 113 ± 1.5 μm before and after aberration correction, respectively, for the area, indicated as a white dashed box in (d). (h) and (i) same as (f) and (g), respectively, for the depth of 122 ± 1.5 μm. Color bar, intensity normalized by the maximum intensity in (i). Scale bars indicate 30 μm in (a), (b) and (d), and 10 μm in (e)–(i). This figure was adopted from [114].

hidden in the recorded reflection matrix of a thick scattering sample will be essential to further extend the imaging depth. This task is likely to demand new physical insights and the active use of computational resources.

Aside from the technical advances, it will also be important to find killer applications of the reflection matrix approach for its long-term establishment. Label-free detection is one of its major strengths, but it can only be meaningful in medicine where administration of exogenous labeling agents is not available. This means that long-term extensive collaborations with medical doctors need to be formulated. Meanwhile, the expansion of its approach as a wavefront sensing AO for other fluorescence imaging modalities can find its use in the near term for immediate use in biological studies using tissue slices and animals.

Acknowledgments

10. Broadband reflection matrix: deterministic and learning-based approaches to deep imaging

Alexandre Aubry and Sebastien Popoff
Institut Langevin, ESPCI, PSL University, CNRS, Paris, France

Status

In wave imaging, one aims at characterizing an unknown environment by actively probing it and then recording the waves reflected by the medium. This is, for example, the principle of optical coherence tomography for light. However, wave propagation from the sensors to the focal plane is often degraded by the heterogeneities of the medium itself. They can induce wavefront distortions (aberrations) and multiple scattering events that can strongly degrade the image resolution and contrast (figure 14). However, the emergence of high-resolution sensor arrays and recent advances in data science pave a way toward the breaking of these fundamental limits for optical deep imaging.

To that aim, a matrix formalism is the perfect tool to capture the input–output correlations of the light scattered by the medium. Indeed, the Holy Grail for imaging is to have access to the transmission matrix **T** that connects any point inside the medium to a sensor array outside (figure 14(h)). The experimental access to the **T**-matrix has allowed experimentalists to take advantage of multiple scattering for optimal light focusing and communication across a diffusive layer or a multimode fiber [83]. However, the transmission configuration is not adapted to noninvasive and/or *in vivo* imaging of biological tissues. The reflection matrix **R** that links the incoming and outgoing waves recorded by the sensor array should then be considered. To retrieve **T** from **R**, both deterministic and learning-based approaches have been proposed.

Inspired by adaptive optics, deterministic approaches take advantage of the correlations exhibited by scattered light over coherence volumes called isoplanatic patches [112, 118]. Relying on the optical memory effect (see section 14 by Katz), such correlations can be exploited to compensate for low-order aberrations induced by forward scattering. Unfortunately, beyond one transport mean free path ($\ell_t \sim 1$ mm in biological tissues), waves lose the memory of their initial direction and start to follow a random walk that requires a precise knowledge of the microscopic properties of the medium to be harnessed. This is where a learning-based approach can be fruitful. Nevertheless, it requires a large training set and experimental results have so far only been obtained for thin diffusers [119].

Current and future challenges
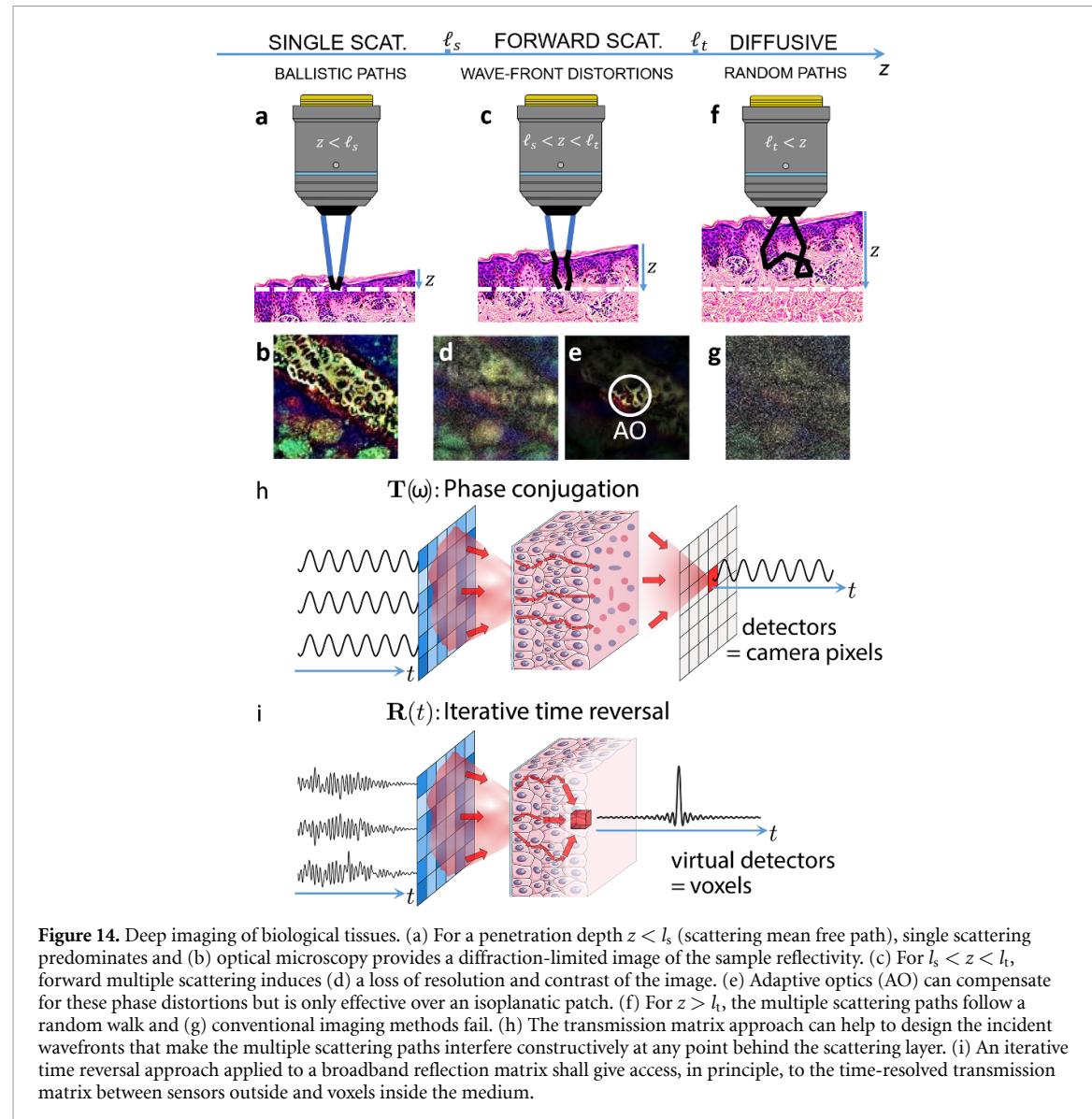
Physical insights, used in deterministic approaches, and measured data, used as training sets in learning-based approaches, both provide information about the propagation of light in inhomogeneous media. However, they are mostly exploited separately in current imaging techniques, and both approaches have their limits.

Until now, matrix imaging has relied on singly scattered and forward multiply-scattered photons, the number of which decays exponentially with the penetration depth. These photons exhibit a deterministic time of flight and are currently discriminated from the diffuse background by: (a) a time gating process; (b) a spatial compensation of their phase distortions. Nevertheless, in the future, one will have to play with both spatial and temporal degrees of freedom in order to harness multiply scattered waves. The measurement of a broadband **R**-matrix and a spatio-frequency analysis of its correlations should be coupled to learning based methods in order to retrieve a time-dependent **T**-matrix that will allow using the medium heterogeneities as a scattering lens and extend the penetration depth of matrix imaging beyond the transport mean free path (figure 14(i)). Such an approach can be rewarding since scattering can increase the effective numerical aperture of the imaging system and lead to super-resolution [120].

With regard to learning-based approaches, models such as deep learning (DL) ones were developed initially for problems where the underlying model is not known, e.g. we do not know a mathematical formula that allows identifying a cat from a dog in a picture. This lack of information is replaced by a large number of parameters that have to be trained using large data sets. As the complexity of the task increases, so does the risk of not converging to a solution that generalizes well for unknown configurations (overfitting). This likely explains why DL approaches have so far not been successful in predicting the transmission properties of an inhomogeneous medium in the multiple scattering regime. Finding a way to efficiently combine physical insights and learning approaches may be the key to retrieve transmission information from the **R**-matrix in multiple scattering media.

Advances in science and technology to meet challenges

To address the multiple scattering limit in optics, the challenges to be met are both experimental and computational.

Figure 14. Deep imaging of biological tissues. (a) For a penetration depth $z < l_s$ (scattering mean free path), single scattering predominates and (b) optical microscopy provides a diffraction-limited image of the sample reflectivity. (c) For $l_s < z < l_t$, forward multiple scattering induces (d) a loss of resolution and contrast of the image. (e) Adaptive optics (AO) can compensate for these phase distortions but is only effective over an isoplanatic patch. (f) For $z > l_t$, the multiple scattering paths follow a random walk and (g) conventional imaging methods fail. (h) The transmission matrix approach can help to design the incident wavefronts that make the multiple scattering paths interfere constructively at any point behind the scattering layer. (i) An iterative time reversal approach applied to a broadband reflection matrix shall give access, in principle, to the time-resolved transmission matrix between sensors outside and voxels inside the medium.

From an experimental point of view, the challenge is to record the **R**-matrix over a broad bandwidth in an acquisition time ideally smaller than the decorrelation time of the medium. This can be a drastic barrier for living tissues which exhibit a decorrelation time ranging from 50 ms to 2.5 s depending on the level of immobilization [121]. Two strategies can be followed to circumvent that key issue: (a) reduce the number of input illuminations and use physical insights to retrieve the complete information thanks to compressed sensing or model-based approaches; (b) develop a dynamic matrix approach of optical imaging by considering e.g. the generalized Wigner–Smith operator [122] in order to discriminate scattering paths as a function of their decorrelation time and address them independently. Interestingly, dynamic scattering can give access to a large number of speckle realizations for each voxel which can be used, in return, to extract the **T**-matrix without relying on isoplanicity.

From a computational point of view, the training of numerical models designed to incorporate physical insights shows promising results, e.g. demonstrating the compensation of aberrations in optical measurements [123] or predicting the transmission properties of thin diffusers [124]. Exploiting these insights has two interesting consequences: (a) by drastically restricting the space of solutions, it limits overfitting and reduces the amount of information required for the training process; (b) accessing the model parameters after training could allow predicting various properties of the physical system.

Using DL frameworks one can create physics-inspired models for light propagation inside inhomogeneous media. The propagation equation, its invariants and/or its statistical properties can be incorporated into numerical models. For instance, for biological tissues, where the scattering is anisotropic, light propagation is well modeled by a series of diffraction events by thin diffusers with free space propagation in between [125] (figure 15). One can then envision models that mimic these effects using layers
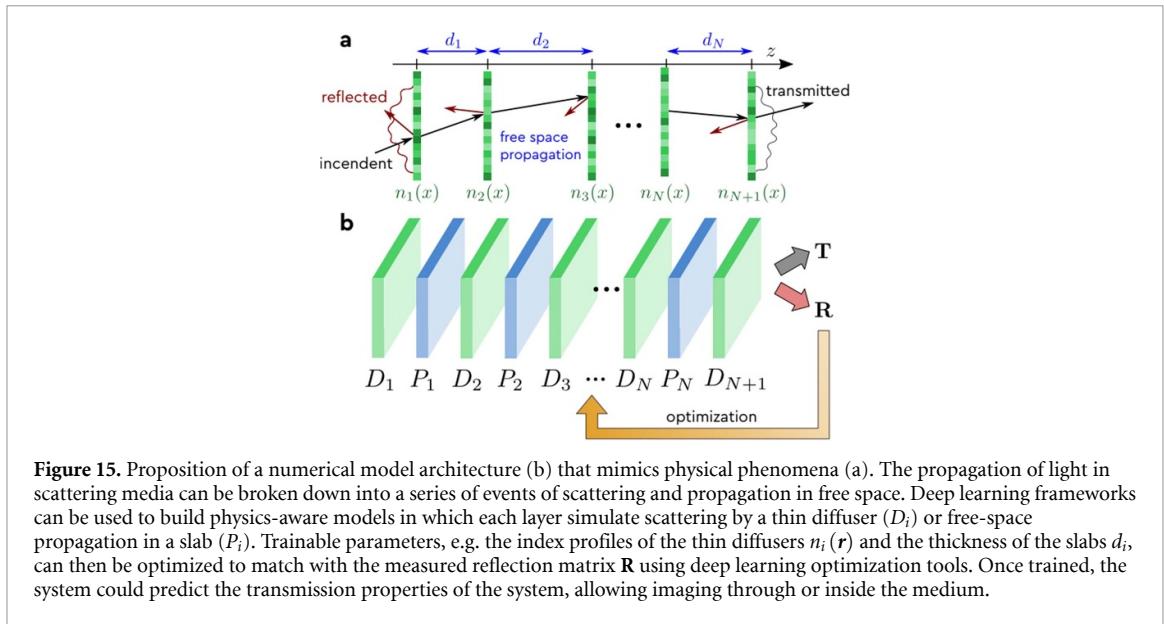
Figure 15. Proposition of a numerical model architecture (b) that mimics physical phenomena (a). The propagation of light in scattering media can be broken down into a series of events of scattering and propagation in free space. Deep learning frameworks can be used to build physics-aware models in which each layer simulate scattering by a thin diffuser (D_i) or free-space propagation in a slab (P_i). Trainable parameters, e.g. the index profiles of the thin diffusers $n_i(\mathbf{r})$ and the thickness of the slabs d_i, can then be optimized to match with the measured reflection matrix **R** using deep learning optimization tools. Once trained, the system could predict the transmission properties of the system, allowing imaging through or inside the medium.

with trainable parameters. Once trained on a measured **R**-matrix, it can be used to predict the associated **T**-matrix.

Concluding remarks

Predicting transmission properties from non-invasive and label-free reflection measurements is a subject of paramount importance with a wide range of applications. In biomedical imaging, the effort was originally oriented toward ballistic and forward-scattered photons, which limits the penetration depth to one transport mean free path. To reach greater depths, it is necessary to harness multiply-scattered photons, whose trajectories cannot be *a priori* predicted. To that aim, a spatio-temporal control of light is required. On the experimental side, the acquisition of a broadband **R**-matrix can provide a post-processing solution to this challenging problem. On the computational side, the correlation properties of this matrix can feed a physical model whose numerous parameters can be adjusted through learning-based methods. The combination of deterministic and data-driven approaches constitutes a promising route toward the realization of an old dream researchers in optics have been chasing for ages: seeing in or through the fog.

Acknowledgments

11. Use of the linear scattering matrix for nonlinear coherent optical imaging at large depths in biological tissues

Sophie Brasselet and Matthias Hofer
Aix Marseille University, CNRS, Centrale Marseille, Institut Fresnel, F-13013 Marseille, France
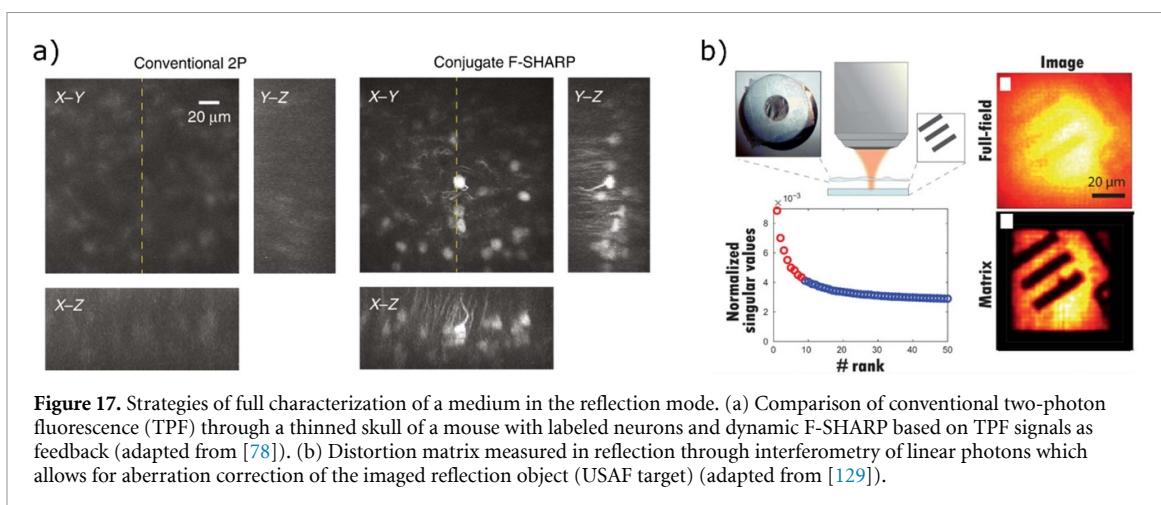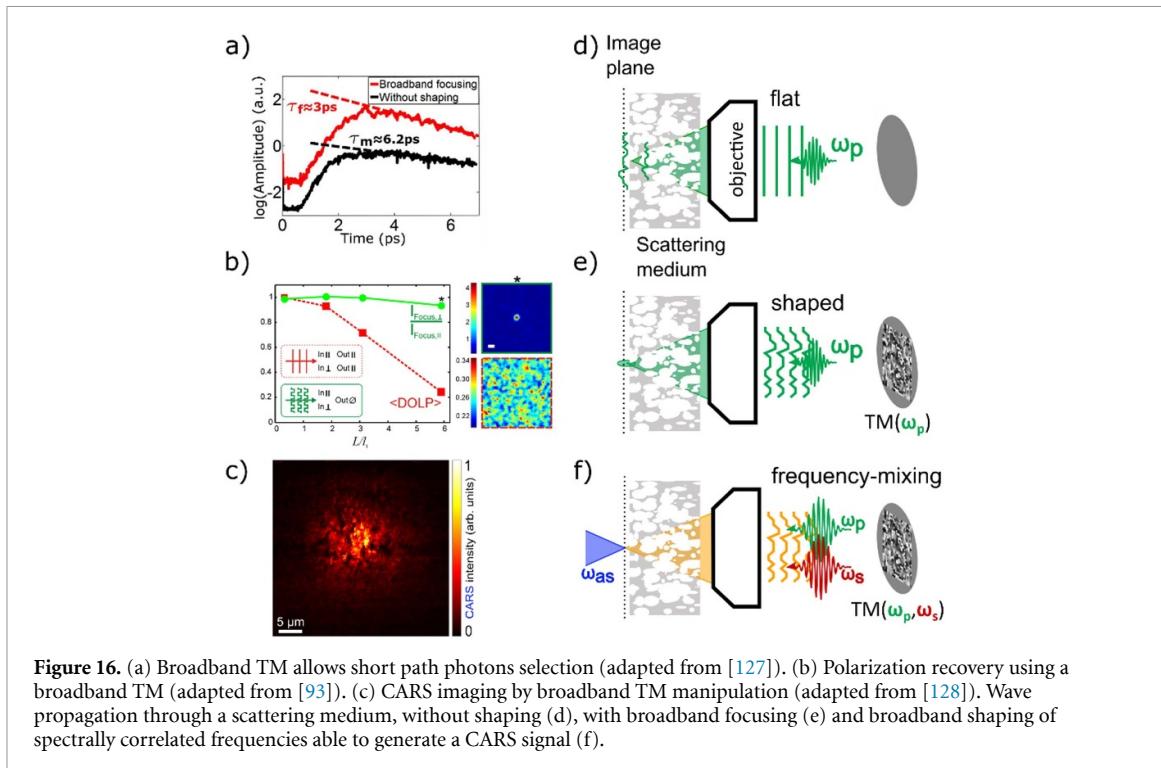
Status

Scanning nonlinear microscopy is a widely used approach in biological imaging, with the advantage of benefiting from label-free optical contrasts that are specific to intrinsic tissue properties. Nonlinear optical imaging has first exploited two-photon excitation contrasts, through either incoherent (two-photon fluorescence) or coherent (second-harmonic generation, SHG) processes, then reached higher-order contrasts thanks to progress made by pulsed laser sources. Today, three-photon fluorescence, third-harmonic generation and four-wave mixing (FWM) processes based on the coherent mixing of three wavelengths are current imaging tools applied to neuroimaging as well as in research on pathologies such as in cancer or immunology. The requirements of nonlinear imaging are, however, stringent, since it necessitates the spatio-temporal coherent superposition of focused near-infrared laser pulses, possibly at different frequencies, that are scanned over the sample volume with sub-micrometric resolution. This quality is rapidly lost when imaging at depths larger than a few hundred micrometers in biological tissues, e.g. a few scattering mean free paths. Preserving a high focus quality in space and time is at the center of strategies based on optimization and adaptive optics, which rely on the natural selection of coherent constructive optical paths by nonlinear feedback such as two/three-photon fluorescence signals or SHG. In parallel, the development of strategies to refocus incident beams based on the manipulation of the scattering matrix either in transmission (see section 6) or reflection (see sections 8 and 9) has seen very fast technological and conceptual progress. Learning the medium's scattering matrix by experimentally measuring the relation between incoming and outgoing fields is particularly interesting to master wavefront reversal processes in a deterministic way, but also to investigate how field degradations of input focused beams relate to the spatial, temporal and polarization correlation properties of the medium. Accessing such information is also crucial to determine and decipher strategies to correct not only for smooth aberrations but also for more complex propagation perturbations due to scattering. This section describes recent strategies based on linear photon manipulation to generate nonlinear signals through and inside biological tissues, as well as the challenges still to be overcome. Here we describe the context of pure optical control; methods using other contrasts such as ultrasound can be found in other sections.

Current and future challenges

The coherent manipulation of linear photons opens interesting routes for the excitation of nonlinear mechanisms; however, the necessity to preserve short pulses (femtosecond to picosecond range) synchronized in space and time for scanning nonlinear imaging brings additional challenges compared to linear optics. The randomization of optical propagation in a scattering medium breaks the coherence propagation of pulses and distorts the pulse profiles into spatio-temporal speckles, also randomizing their spectral phase. Linear feedback control is nevertheless intrinsically limited by the correlation lengths of the medium along all dimensions (space, time/spectrum but also polarization). Elaborating on this property, a complete spatio-temporal control of a focus was recently demonstrated in the Gigan lab by the measurement and manipulation of a multi-spectral transmission matrix (TM) of a medium made of a stack of monochromatic, initially uncorrelated TMs, in a scheme that is also transposable in the time domain via time-gated TMs [126]. Focusing all components in the same output spatial position with accurate spectral phase/time control, enabled deterministic control of the output pulse time profile. More recently, it was found that by measuring this matrix with a broadband pulse, a transform-limited refocus naturally forms [127] (figure 16). The self-reference interferometry used to measure the matrix creates an intrinsic coherent selection of low propagation path photons in the medium, which has been shown to lead to strong nonlinear SHG signals after refocusing through a thick scattering biological medium as well as a natural polarization recovery [93]. Using a similar configuration in frequency mixing processes could open the way to the not yet much explored FWM manipulation in scattering media, for which a particularly interesting contrast is coherent anti-Stokes Raman scattering (CARS). This process necessitates two distant wavelengths from short pulses to be overlapped coherently, whose frequency difference fits with the chemical vibration of the medium. Thanks to the manipulation of spectrally correlated TMs for which two ~150 fs pulses were manipulated at about 100 nm wavelength distances, the recovery of a CARS signal was made possible through a thick scattering medium [128]. In this application, knowledge of the spectral correlation properties as well as spectral–spatial coupling in the medium is crucial [125]. Yet, while these demonstrations make it clear that manipulating the linear incident photons leads to impressive recoveries of

Figure 16. (a) Broadband TM allows short path photons selection (adapted from [127]). (b) Polarization recovery using a broadband TM (adapted from [93]). (c) CARS imaging by broadband TM manipulation (adapted from [128]). Wave propagation through a scattering medium, without shaping (d), with broadband focusing (e) and broadband shaping of spectrally correlated frequencies able to generate a CARS signal (f).


Figure 17. Strategies of full characterization of a medium in the reflection mode. (a) Comparison of conventional two-photon fluorescence (TPF) through a thinned skull of a mouse with labeled neurons and dynamic F-SHARP based on TPF signals as feedback (adapted from [78]). (b) Distortion matrix measured in reflection through interferometry of linear photons which allows for aberration correction of the imaged reflection object (USAF target) (adapted from [129]).

nonlinear polarized optical signals at large depths in transmission, it needs to be transposed to a reflection geometry to be pertinent for microscopy imaging *in vivo*.

Advances in science and technology to meet challenges

Strategies to transpose the control of complex waves in reflection, in the linear optical regime, hold great promise for nonlinear coherent optical imaging. The first set of strategies is based on an *in situ* characterization of the scattered optical wavefront inside the medium by linear interferometry in the presence of nonlinear signal generation inside the medium. Monitoring of *in situ* wavefronts has been achieved by focus scanning holographic aberration probing followed by wavefront conjugation [78]. More recently, dynamic adaptive scattering compensation holography has exploited similar principles with iterative wavefront front implementations [79]. These approaches have allowed two-photon fluorescence imaging with high resolution over extended fields of view at a few hundred micrometers depth inside a mouse brain. A second set of strategies consists in measuring the reflection matrix measurement and refocusing light by phase front reversal. Constructing a distortion matrix to connect scanning focuses with reflected wavefronts, its singular value decomposition has allowed us to correct for high-order aberrations and forward multiple scattering over isoplanatic patches at a depth of ten scattering mean free paths in the turbid cornea [129] (figure 17). Using a related approach, laser scanning reflection-matrix microscopy has

allowed correcting for the matrix aberration components and generating reflectance and two-photon images of axons underneath an intact mouse skull [114]. Finally, an emerging strategy aims at modeling the medium and computationally correcting for propagation distortions to retrieve an image [124]. Capitalizing on the possibility to intrinsically monitor optical propagation properties in a complex sample, most of these strategies are able to correct for both smooth aberrations and scattering distortions and overcome the limiting memory range of the medium.

Concluding remarks
Challenges remain to accommodate the complexity of explored media and adapt nonlinear imaging to requirements in nanoscience, biology and biomedical optics. Interestingly, novel emerging schemes that exploit reflection-wavefront correction are being developed fast and in parallel with novel nonlinear imaging tools that are compatible, such as spectral focusing or light sheet microscopy. Among the directions followed in the field of linear photon manipulation, large progresses on both technological and computational tools will most probably allow future steps toward dynamic, high-resolution and large-field-of-view tissue imaging in depth.

Acknowledgments

12. Deep learning for imaging through complex media

Lei Tian[1,2]
[1] Electrical and Computer Engineering, Boston University, United States of America
[2] Department of Biomedical Engineering, Boston University, United States of America

Status

Deep learning (DL) has shown tremendous success in solving ill-posed computational imaging problems. Interested readers can refer to a comprehensive review on this topic in [130]. Within these computational imaging applications, one of the prevalent problems is imaging through complex media, which is our focus in this section.
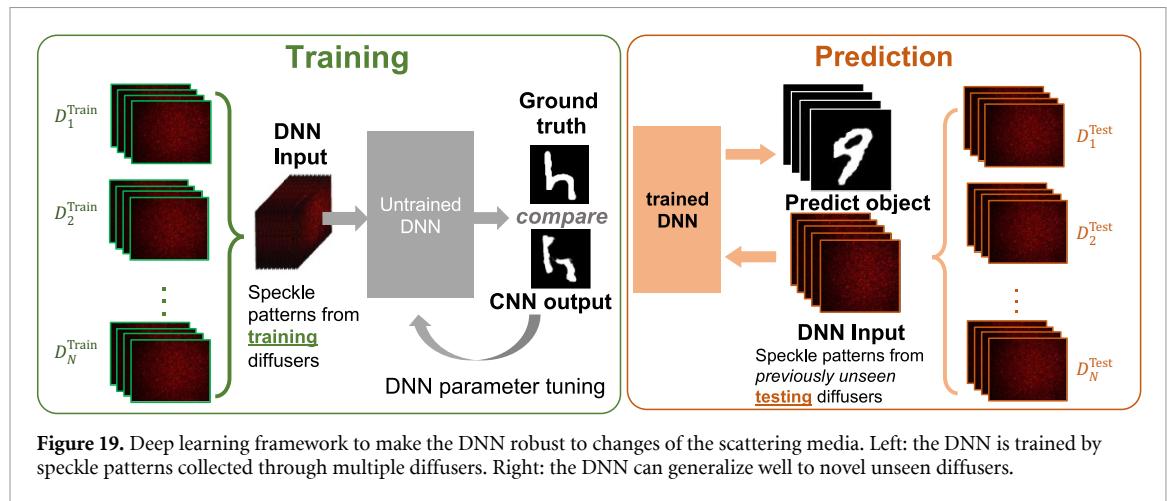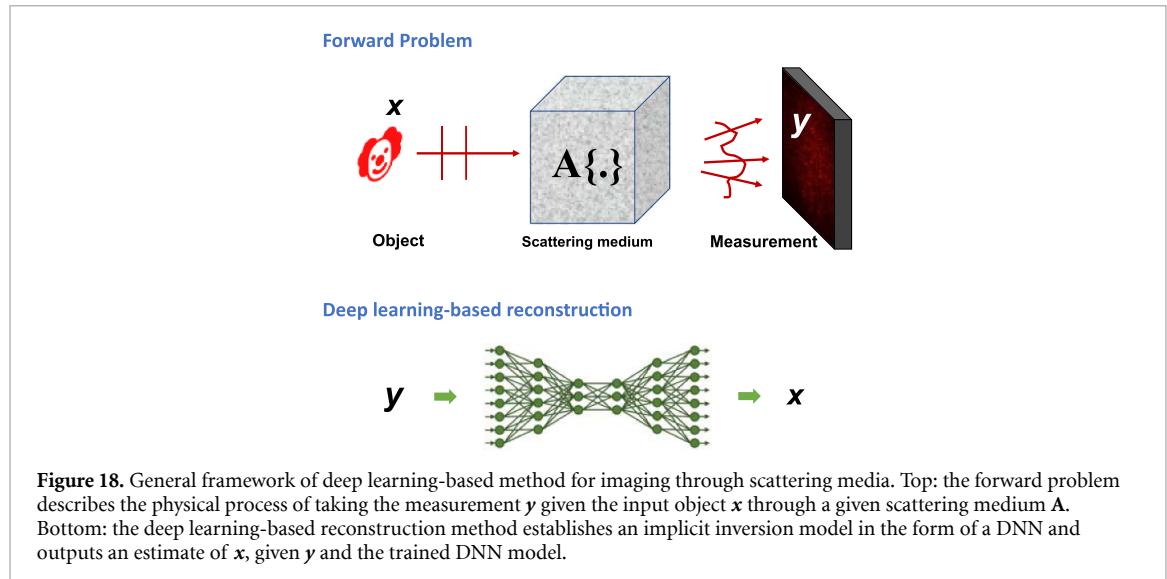
Recovering the object information from scattering measurements can be treated using a computational imaging framework, which consists of a forward problem and an inverse problem. The forward problem describes the formation process of measurement *y* given the input object *x* (figure 18 top). The inverse problem seeks a solution of *x* given the measurement *y*. To solve this inverse problem, significant progress has been made using physical model-based techniques, such as those based on the memory effect and transmission matrix theory, which are detailed in other sections of this article. Due to the underlying assumptions in these models, the recovery is often limited by the field of view (FoV), the system's calibration requirement and stability. Instead of relying on a physical model, DL instead takes a data-driven approach to solve the inverse problem, in which an implicit inversion model, in the form of a deep neural network (DNN), is learned from a large training dataset (figure 18 bottom). The main insight from recent works is that by intelligently engineering different training conditions, a DNN-based model can increase the FoV, relax the calibration requirement, and improve the system's stability. In the following, we highlight a few notable advances.

The first successful demonstration of using DL to overcome the FoV limitation imposed by the memory effect (discussed in section 13) is shown in [131]. The DNN is trained to recover the object directly from a speckle pattern. By training the DNN using a diverse image dataset captured on a fixed diffuser, it can generalize over different objects and achieves diffraction-limited resolution across an FoV well beyond the isoplanatic region of the system. However, this network is susceptible to changes in the scattering medium. To overcome this limitation, a different training strategy is proposed in [132]. By incorporating variations induced by changes in the scattering media itself during training, the DNN is able to learn 'hidden' correlation information from multiple realizations of a random medium. Specifically, the authors show that, by training a DNN on multiple diffusers with the same macroscopic property, it can make high-quality predictions through different unseen diffusers (figure 19). Recently, the unsupervised dimension reduction technique has been used to provide additional insights into this learning process [133]. A similar strategy has been successfully applied to imaging through nonstatic thick turbid media [134].

Current and future challenges

Despite recent advances, multiple challenges remain to be solved to make the DL techniques applicable in broader imaging scenarios, as outlined below:

(a) **Need for a large-scale and diverse paired training dataset.** The supervised learning framework used in the existing techniques dictates that paired input and output images are required to train the DNN. In general, both the scale and the diversity of the dataset required for training a generalizable DL model can be challenging in many practical applications, such as biomedical microscopy. We can further dissect this issue into several scenarios.
  1. **Volumetric imaging.** In all the existing work reviewed here, the training input images are generated by a spatial light modulator. This imposes several assumptions about the object, including (a) it must be 2D planar, (b) no other object sources are present before or after the 2D plane of interest. It is challenging to directly apply the existing training strategies and DNN architectures to volumetric 3D imaging applications.
  2. **Imaging objects inside a scattering medium.** Another limitation comes from the requirement for direct access to both the input and output planes during the training process. This becomes challenging when the objects are buried inside a continuously distributed scattering medium.
  3. **Imaging in reflection geometry.** A related challenge is when imaging objects inside a scattering medium, while measurements can only be made outside the medium.
(b) **Generalization to different scattering conditions.** Although advances have been made to make the DL model generalizable to scattering media with the macroscopic property, i.e. the same scattering condition, the model is still susceptible to changes to the scattering conditions, such as changes in the

Figure 18. General framework of deep learning-based method for imaging through scattering media. Top: the forward problem describes the physical process of taking the measurement *y* given the input object *x* through a given scattering medium **A**. Bottom: the deep learning-based reconstruction method establishes an implicit inversion model in the form of a DNN and outputs an estimate of *x*, given *y* and the trained DNN model.

Figure 19. Deep learning framework to make the DNN robust to changes of the scattering media. Left: the DNN is trained by speckle patterns collected through multiple diffusers. Right: the DNN can generalize well to novel unseen diffusers.

scattering density and scattering mean free path. Innovations in both training strategies and DNN architectures are needed to make the DL model robust over a wide range of scattering conditions.

Advances in science and technology to meet challenges

Here we outline several promising directions to pursue to overcome the above challenges and further push the fundamental limits of imaging in complex media using DL.

(a) **Physics-informed learning.** The large training dataset requirement of supervised learning techniques stems from its pure data-driven framework without using any knowledge of the physics. However, many physical insights and models are available and can be utilized to describe the scattering measurements. As a result, it is conceivable that physics-informed learning approaches, which synergistically combine physical models and DL, can overcome many of the existing challenges. For example, Metzler *et al* showed that a DNN robust to low signal-to-noise ratio in non-line-of-sight imaging can be trained by taking the autocorrelation of the speckle pattern as the input [135]. This data preprocessing step directly draws physical insights from classical correlography theory.

(b) **Multiple-scattering simulator-based training.** To alleviate the need to physically acquire experimental training data, another possibility is to use a physics simulator to generate the training data. To simulate a large-scale scattering measurement dataset, the simulator needs to be both accurate and computationally efficient. An additional benefit of this simulator-based training is that it is not limited to any specific imaging geometry. For example, Matlock *et al* showed that a DNN that is generalizable to experimental measurements on 3D samples can be trained using a multiple-scattering simulator based on an accurate and efficient split-step non-paraxial beam propagation model [136].

(c) **Exploiting correlations between transmission and reflection measurements.** To address the challenges associated with reflection imaging, another promising direction is to exploit the speckle correlations between the transmission and reflection measurements. For example, Skarsoulisa *et al* recently showed that a DNN can be trained to predict the speckle patterns through a scattering medium purely based on the pattern measured in the reflection [119].

(d) **Adaptive learning framework.** To build a DL model that is robust over a wide range of scattering conditions, adaptive DNN architecture is a promising direction to investigate. For example, Tahir *et al* recently proposed a new dynamic synthesis network architecture that can dynamically adjust the DNN's model weights and adapt to different scattering conditions [137].

Concluding remarks

Recent advances in DL have shown the potential to push the fundamental limit for imaging in complex media. By combining new physical insights in scattering physics with a novel learning framework, we expect novel imaging and sensing techniques will continue to emerge and make their way to practical applications in many impactful areas, such as biomedical microscopy, metrology, and material science.

Acknowledgment

13. Model-based wavefront shaping

Ivo M Vellekoop
Department of Science and Technology, University of Twente, Enschede, The Netherlands

Status

Most approaches to imaging through scattering rely on the optical memory effect in one way or another. One approach is to use wavefront shaping (WFS) with feedback from a guidestar or a detector to form a focus (e.g. [138], cf section 5), and then use the memory effect to raster-scan this focus for microscopy [45, 139, 140]. Sometimes, we can even use the memory effect by itself for computational imaging (see section 13). Unfortunately, the optical memory effect only has a significant range for objects placed far behind a thin scattering layer [141], or inside forward scattering materials, such as biological tissue [67].

Without the optical memory effect, the possibilities for deep imaging are limited; if we can only focus onto the guidestar itself, we will get a 'single-pixel image.' An interesting solution is to use ultrasound tagging to define a 'movable' guide star (section 5). This solution does, however, have the drawback of severely decreasing the resolution and contrast of the focus.

Model-based (MB) WFS represents a completely different method that neither requires guidestars nor the optical memory effect. The idea is simple: if we have an accurate refractive index (RI) model of the scattering structure, we can *compute* how to form a focus at any arbitrary point inside the sample.

Of course, one typically does not have an exact model of the structure. In many cases, however, *a priori* knowledge about the sample can be combined with additional measurements to construct the model. A rudimentary demonstration of this concept was given in [142], where the structure was a flat piece of glass with known thickness and RI. From this model the wavefront corrections for aberration-free focusing at any depth can easily be computed. A more advanced example is the construction of a model of a multimode fiber [143]. By fitting a 12-parameter model to calibration measurements, the fiber can be digitally modeled to compute wavefronts for focusing at arbitrary points through it.

The use of MB-WFS to see through highly scattering structures was first demonstrated in [124]; see figure 20. Here, a rough scattering surface was imaged from the outside, and these images were converted to a three-dimensional RI model. MB-WFS resulted in high-quality wavefront corrections even at depths where guidestar-based techniques fail due to the low signal-to-noise ratio of the feedback signal.

Current and future challenges
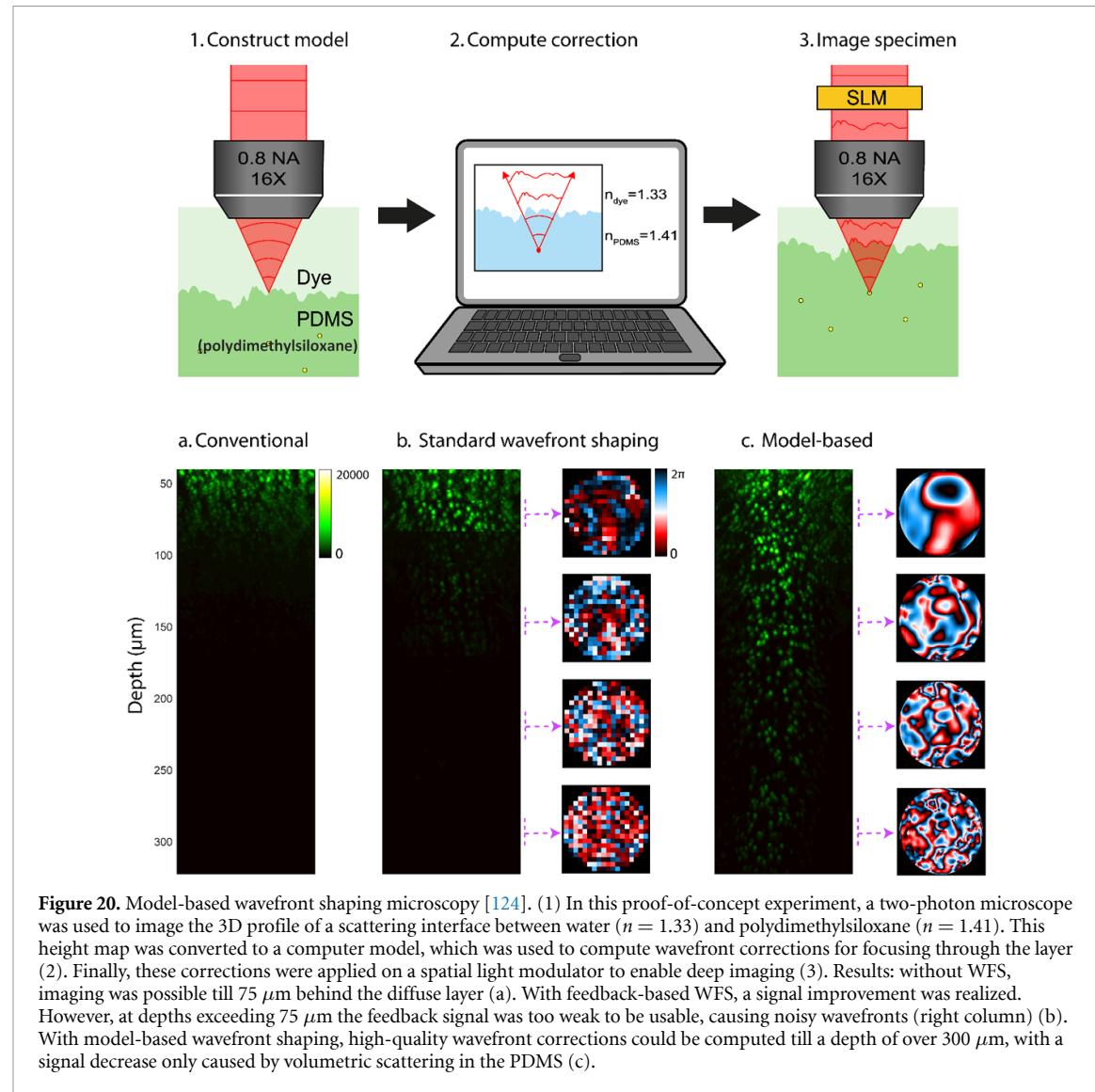
These promising new approaches introduce a class of challenges that are new to the field of wavefront shaping:

(a) **RI model reconstruction.** First of all, it is essential to have a sufficiently accurate model of the RI. A challenge here is that most tomographic techniques are developed in the weak scattering regime where the Rytov approximation, first-order Born approximation, or geometrical optics are applicable. When scattering becomes more dominant, unfortunately, these methods no longer produce correct results, so alternatives are needed. The alternative of directly mapping the surface (figure 20) does work for micrometer-scale irregularities. However, the challenge here is to extend the concept to multi-layer or truly volumetric samples.

(b) **Fast light propagation simulations.** A practical challenge is to make these computations fast enough for real-time imaging. In particular, when the memory effect is very small or absent, a new wavefront needs to be computed for every point in the image. These computations currently take seconds to minutes, making them the bottleneck for MB imaging.

(c) **Coordinate mapping.** An experimental challenge is to achieve a true 1:1 mapping of the 'virtual' coordinates used in the computer model, and 'physical' coordinate spaces spanned by SLM pixels, camera pixels, galvo scan angles, etc.

Advances in science and technology to meet challenges

Rapid progress is being made to meet these challenges. Some of the highlights are:

(a) **RI reconstruction algorithms and iterative measurements.** The need for RI reconstruction inside scattering materials calls for the development of reconstruction algorithms that are robust against multiple scattering. Promising developments in this direction are the development of optical coherence refraction tomography [60], neural-network-based methods [144] and reconstruction algorithms specifically designed for strong scattering [145].

Figure 20. Model-based wavefront shaping microscopy [124]. (1) In this proof-of-concept experiment, a two-photon microscope was used to image the 3D profile of a scattering interface between water ($n = 1.33$) and polydimethylsiloxane ($n = 1.41$). This height map was converted to a computer model, which was used to compute wavefront corrections for focusing through the layer (2). Finally, these corrections were applied on a spatial light modulator to enable deep imaging (3). Results: without WFS, imaging was possible till 75 μm behind the diffuse layer (a). With feedback-based WFS, a signal improvement was realized. However, at depths exceeding 75 μm the feedback signal was too weak to be usable, causing noisy wavefronts (right column) (b). With model-based wavefront shaping, high-quality wavefront corrections could be computed till a depth of over 300 μm, with a signal decrease only caused by volumetric scattering in the PDMS (c).

(b) **Light propagation algorithms and parallel computation.** Recently developed solvers can solve Maxwell's equations in 3D media of $\sim 10^4$ cubic wavelengths in a matter of seconds on a single graphics processing unit [146]. Still, when the scattering structure is millimeter-sized (10^{10} cubic wavelengths), faster, less accurate, algorithms are more appropriate, such as angular spectrum methods [124, 144, 145] or ray tracing [60].

(c) **Automated alignment and calibration.** These coordinate mapping challenges are very similar to the challenges encountered in digital optical phase conjugation. An interesting development in this field is the development of fully automated calibration protocols that are even capable of digitally correcting alignment imperfections [147].

Concluding remarks

After feedback-based wavefront shaping and phase conjugation, MB-WFS provides a third route to focusing light inside scattering materials. This new approach does not rely on guidestars or on the optical memory effect. Rather, it uses a variety of algorithms for RI mapping, light propagation computations, and automated alignment, combined with *a priori* knowledge about the structure. Interestingly, this new route shifts the problem of deep imaging from optics to a multidisciplinary research field incorporating inverse problem methods, numerical mathematics, cloud computing, and artificial intelligence.

Acknowledgments

14. Memory-effect-based imaging in complex media

Ori Katz
Department of Applied Physics, Hebrew University of Jerusalem, Jerusalem, Israel

Status

Scattering-induced distortions in complex media are one of the major hurdles for imaging in many applications in optics, from astronomical observations through the turbulent atmosphere, through imaging in foggy conditions, to deep-tissue imaging. Interestingly, this challenge is encountered in several domains beyond optics, from acoustic imaging to geophysics. While wavefront shaping allows one to undo scattering and focus to a diffraction-limited bright spot even through multiply scattering samples, *imaging* requires the ability to undo scattering from (or to) *multiple* points in the desired field of view (FoV). In general, one has thus to find and apply a large number of different wavefront corrections that correspond to all points in the FoV, making *imaging* in complex media a much more difficult challenge than single-point *focusing*.

However, what may alleviate the problem in many instances is if a single wavefront correction can be effective over more than a single point in the FoV. Such 'shift invariance' of the wavefront correction is termed 'isoplanatism' in the fields of adaptive optics and acoustics, and it is in essence the shift (or more precisely tilt) invariance of the scattering point-spread function, or Green function. Surprisingly enough, even thick, multiply scattering diffusive samples can scatter light in an isoplanatic fashion [2], meaning that waves that illuminate the medium at slightly different angles, scatter to nearly identical speckle patterns that propagate at corresponding relative angles (figure 21(a)). This effect, termed the angular optical 'memory effect,' was first discovered and characterized in the 1980s [2]. Strikingly, the memory effect exists even at depths well beyond the transport mean free path, l_t, where the propagation direction has been totally scrambled by multiple scattering.
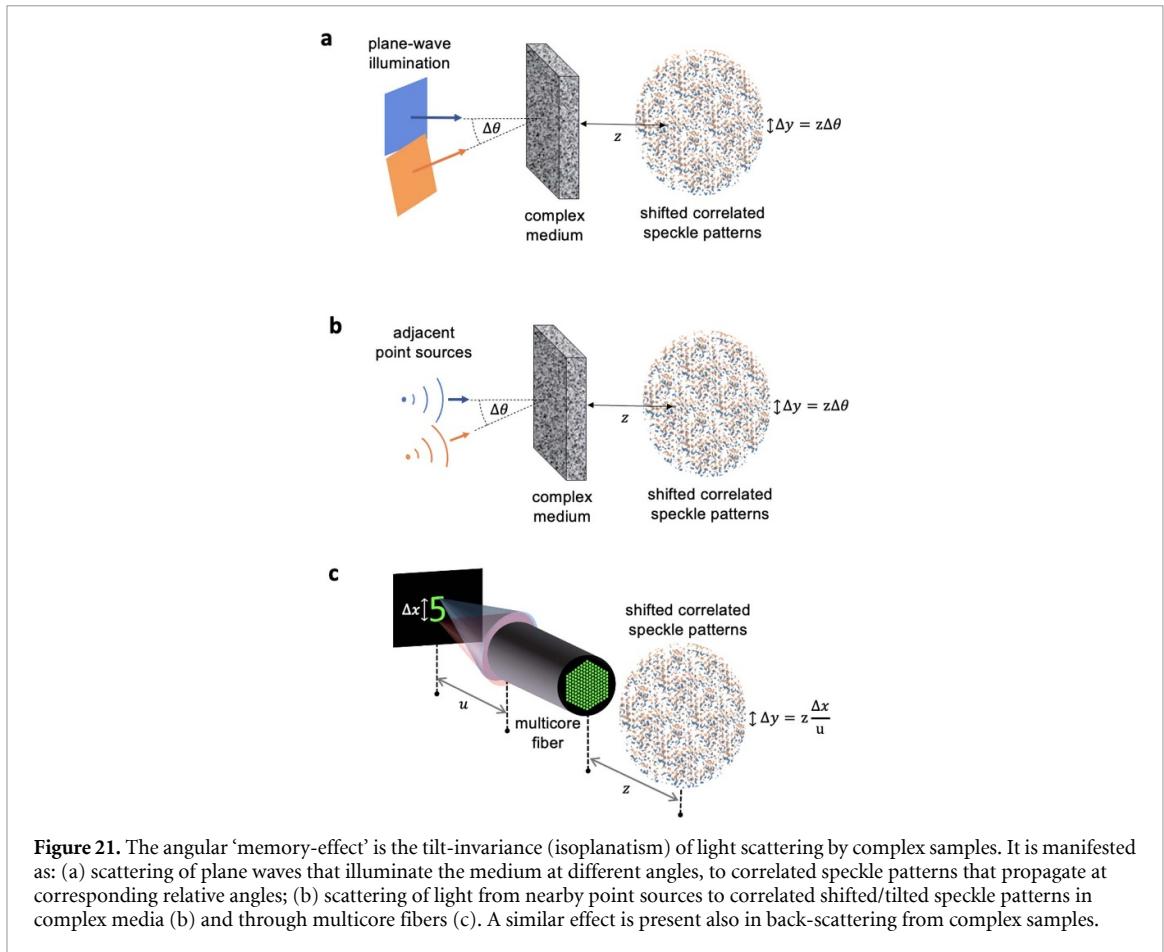
A direct implication of the 'memory-effect' isoplanatism is that a single wavefront correction can be used to scan a wavefront-shaped focus within the memory-effect angular range (also termed the 'isoplanatic patch') to produce an image [139] (figure 22(a)). Thanks to Helmholtz reciprocity, a widefield single-shot variant of this approach can be performed (figure 22(b)); since light from adjacent point sources is scattered to highly correlated speckle patterns [2], they can all be corrected *simultaneously* by the same static wavefront correction [148] (figure 22(b)). These approaches to imaging are based on the physical wavefront correction of a single point. The wavefront correction can be directly found by invasive access to the target plane [139], e.g. by implanting a point source 'guidestar' [148]. However, advanced approaches currently allow noninvasive wavefront correction, e.g. by optimizing a nonlinear signal [149], or an image contrast metric [150] (figure 22(b); see section 7). Interestingly, the angular memory effect is present also in reflection from complex samples such as white painted walls, and in light propagation through multi-core fibers (figure 21(c)), opening the path to looking 'around corners' [2, 148], and to lensless diffraction-limited endoscopy [151] (see section 18).

As was first suggested by Freund three decades ago [2], 'memory-effect' correlations allow imaging even without a physical wavefront correction. The first realization in multiply scattering media was demonstrated by scanning unknown (but correlated) speckle patterns over a fluorescence target (figure 21(a)), and computationally reconstructing the image from the spatial autocorrelations of the measured patterns using phase retrieval [152]. Shortly after, it was shown that the same autocorrelation information can be retrieved from a single-shot image of the scattered light [153, 154] (figure 22(c)), bringing the principles of Labeyrie's 'stellar speckle interferometry from astronomy to complex media [153].

Current and future challenges

The major limitations of using the memory effect for imaging are its small FoV and limited imaging depth, as well as its limited spectral bandwidth. While the angular memory effect is a universal property of multiple-scattering samples, its angular range is inversely proportional to the sample thickness, L. In the diffusive regime, i.e. at $L \gg l_t$, the memory effect angular range is $\Delta\theta_{FoV} \approx \frac{\lambda}{\pi L}$. The imaging FoV, which is the product of $\Delta\theta_{FoV}$ and the imaging depth, is thus unfortunately of the order of a wavelength—too small for most applications. Nonetheless, the FoV can be larger when imaging targets that are located at a standoff distance from a thin scattering layer (e.g. in an 'eggshell' geometry), or when imaging 'around corners', where the angular memory-effect range in reflection is $\Delta\theta_{FoV} \approx \frac{\lambda}{\pi l_t}$. The imaging FoV can also be somewhat larger than a wavelength when imaging through biological tissues at depths smaller than l_t [67]. In addition, the large anisotropy of the scattering in soft tissues gives rise to speckle correlations also for transverse translations of the incident wavefront at such depths [67], which may also be exploited for imaging.

The isoplanatic patch size limitation can be overcome by mosaicking multiple isoplanatic patches into a single large-FoV image. This can be done by separating the different isoplanatic patches by decomposition of

Figure 21. The angular 'memory-effect' is the tilt-invariance (isoplanatism) of light scattering by complex samples. It is manifested as: (a) scattering of plane waves that illuminate the medium at different angles, to correlated speckle patterns that propagate at corresponding relative angles; (b) scattering of light from nearby point sources to correlated shifted/tilted speckle patterns in complex media (b) and through multicore fibers (c). A similar effect is present also in back-scattering from complex samples.

the medium's reflection matrix (see sections 9 and 10), or of the matrix containing scattered fluorescence patterns (see section 7). Another approach to enlarge the FoV is to physically limit the sample probing using a probe that is smaller than the isoplanatic patch. This was recently realized via localized acousto-optic tagging followed by a ptychographic reconstruction [155].

The advanced computational reconstructions of the matrix-based approaches or ptychographic techniques do not only allow wider FoV imaging but also address the convergence instability of the iterative phase-retrieval algorithms used in the first memory-effect works [151–153]. Another possibility to overcome the need for phase retrieval is through the calculation of the scattered light bispectrum [156], as first developed for astronomical observations.

Another fundamental challenge is in three-dimensional imaging, which is addressed to some extent by time-gating in either reflection-matrix measurements, which may also increase the angular correlation range [66].

Finally, a major challenge is in performing a large number of required measurements in an acquisition time that is shorter than the sample decorrelation time. One potentially interesting way around this is to exploit the sample dynamics to retrieve additional information from multiple speckle realizations [155], rather than to try to overcome it.

Advances in science and technology to meet challenges

The depth, FoV, and speed limitations of memory-effect-based imaging require significant advances in both technology and scientific approaches. A straightforward step to extend the FoV and imaging depth is to utilize longer infrared wavelengths for imaging, possibly using high-resolution InGaAs cameras for detection. Another step forward would be in boosting the acquisition speed by using high-speed cameras, fast spatial light modulators, and parallelized acquisition schemes, potentially exploiting spectral information.

The combination of memory-effect-based imaging with acoustic tagging carries interesting potential for combining the benefits of both modalities: the high resolution of light and the large penetration depth of ultrasound. However, the current implementations (e.g. [155]) are too slow for most applications, and still rely on a memory-effect range that is larger than the acoustic focal spot.
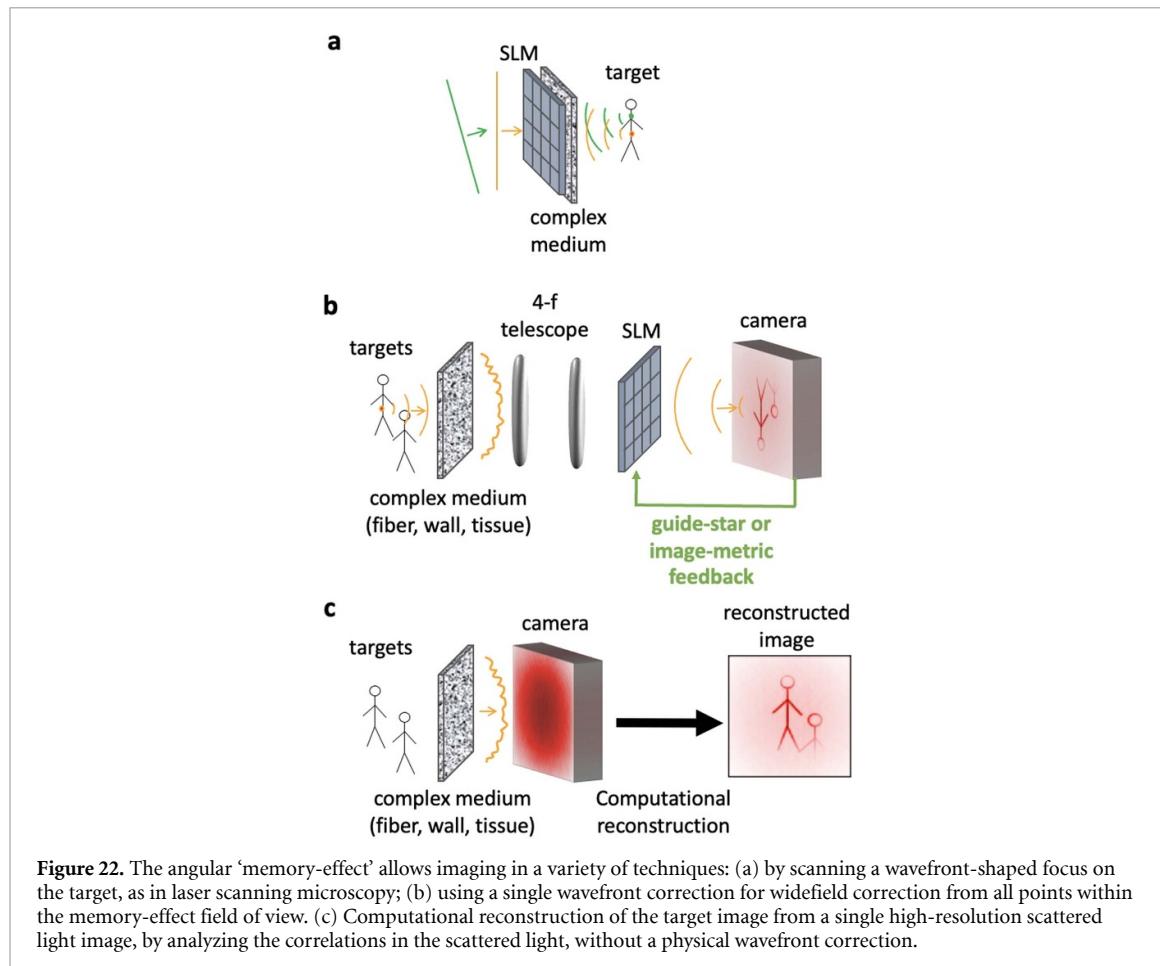
Figure 22. The angular 'memory-effect' allows imaging in a variety of techniques: (a) by scanning a wavefront-shaped focus on the target, as in laser scanning microscopy; (b) using a single wavefront correction for widefield correction from all points within the memory-effect field of view. (c) Computational reconstruction of the target image from a single high-resolution scattered light image, by analyzing the correlations in the scattered light, without a physical wavefront correction.

Deep-learning-based approaches carry huge potential as they can in principle address all current challenges (namely the number of measurements, parallelization, reconstruction stability, FoV, and sample dynamics). Deep learning has been recently shown to generalize correlation-based reconstruction beyond angular or translational correlations, and to include model-based physical insights (see section 12). As in most deep-learning works, the limited interpretability ('black-box'-iness), and the limited generalizability may present drawbacks, but their full promising potential is yet to be realized.

Finally, a fundamental limitation of deep imaging is the limited photon budget: the deeper one tries to image, the more speckle grains (modes) each photon is scattered to. This necessitates higher-resolution wavefront shaping, highly sensitive detectors, and more noise-robust computational approaches.

Concluding remarks

The fact that multiply scattered diffuse light has inherent correlations is at first glance surprising, and indeed gives rise to some counterintuitive results, such as the ability to look around corners. However, intuition for the existence of angular correlations emerges from the fact that illuminating a point on a sample facet results in a bright halo only around the illumination point. The angular correlations are simply the manifestation of this effect in the Fourier domain [2]. Thus, one should not be surprised that some imaging information is contained in scattered light. How to distill this information in the fastest and most efficient manner such that it can be used most effectively in real-life applications is yet to be found. Combining spatial and temporal gating, matrix-based decomposition, generalized correlations and deep-learning reconstruction represent a potentially interesting path toward this goal.

Acknowledgments

15. Information from correlations

Jacopo Bertolotti
School of Physics and Astronomy, University of Exeter, Exeter EX4 4QL, United Kingdom

Status

Multiple scattering of light in biological tissues, clouds, etc is so complex and dependent on so many tiny details that it is tempting to pretend that the whole process is random and only deal with the relative simplicity of the diffusion approximation. The price one pays for that simplicity is big, as true randomness means that information is forever lost, and therefore there is only so much we can do if we want to image an object through a scattering layer. Despite its complexity, multiple scattering is still a perfectly deterministic process, and for the typical powers involved in imaging, it is also often a completely linear one. As a result, all the information contained in the signal before it was scattered must still be present after it has been scattered. In this sense, multiple scattering effectively performs a rotation in a very high-dimensional space [2]. If we knew this rotation (the scattering matrix) we could invert it [157], but otherwise the information is now spread out and only visible in the form of correlations between the intensity at different points.

As shown if figure 23, speckle correlations come in many forms, each carrying a bit of the desired information. The most commonly used speckle correlation in imaging is the optical memory effect, i.e. the fact that, by tilting the incident beam, the transmitted speckle will tilt by the same angle, as long as the angle is not too large (isoplanatism) [158]. This correlation is a useful tool to image through a scattering layer, because it gives you information about what is happening on the hidden side of the layer using only information measured on the accessible one, thus allowing noninvasive imaging [152] (see section 13).

The success of methods based on the memory effect suggests that, among the many possible correlations that we can find in speckle patterns, the easiest to exploit are those that contain mutual information between the region where the hidden object is and the region we can freely measure.

Current and future challenges

The main limitations to the use of correlations for imaging are that they are often weak, as most correlations decrease with the 'dimensionless conductance' g, which is very large for most scattering media [159]. Furthermore, most correlations are probabilistic in nature, requiring some form of averaging over disorder to extract an image. In this respect the optical memory effect is an outlier, being a perfect ($C = 1$) and deterministic correlation, as long as the angles involved are small enough.

Another complication is that there are many ways in which mutual information between one part of the scattered field and another can manifest. Two-point correlations in a single speckle pattern have an elegant classification in terms of how the correlation decreases with the distance between the two points, but other forms of correlation, e.g. three-point correlations (bispectrum) [160], are difficult to classify using that framework. This is, of course, both a challenge and an opportunity, as it is possible to find useful mutual information in many places. For instance, linear scattering preserves spatial coherence, so one can estimate the extension of a source hidden in a turbid medium by looking at the signal spatial coherence [87] (see section 6).

The presence of as yet undiscovered or unexploited speckle correlations is also why machine learning-based techniques can work on systems they were never trained on. Although we are not aware of them, a properly trained neural network can find and exploit correlations that are not sample-specific, thus enabling it to recover the desired image even when the scattering system is different from the one(s) used for the training [132] (see section 11). The challenge here is that, while the success of machine learning tells us that the correlations are there, there is no obvious way to find out which correlations are being exploited and thus use them for other imaging techniques.

Advances in science and technology to meet challenges

Starting with the work of Feng *et al* in 1988 [141], where the first speckle correlations were described and classified, there has been a lot of interest in the properties of speckles, and in recent years a number of new correlations have been characterized, from the 'tilt–tilt' memory effect [161] through the 'chromato-axial' memory effect [125] to the 'transmission-reflection' correlations [162], and others. All these new correlations allow us to push the boundaries of what can be done for imaging through scattering media, but there has been no coordinated effort to make the search for new correlations more systematic yet.

Measuring speckle correlations often entails measuring small signals over large backgrounds, and/or having to average over a large ensemble, which requires fast detectors with large dynamic ranges. At the same time, fast measurements almost invariably mean less light per time bin, which exacerbates the dynamic range
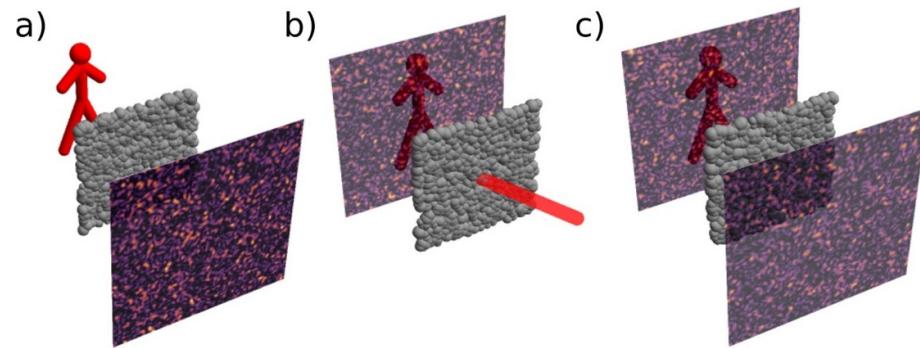
Figure 23. Different kinds of correlations give us different kinds of information. (a) When the light coming from an object is scrambled by a scattering layer, the resulting speckle will depend on the properties of the object, e.g. its spatial coherence. (b) If we can control the input light, the pattern illuminating the object will depend on the properties of the scattering medium, e.g. the optical memory effect range will depend mostly on the layer thickness. (c) The scattered light that goes back in our direction is correlated with the scattered light illuminating the hidden object, so we can use that to retrieve an image.

problem, as the signal one wants to measure can be on the limits of sensitivity. This conundrum has no easy solution, and improvements will require performance increases on all fronts for cameras.

The number of modes over which the information is spread out is geometry-dependent, but in most cases it grows approximately quadratically with the thickness-to-wavelength ratio, which means that correlations tend to become weaker, and thus harder to measure and exploit, for thick scattering media. Currently, this is one of the main roadblocks to the real-world application of any correlation-based imaging technique (see section 13). Using longer wavelengths ameliorates the problem, as does using media that are mostly forward scattering [163], but this is the most important problem to solve in the near to medium future. A possible way forward is to use several correlations at the same time, and combine the small amount of information that can be gathered by each to obtain a more complete picture.

Concluding remarks

Linear multiple scattering does not change the information content of a wavefront but scrambles it. In principle this scrambling can be reversed, but this requires a complete characterization of the system. Whenever this is not possible, we need to extract as much information as possible from the apparently random speckle patterns. This is possible because speckle patterns are not really random, and the information we seek is now encoded in their correlations. The large variety of correlations present is both a challenge and an opportunity, and with only a handful of correlations that have been studied and understood, this field is still in its infancy.

Acknowledgment

16. Computational imaging with randomness

Ryoichi Horisaki
The University of Tokyo, Japan

Status

Recent advances in information science, such as compressive sensing and machine learning, have contributed to various fields, imaging being a typical example. In particular, computational imaging, which is a powerful framework for developing innovative photography and display systems by combining optical and computational processes, is an attractive field in which to apply state-of-the-art tools in information science to optics [164]. Simplification of optical hardware, enhancement of imaging performance, nonconventional imaging modalities and applications have been studied in the field of computational imaging. Established examples of computational imaging include computed tomography, digital holography, and computer-generated holography. The advances in information science mentioned above and the rapidly growing power of computer hardware, such as graphics processing units, are driving forces in the field of computational imaging.

Optical modulation with randomness has been used in computational imaging, as shown in figure 24. Random processes have some interesting features such as broad frequency spectra and low cross-correlation. There are two examples that exploit these features: (a) Pinhole cameras are the simplest optical modality in lensless imaging. To enhance the spatial resolution based on geometrical optics, the pinhole must be small, but this decreases the light efficiency, and vice versa. Thus, pinhole cameras have a serious tradeoff between spatial resolution and light efficiency. Coded aperture imaging employs random pinhole arrays and a computational deconvolution process to overcome this tradeoff in lensless imaging [165]. (b) Optical information is multidimensional and includes, for example, three-dimensional spatial position, wavelength, time, etc, but image sensors are two-dimensional. To compensate for this dimensional gap between the object and the sensor, the resolution along a certain dimension, such as space or time, is generally compromised in conventional multidimensional imaging. Compressive sensing is an innovative sampling framework for capturing object information with fewer measurements compared with the sampling theorem, thus overcoming the above compromise [166]. It is based on dimensionality reduction with random projection and computational reconstruction with a sparsity constraint. Single-shot multidimensional imaging, such as single-shot depth imaging and single-shot spectral imaging, has been realized by using random processes implemented with scattering media [167].

Current and future challenges

The transmission matrix (TM) represents the linear input/output relationship through scattering processes, and it has been used for imaging and focusing through scattering media. One advantage of the transmission-matrix-based approach is the ability to achieve single-shot imaging and focusing through scattering media after a calibration process for observing the TM [168]. However, this approach requires costly and careful calibration processes, such as an interferometrical optical setup with no stray light. To address this issue, we present a machine learning approach for estimating the input/output relationship through a scattering process. This approach is applicable for observing not only linear relationships but also nonlinear ones, and it alleviates the requirements for the calibration process. Imaging and focusing based on this machine learning approach have been demonstrated with a simple non-interferometric setup [169, 170]. One challenge with this learning-based method is the tradeoff between the generalization capability and imaging performance.

Speckle-correlation imaging is also an approach for imaging through scattering media [152]. An advantage of speckle-correlation imaging over other methods, including the approach based on the TM, is its noninvasiveness. In speckle-correlation imaging, by assuming shift invariance of the scattering process, it is not necessary to access the region inside or behind the scattering media for the calibration mentioned above. The shift invariance is called the memory effect, and it enables us to approximately identify the autocorrelation of the object and that of the captured speckle image. The lateral memory effect has realized two-dimensional speckle-correlation imaging. We have extended two-dimensional speckle-correlation imaging to three-dimensional cases and have demonstrated single-shot depth imaging through scattering media with an axial memory effect, where the speckle is laterally scaled when the object is axially shifted [171]. The object is reconstructed from a single speckle image with a three-dimensional correlation process and a three-dimensional phase retrieval process. Similarly, we have also presented single-shot spectral imaging through scattering media with a spectral memory effect [172]. These methods have realized calibration-free multidimensional imaging. However, the memory effect is a serious limitation of these methods and restricts the applications of speckle-correlation imaging.
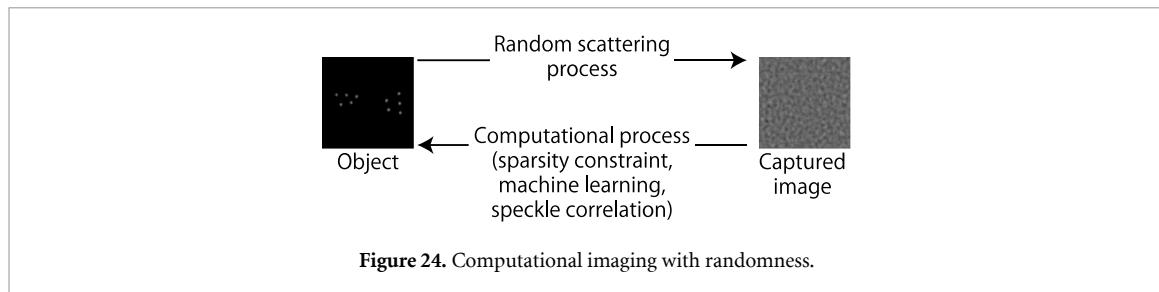
Figure 24. Computational imaging with randomness.

Advances in science and technology to meet challenges

To address the issues in imaging through scattering media mentioned above, state-of-the-art technologies in information science, such as deep learning and unsupervised learning, can be important. Cross-disciplinary approaches might also contribute to overcoming these issues. Computational imaging is one such approach in which optics and information science are combined. Further crossovers, including biomedicine and chemistry, are necessary to make the current approaches for imaging through scattering media more practical and more general.

Concluding remarks

We present the current situation, future issues, and possibilities in computational imaging with randomness. Computational imaging has contributed to imaging through scattering media, and various promising methods have been reported, such as compressive sensing, transmission-matrix-based imaging, and speckle-correlation imaging. However, crucial issues still remain. Further interdisciplinary approaches, not only optics and computer science, may contribute to this field.

17. Sculpted illumination for deep tissue imaging and interrogation

Vincent R Curtis[1], Laura Waller[2] and Nicolas C Pégard[1,3,4]
[1] Department of Applied Physical Sciences, UNC Chapel Hill, United States of America
[2] Department of Electrical Engineering and Computer Sciences, UC Berkeley, United States of America
[3] Department of Biomedical Engineering, UNC Chapel Hill, United States of America
[4] UNC Neuroscience Centre, UNC Chapel Hill, United States of America

Status

Scattering and aberrations in dense biological tissue are a major barrier to imaging beyond superficial depths. To observe deeper layers, a popular strategy is to illuminate samples with engineered light to capture optically encoded information that static illumination cannot. Scanning techniques such as multiphoton and confocal microscopy concentrate light to isolate signal from noise and scattered photons, but they introduce tradeoffs between imaging speed, spatial resolution, and light exposure. More efficient imaging strategies, such as compressed Hadamard imaging [173] and Fourier ptychographic microscopy [145], leverage custom illumination and computation to enhance diversity in the recorded data, followed by the reconstruction of deep images.

The success of many of these imaging strategies currently depends on advanced light sculpting techniques such as computer-generated holography (CGH), where algorithms control spatial light modulators (SLMs), either to rectify aberrations [25] (figure 25(a)) or to focus light deep into tissue [79]. These wavefront engineering methods are routinely used in ground telescopes to undo atmospheric distortions, but they are inadequate for deep tissue imaging because dense aggregations of living cells disturb the free propagation of light with far more degrees of freedom (DoF) than there are pixels in the SLM. Hence, new illumination techniques that can sculpt light with many more degrees of control to synthesize incoherent distributions [174] or light fields [175] are critically needed for next-generation deep tissue imaging.

Another critical aspect to the performance of deep imaging techniques is managing the joint operation of image acquisition and illumination hardware operating simultaneously in closed-loop systems [79, 173, 176]. Since the number of possible sampling modalities is too large to be explored exhaustively, the integration of advanced optical hardware in future deep imaging methods must be met with equally advanced computational methods and smart sampling strategies to collect as much optically encoded information as possible within the available observation time window.

Current and future challenges

Perhaps the most important current challenge in the development of high-performance optical instrumentation is the need to innovate with commercially available equipment. SLMs and digital micromirror devices are only commonly available today because they are mass-produced for video projection. Likewise, the video game industry drives the development of graphics processing units, which are at the heart of scientific computation. As a result, while many research groups have conceptualized innovative technologies to push the limits of deep imaging beyond the state-of-the-art, experimental implementations are routinely biased toward readily available mass-produced hardware. While gaps between accessible technology and experimental needs can sometimes be filled with additional computational resources, the additional data processing steps that are required eventually affect imaging performance.

Significant work remains to be done to improve light sculpting technology and compensate for dense scattering in tissue. Existing light sculpting techniques operating with SLMs can only modulate the phase or the amplitude of a single coherent wavefront. For each square millimeter of tissue surface (figure 25(a)) they enable, at best, a few million pixels of control. Conversely, deep tissue imaging at depths as short as 200 micrometers requires the compensation of hundreds of millions of aberrating features per square millimeter. Dense layers of cells disturb the free propagation of light, both spatially and in the angular domain, and repeatedly. The 3D accumulated effects yield complex, incoherent distributions of light (figure 25(b)) that cannot be approximated accurately by a single engineered 2D coherent wave. As a result of this dimensional discrepancy, even the most advanced adaptive wavefront shaping techniques do not have enough degrees of control to address scattering in deep tissue.

Progress in both light sculpting and camera technologies dramatically increases both the amount and the rate of optically encoded data that can be exchanged between a computer and biological samples. New algorithms must be developed to control both ends of the acquisition process and obtain the most informative final image within a biologically defined time window. These algorithms must be capable of managing user input, controlling hardware, and analyzing data simultaneously. By collecting information about the sample in real time the most efficient frameworks will be able to identify the most informative sampling strategy with instantaneous and partial information.
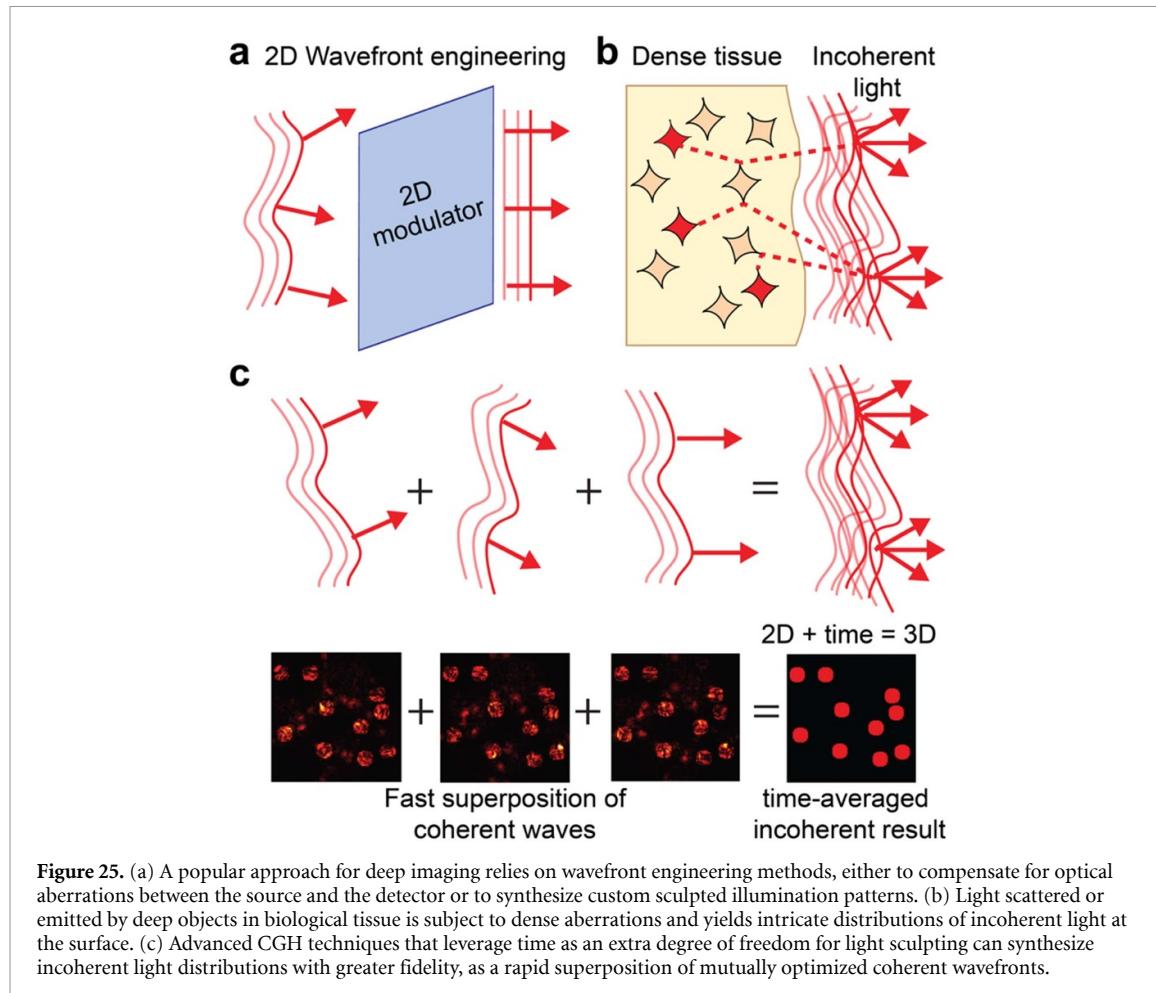
Figure 25. (a) A popular approach for deep imaging relies on wavefront engineering methods, either to compensate for optical aberrations between the source and the detector or to synthesize custom sculpted illumination patterns. (b) Light scattered or emitted by deep objects in biological tissue is subject to dense aberrations and yields intricate distributions of incoherent light at the surface. (c) Advanced CGH techniques that leverage time as an extra degree of freedom for light sculpting can synthesize incoherent light distributions with greater fidelity, as a rapid superposition of mutually optimized coherent wavefronts.

Advances in science and technology to meet challenges

We expect that ongoing and rapid progress in custom, low-volume optoelectronic device manufacturing will open the door to innovative task-driven hardware designs. Custom light modulators tailored for laser beam fast focusing applications have already demonstrated superior capabilities compared to systems designed with commercial, rectangular pixel array modulators [177].

The development of light sculpting technology for deep tissue focusing will require pushing the capabilities of existing hardware and algorithms to obtain the additional DoF needed to engineer light through billions of aberrating features. Perhaps a promising path is to explore the untapped potential of high-speed modulators and leverage time to sculpt light with many more degrees of control than static modulators. Promising results have already been obtained with dynamic computer-generated holography [174] to achieve realistic 3D image renderings in the human eye, by approximating incoherent distributions as a superposition of mutually optimized coherent waves (figure 25(c)). This methodology has the potential to achieve the necessary gap in performance to focus light precisely through dense biological tissue.

The combination of high-throughput sensing and light sculpting technologies enables innovative closed-loop imaging modalities for which new algorithms must be developed. The magnitude of data exchange required to view a sample is too large to be stored, making offline processing suboptimal. Real-time data-driven frameworks that can continuously collect, process, and use information gathered from a changing environment to inform and improve the sampling strategy are preferred. For instance, online optical aberration correction algorithms [178] gradually improve image quality and facilitate the long-term monitoring of living tissue. Deep learning (DL) models are particularly amenable to handling this type of two-way data stream at high speeds. Their reconfigurable structure can be adjusted on demand with learning algorithms as new data become available during operation. DL models have already dramatically accelerated CGH [179] and are now routinely used in image acquisition and processing. By leveraging DL methods to simultaneously take control of illumination and acquisition hardware [176], self-adjusting imaging systems eliminate sources of human bias and pave the way for more stable and reproducible imaging experiments.

Concluding remarks

The joint development of high-performance sculpted illumination and smart algorithms for online data analysis is critical to enable progress in deep tissue imaging technology. Although this strategy may bring deep imaging capabilities closer to the theoretical limits of accessible depth in biological tissue, many technological and scientific challenges remain to be addressed. Open research avenues include high-performance optoelectronic hardware, optical instrumentation design, and new algorithms for fast, sample-driven acquisition and processing of optically encoded information. In this interdisciplinary area, collaborative projects that explore innovation along multiple directions in parallel are expected to achieve the greatest breakthroughs in performance.

Acknowledgments

18. Multimode-fiber-based holographic endomicroscopy

David B Phillips[1] *and Tomáš Čižmár*[2,3]

[1] School of Physics and Astronomy, University of Exeter, Exeter, EX4 4QL, United Kingdom
[2] Leibniz Institute of Photonic Technology, Albert-Einstein-Straße 9, 07745 Jena, Germany
[3] Institute of Scientific Instruments of the Czech Academy of Sciences, Královopolská 147, 612 64 Brno, Czech Republic

Status

Optical imaging through scattering media, such as living tissue, is a grand challenge in biophotonics. Such a capability promises visualization of structures deep inside the body using non-ionizing light. In this section we focus on techniques to image through hair-thin strands of multimode optical fiber (MMF), enabling their deployment as endomicroscopes capable of conveying high-resolution images and video from the tip of a needle.
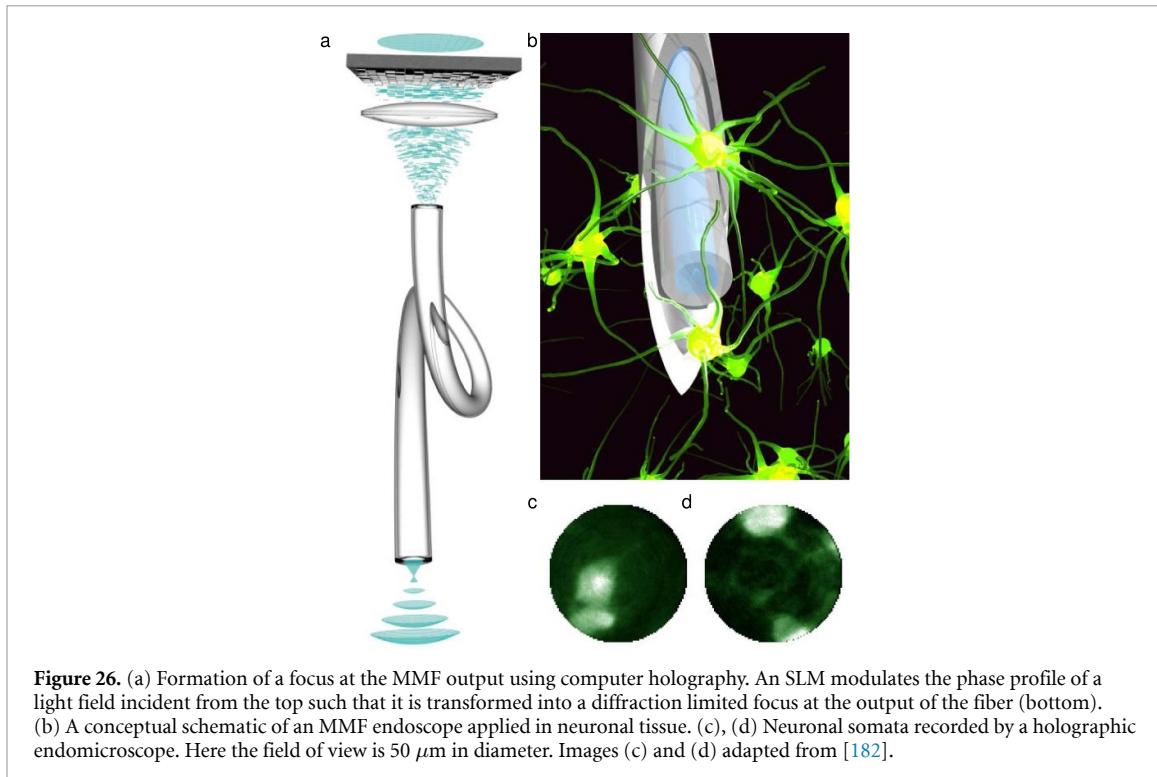
Recovery of images from light signals that have been randomized by propagation through a MMF was first demonstrated in 1967 using analog holography [180]. Despite this achievement, it took the next four decades for our understanding of light scattering in complex media and the development of digital wavefront manipulation techniques to become sufficiently mature to target real applications. Modern MMF-based endoscopes utilize high-fidelity spatial control over the amplitude, phase and polarization of light in order to achieve close-to-perfect generation of the desired optical fields at the distal facet (i.e. far end) of a MMF [143]. In imaging applications, these fields most commonly take the form of diffraction-limited foci which are used to scan the scene point by point. Specialized techniques are already able to use MMFs to funnel various forms of modern microscopy techniques, as well as spectroscopy and the methods of optical manipulation, into locations with restricted access [181]. In particular, holographic endoscopes have become an exciting technological candidate for *in vivo* neuroscience, promising micrometer resolution observations of fluorescently labeled neurons residing deep within the living brain [56, 182], as shown in figure 26. To date, these systems have been tested on mouse models, but they are readily scalable to the size of non-human primates and, ultimately, humans.

Based on the geometry of the MMF, the size of the field of view can vary between 10 s and 100 s of μm (when imaging in the vicinity of the distal facet of the MMF) and the numerical aperture ranges between 0.1 and 1. With current light modulation technology, imaging at a few frames per second is achievable with these systems. A unique feature of MMF-based holographic endoscopes is their ability to arbitrarily alter their working distance and observe objects located right on the distal facet, or move the imaging plane away from the end of the fiber as far as the strength of the returning signals allows. In combination with time-of-flight detection, MMF-based endoscopes can nowadays also offer depth-perception in macroscopic three-dimensional scenes. Such far-field holographic endoscopes look set to further expand the range of applications within the biomedical and industrial inspection domains [183].

Current and future challenges

Scanning imaging through an MMF requires the acquisition of the fiber's transmission matrix (TM), which describes how light fields at either side of any linearly scattering medium are connected [157]. More precisely, the TM of an MMF is a linear matrix operator relating how any input field is transformed via propagation through the fiber. TM acquisition generally requires access to both ends of the MMF: a sequence of known input fields are propagated through the fiber (of a number that should exceed the fiber's mode capacity), and the output fields are holographically measured using an optical setup with interferometric stability. Once the TM is recovered, it can be used to predict the input field required to generate any desired output (within the spatial bandwidth of the fiber), such as a focused spot. A key challenge is that the TM of current fiber technology is highly sensitive to mechanical or thermal perturbations—so if the fiber is contorted or changes temperature during use as an endoscope, its TM is altered in an unknown way, and the pre-calibration is no longer valid. This reduces the fidelity of light control at the distal facet, and ultimately disrupts imaging capabilities.

Other challenges pertain to improving the resolution, frame rate, and signal-to-noise ratio of microscopy techniques it is possible to deliver through optical fibers. Although MMF endoscopy has proven itself capable of adopting numerous scanning-based imaging techniques, it remains highly desirable to extend its portfolio also to prominent wide-field approaches, including super-resolution PALM or STORM, as well as structured-illumination and volumetric (e.g. light-sheet) imaging modalities.

Figure 26. (a) Formation of a focus at the MMF output using computer holography. An SLM modulates the phase profile of a light field incident from the top such that it is transformed into a diffraction limited focus at the output of the fiber (bottom). (b) A conceptual schematic of an MMF endoscope applied in neuronal tissue. (c), (d) Neuronal somata recorded by a holographic endomicroscope. Here the field of view is 50 μm in diameter. Images (c) and (d) adapted from [182].

Advances in science and technology to meet challenges

There are a range of emerging advances that offer routes to overcome these challenges. Several developments show promise in managing and ultimately alleviating the extreme mechanical sensitivity of holographic endomicroscopy. By virtue of its cylindrical symmetry, the TM of an MMF is not completely random, but contains hidden correlations that become evident when it is represented in a well-chosen basis. In particular, by solving the wave equation in cylindrical coordinates, a set of circularly polarized propagation-invariant eigenmodes (PIMs) can be derived. These PIMs form a basis in which the experimental TM of a short length of MMF will be sparse and strongly diagonal, as shown in figures 27(a)–(c). Recent work has shown that these features allow prediction of how the TM will be modified when the fiber bends [143]; see figures 27(d) and (e). They also constitute prior knowledge which can be used to vastly reduce the number of probe fields required to measure the TM, thus significantly speeding up the pre-calibration process [184]; see figures 27(f) and (g). Furthermore, such correlations also enable an estimate of the TM to be derived with access only to the input end of the fiber by placing a guidestar at the distal facet—meaning re-calibration of a perturbed MMF-based endoscope can be performed *in situ* [185]. In parallel to these concepts, there is interest in developing new fibers that are more stable to perturbations, with recent work suggesting this may also be possible.

There are two main routes to turning MMF-based endoscopes into single-shot wide-field (scanner-less) imaging devices. The first involves building a mode converter [186] that is able to physically reconstruct an image from MMF-delivered light by unscrambling all modes simultaneously. This method has already been demonstrated using a single diffractive element; however, this design suffers from prohibitively low conversion efficiency which is incompatible with fluorescence microscopy [187]. More complicated designs will be necessary to achieve such transformations more efficiently, with the added challenge that they must be able to dynamically adapt to apply new transformations if the fiber itself bends. The second suite of methods relies on computational approaches to recover images from the MMF-randomized signals with no further physical light modulation. However, such an inverse problem is very poorly conditioned, and therefore due to their profound sensitivity to noise computational algorithms can only provide useful results when imaging very sparse scenes [188]. Practical solutions are likely to involve a combination of both physical and computational techniques.

Finally, rapid light modulation devices, such as digital micro-mirror devices (DMDs) and high-speed phase-only spatial light modulators, currently underpin holographic endoscopic techniques. DMDs can operate at tens of kHz, but are highly inefficient and are only practical for narrowband sources. SLMs are
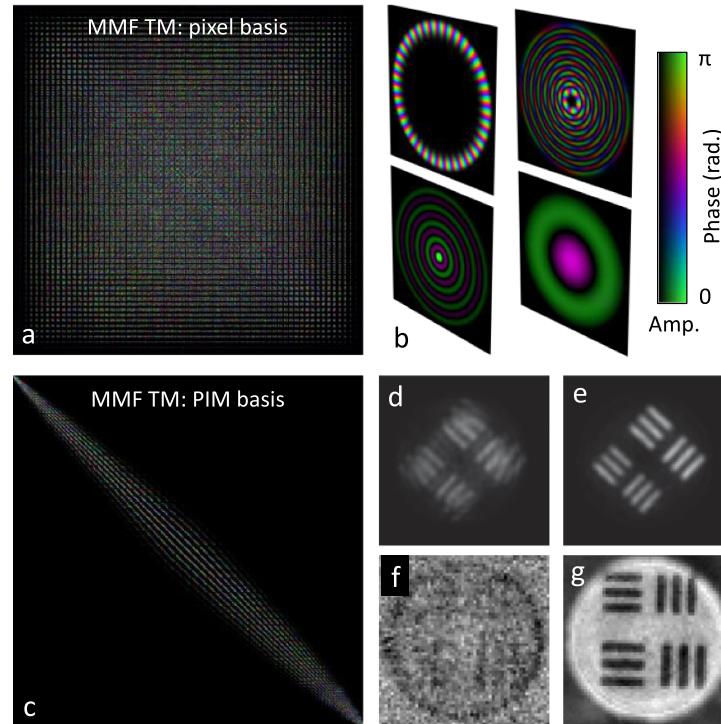
Figure 27. (**a**) Example of the TM of an MMF represented in the pixel basis. (b) Four examples of PIMs that propagate with a constant spatial profile through an ideal MMF. (**c**) Example of the same TM as in part (a), now represented in the PIM basis. In this case the TM is strongly diagonal, with the remaining spread in the power into off-diagonal elements due to imperfect alignment and limited knowledge of the geometric fiber parameters. (d) Imaging quality through a MMF that has been bent after calibration. (e) Image quality restored after prediction of new TM accounting for bending ((d), (e) adapted from [143]). (f) Imaging quality through a MMF having only measured 5% of the full TM. (g) Imaging using the same TM calibration data as in part (f), but now incorporating priors to estimate a more faithful TM ((f), (g), adapted from [184]).

more efficient yet offer considerably slower modulation rates. New light modulation techniques are needed to overcome these limitations, and one avenue may be the fast piston-based DMD equivalents that are on the horizon.

Concluding remarks

Over the last decade there has been an explosion of interest in holographic endo-microscopy, driven by key breakthroughs such as the transmission matrix concept and the advent of high-speed digital light shaping techniques. Holographic endoscopes have already been employed to image neurons deep inside living brain tissue, and emerging applications also include depth perception and industrial inspection endoscopy. In parallel, extensive efforts in basic research are focused on overcoming the remaining challenges, particularly the sensitivity of MMF calibration to mechanical fiber deformations and moving from scanning-based to single-shot widefield imaging modalities. Progress so far has impacted numerous domains beyond endoscopic imaging, including high-capacity optical communications, optical computing and quantum optics, to name a few. Looking forward, we foresee a continued expansion of activity in this exciting area of complex media photonics.

Acknowledgments

19. Ultra-thin imaging endoscope using multi-core fiber

Hervé Rigneault[1] and Esben Ravn Andresen[2]
[1] Aix Marseille University, CNRS, Centrale Marseille, Institut Fresnel, F-13013 Marseille, France
[2] Université de Lille, CNRS UMR 8523—PhLAM—Laboratoire de Physique des Lasers, Atomes et Molécules, F-59000 Lille, France

Status

In the same year that a fiber-optic lensless endoscope based on multimode fiber was demonstrated [189], a lensless endoscope based on multi-core fiber (figure 28 (a1)) was also demonstrated [190]. Both represent the vision of lensless endoscopes: an ultra-thin endoscope whose diameter reduces to the size of the fiber itself ($\sim$100 μm). Having no further distal optics, the lensless endoscope uses a wavefront shaping element on its proximal side to control the phase of the fiber modes at the distal side for imaging. The small diameter makes the fiber a minimally invasive imaging probe exquisitely suited to acquire images of cells hidden deep in sensitive tissue which must be left to the highest possible extent undisturbed. For instance, multimode fiber-based lensless endoscopes have already been demonstrated for brain imaging [56, 182, 191].

We may take [56, 182, 191] as a starting point to highlight some universal challenges for lensless endoscopes and how multi-core fiber may aid in overcoming them.

Acquisition rate

In the cited [56, 182, 191] image acquisition is performed by point scanning, and the wavefront shaping element has to display a specific mask for every pixel of the acquired image. The update rate of the wavefront shaping element is thus the limiting factor for the image acquisition rate. Multi-core fibers can overcome this limit under the condition that individual cores do not exchange energy, allowing point scanning by fast scan mirrors [192] by exploiting the so-called memory effect (the ability to translate the distal wavefront with a simple phase tilt at the fiber input side; see section 13).

Two-photon imaging (and nonlinear imaging in general)

In [56, 182, 191] fluorescence contrast was used to benefit from the specificity of contemporary fluorescent reporter molecules. However, narrowband laser sources were used to overcome the low bandwidth of wavefront shaping in multimode fibers and so only one-photon fluorescence contrast was possible. Often two-photon fluorescence contrast is desired for biological imaging, allowing deeper penetration and z-sectioning, but this requires illuminating the sample by a train of ultrashort optical pulses which become stretched by modal dispersion in multimode fibers. Multi-core fibers are exempt from modal dispersion under the condition that all cores are identical, so virtually undistorted transport of femtosecond pulses and two-photon imaging is possible [193]. Additionally, we note that the multi-core fabrication method allows us to include a very high-numerical-aperture inner cladding which is very efficient at collecting fluorescence light [193] (figure 28(a2)).

Current and future challenges
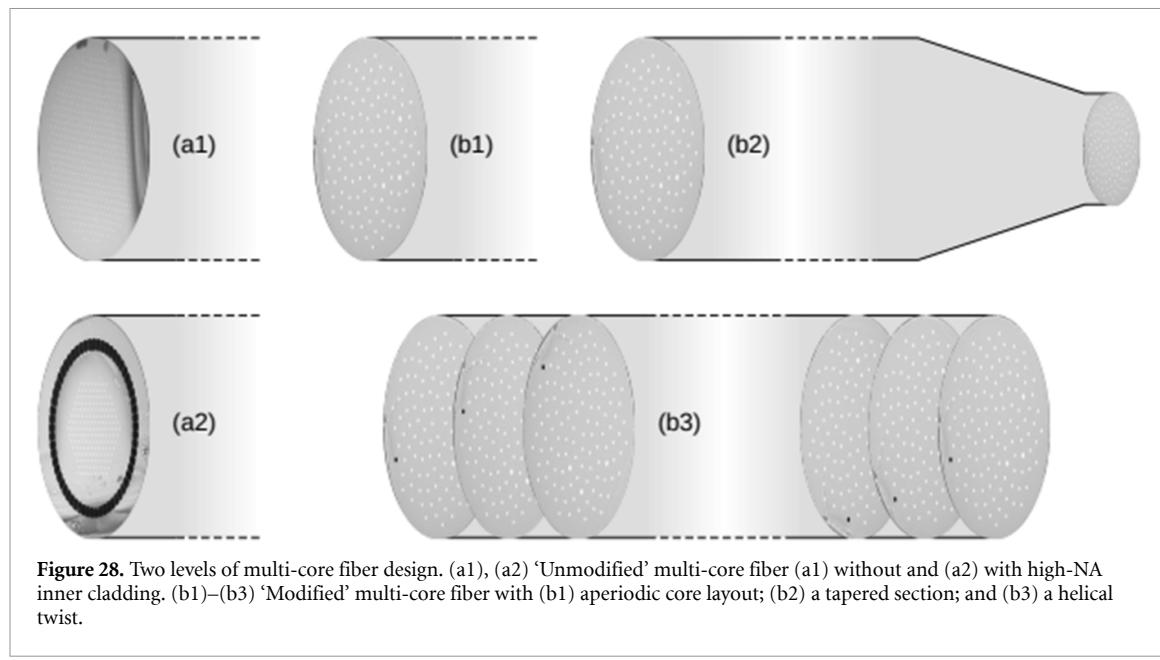
Recent years have seen the exploration of 'modified' multi-core fibers (figures 28(b1)–(b3)) for lensless endoscopes. During fabrication, such modifications can be made before, after, or during the drawing process. Modified multi-core fibers can help address some of the thornier challenges facing multi-core fiber-based lensless endoscopes.

Multiply peaked point spread function (PSF)

Periodicity in the core layout of an unmodified multi-core fiber (figure 28(a1)) has the unwanted consequence of additional intensity maxima in the PSF leading to overlapping replica images. Multi-core fiber with completely aperiodic core structure—for instance a Fermat's golden spiral layout (figure 28(b1))—can be made whose resulting PSF is singly peaked [194].

Strehl ratio

The Fermat's golden spiral multi-core fiber, however, does nothing to resolve another shortcoming of multi-core fibers: the low intensity delivered into the PSF. Indeed, only a small portion (known as the 'Strehl ratio') of the light emitted from the multi-core fiber can be concentrated on a focus by the wavefront shaping element. This is an intrinsic consequence of the low surface coverage of the cores [195], which in turn is a consequence of the large core-to-core distance dictated by the need for low energy exchange between cores. A

Figure 28. Two levels of multi-core fiber design. (a1), (a2) 'Unmodified' multi-core fiber (a1) without and (a2) with high-NA inner cladding. (b1)–(b3) 'Modified' multi-core fiber with (b1) aperiodic core layout; (b2) a tapered section; and (b3) a helical twist.

modification post-drawing of the multi-core fiber tip—a tapering or a homothetic transverse downscaling over a few centimeters (figure 28(b2))—can dramatically increase the PSF intensity while introducing virtually no additional energy exchange and leaving the memory effect intact [196].

Bend resilience

In [56, 182, 191] the endoscope fiber was a few centimeters long multimode fiber which is short enough that it remains rigid at all times. A more ambitious vision of the lensless endoscope calls for a longer fiber that can be free to flex, as this would allow it to be fixed onto a freely moving animal. However, the transmission matrix changes with the fiber conformation, generally rendering the masks displayed on the wavefront shaping element invalid. Multi-core fiber can overcome this challenge in the case where the individual cores follow corkscrew trajectories, i.e. the multi-core fiber is 'twisted' [197] (figure 28(b3)). Such a twisted multi-core fiber remains invariant to conformation as long as the twist period remains small compared to the rate of change of radius of curvature along the fiber. Another strategy has been to monitor in real time the multi-core conformation using double path Mach–Zehnder interferometry and to correct for deformation-induced shifts in focal spot position during raster scanning [198].

Advances in science and technology to meet challenges

Recent progress in additive manufacturing opens new possibilities to 'functionalize' or 'augment' optical fiber properties by 3D printing microstructures at the fiber tip [199]. The coming years could see these new opportunities explored in ultra-thin fiber-optic endoscopes. For instance, we recently explored the possibility to overcome the low Strehl ratio (∼0.01) achievable by multi-core fibers (point 4) by designing a miniature beam combiner that has the property to artificially increase the surface coverage of the cores. Using a combination of microlenses and a 'top lens' the fabricated miniature beam combiner was shown to achieve a Strehl ratio of 0.35 suitable for two-photon imaging (figure 29) [200]. This 3D micro-printing technique is applicable to any type of fiber and so may well have the potential to improve also lensless endoscopes based on multimode fiber. Other improvements that will bring ultra-thin fiber-optic endoscopes closer to applications are expected, such as biocompatible and biodegradable materials or their association, with smart materials allowing their remote conformation control [201].

Concluding remarks

We have seen that most of the challenges brought by ultra-thin fiber-optic endoscopes based on multi-core fiber have solutions that can be realized (inner cladding, aperiodicity, twist, taper or micro-printed beam combiner). The current challenge is to combine all these innovations together into a system that is sufficiently reliable to perform *in vivo* experiments. Forthcoming innovations brought about by additive manufacturing and novel materials are expected to simplify this challenging task.
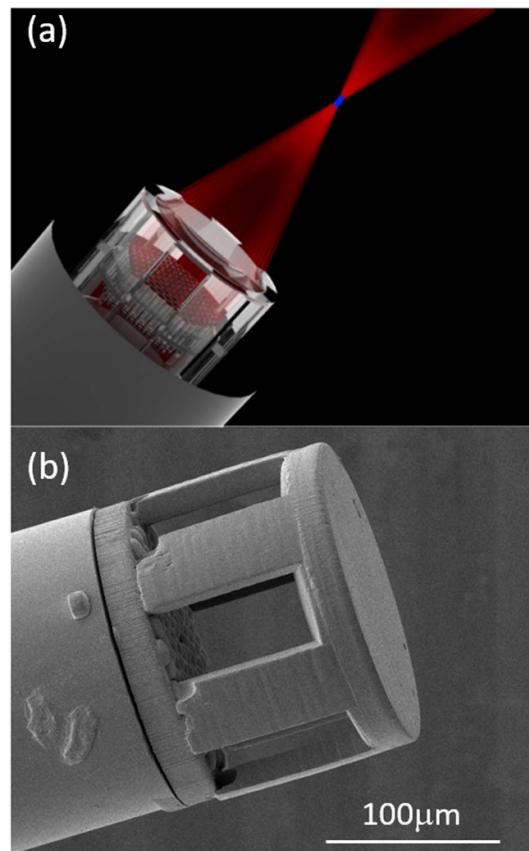
Figure 29. Hyper-telescope micro-printed at the multi-core fiber end and improving the delivered power into the focus spot by ×35. (a) Artist view of the hyper-telescope beam combiner, (b) actual fabrication using micro-printed polymer.

Acknowledgments

20. Learning to image, sense and control with multimode fibers

Babak Rahmani[1], Christophe Moser[1] and Demetri Psaltis[2]
[1] Laboratory of Applied Photonics Devices, School of Engineering, Ecole Polytechnique Fédérale de Lausanne, 1015 Lausanne, Switzerland
[2] Laboratory of Optics, School of Engineering, Ecole Polytechnique Fédérale de Lausanne, 1015 Lausanne, Switzerland

Status

As shown in previous sections, conventional methods of imaging through multimode optical fiber (MMF), such as the gold standard transmission matrix method, require full-field measurements (phase and amplitude) of the fiber's output to construct a mapping between the input and output of the system. The dependence on the phase information makes the system vulnerable as the phase is sensitive to external perturbations. Data-driven methods have been recently proposed to circumvent this problem. These techniques learn statistical characteristics of light propagation using examples of inputs and intensity-only measurements of the output. Within this framework, learning-based methods for imaging through MMFs either a) seek to retrieve the input information (usually a 2D image) entering the fiber from intensity-only measurements of the output or b) seek to obtain the required input pattern that projects a desired target at the distal facet of the fiber. It should be noted that such problems are highly ill-posed as many inputs can result in the same intensity profile at the output of the fiber that only differ in their respective phase information.

The inference of the input of the fiber from intensity-only measurements of its output involves the construction of a backward mapping function that is obtained by minimizing a loss function in the following format:

$$L = M(x, A_\theta(y)) \text{ where } \hat{x} = A_\theta(y)$$

where x and y are the input and output of the system. We note that x in general is complex, whereas y is always a positive real number. $\hat{x}$ is the solution of the this optimization problem. The operator M represents a metric between the predicted output of the deep neural network (DNN) A_θ that is parametrized by θ. The loss function is optimized by taking gradients with respect to the learnable parameters of the mapping function A, i.e. θ, in a process known as gradient descent. Upon convergence, the mapping function is an estimator of the backward mapping of the MMF system that predicts the input patterns of the system from the corresponding outputs.

**Current and future challenges**
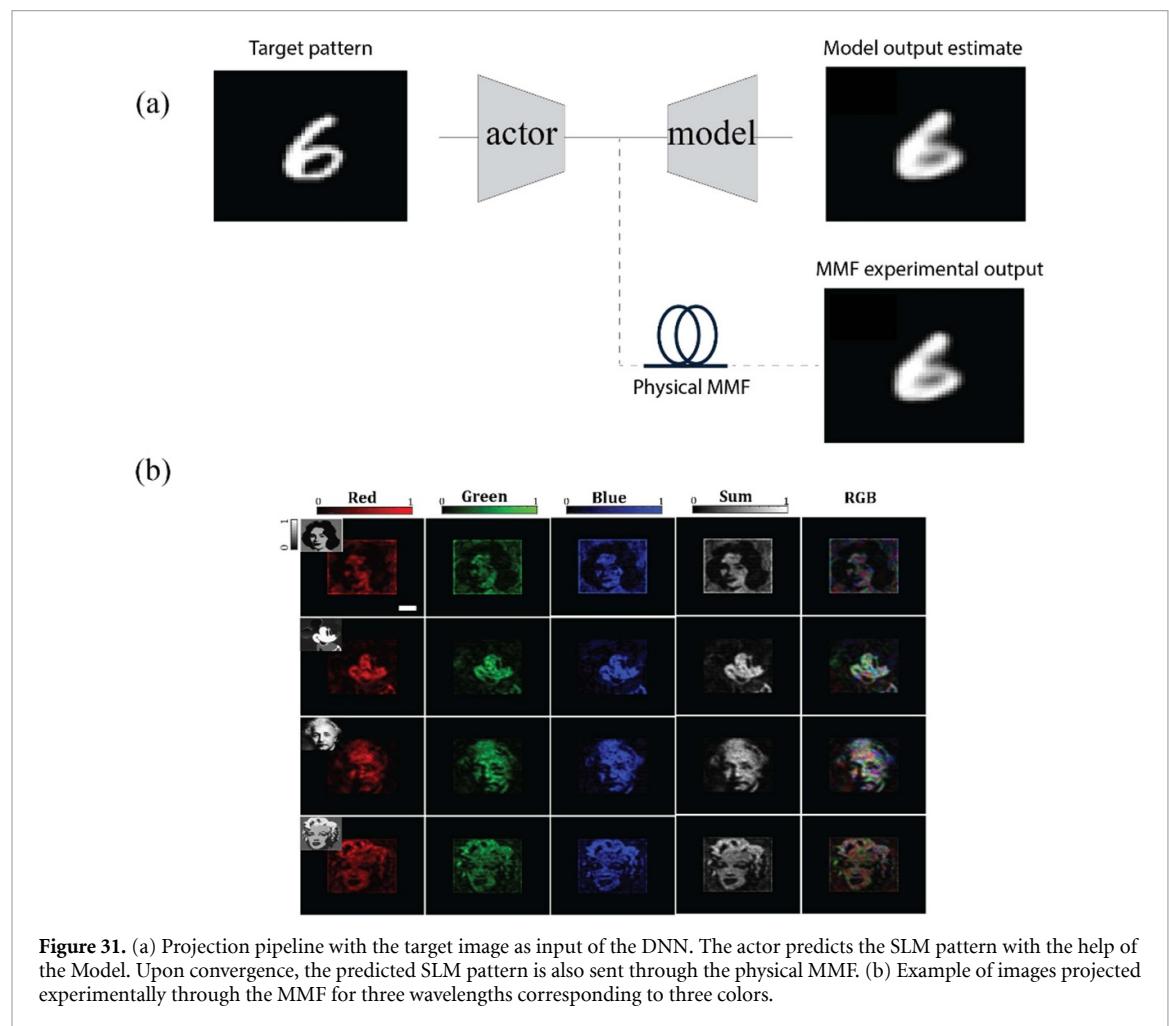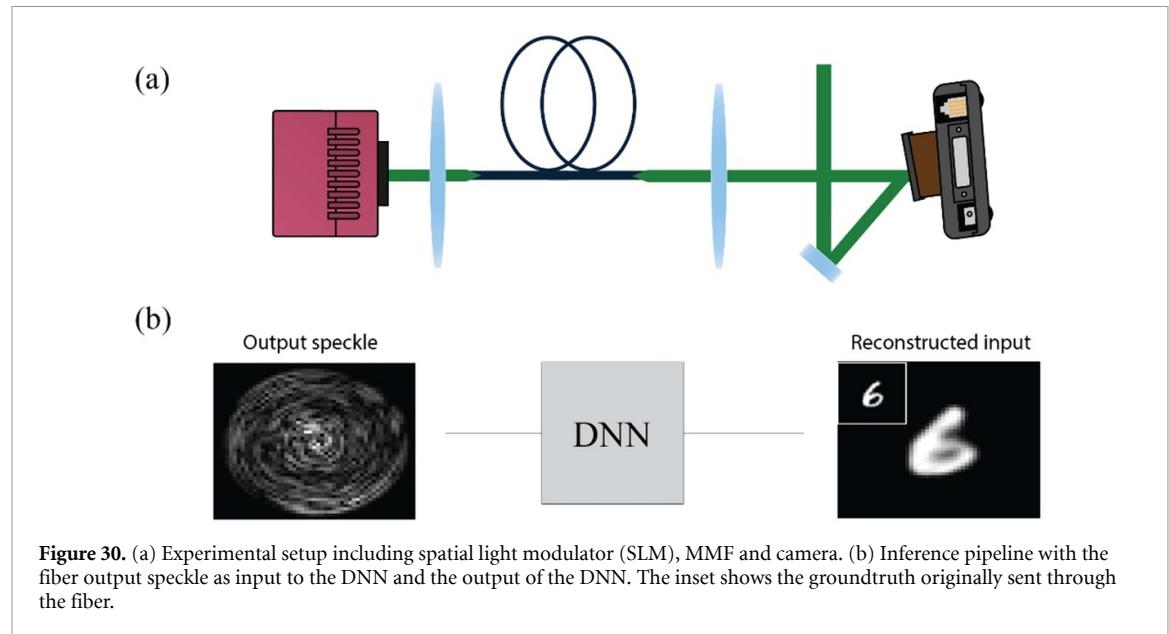
Using convolutional networks, Rahmani *et al* [202], Borhani *et al* [203] and Kakkava *et al* [204] were able to reconstruct sparse-like input images that were scrambled upon propagation through various MMF lengths up to 1 km. Figure 30(a) shows the optical setup that is used in the data collection step. Figure 30(b) depicts an example of a speckle pattern that is fed to the DNN together with its reconstruction. Other authors showed the same performance of the DNNs (2D Pearson correlation around 95%) with more complex input images [205]. Authors in [206] used a simpler DNNs, such as a fully connected single layer for reconstruction of the images scrambled through MMF with comparable fidelity as that of the complex architecture DNNs.

Learning-based methods for projection through MMFs seek to find the correct input pattern that upon propagation through the fiber produces a desired image at its distal side [207, 208]. It is again assumed that the fiber system is characterized without resorting to holographic measurements. Using a more complex training procedure, the authors in [207] were able to project arbitrary images through MMFs for various wavelengths. The training algorithm therein involves the construction of a mapping mimicking the forward propagation of light from the input to the output (Model) followed by learning the backward mapping of the system (Actor). Some sample images projected through the experimental system using the Actor–Model algorithm are plotted in figure 31(b).

The end-to-end characterization of learning-based methods allows for inherent learning of perturbations incurring on the imaging system. Despite severe decorrelation of the imaging system due to external sources of perturbations such as thermal variability and mechanical misalignment, the authors in [207] showed a stable imaging fidelity over several hours.

Another source of perturbation is the drift in the wavelength of the laser source that decorrelates the output intensity with time. In a study conducted by Kakkava *et al* [209–211], it was shown that the DNNs can correct for the decorrelation rendered by the wavelength change of the fiber with an extended bandwidth.

Other researchers investigated the performance of the DNNs under severe mechanical perturbations [212–214]. Specifically, the MMF was positioned in different configurations while examples of inputs and

Figure 30. (a) Experimental setup including spatial light modulator (SLM), MMF and camera. (b) Inference pipeline with the fiber output speckle as input to the DNN and the output of the DNN. The inset shows the groundtruth originally sent through the fiber.

Figure 31. (a) Projection pipeline with the target image as input of the DNN. The actor predicts the SLM pattern with the help of the Model. Upon convergence, the predicted SLM pattern is also sent through the physical MMF. (b) Example of images projected experimentally through the MMF for three wavelengths corresponding to three colors.

outputs were collected. It was shown that DNNs were able to reconstruct the input information sent through the fiber when the DNN was given examples of input–output for all positional configurations. Other lines of work use DNNs to characterize perturbed MMFs for sensing applications such as temperature [215] and mechanical sensors [216, 217]. In addition to sensing in the linear domain, DNNs have started to be used for the characterization of nonlinear dynamics in MMFs. The results of such studies open up a novel perspective for the use of machine learning in multimode fibers [218–221].

21. Transmission eigenchannels in diffusive random media

Hui Cao[1], Alexey Yamilov[2] and Hasan Yılmaz[3]
[1] Department of Applied Physics, Yale University, New Haven, CO, 06520, United States of America
[2] Department of Physics, Missouri University of Science and Technology, Rolla, MI, 65409, United States of America
[3] Institute of Materials Science and Nanotechnology, National Nanotechnology Research Center (UNAM), Bilkent University, Ankara, 06800, Turkey

Status

Coherent control of wave transport by spatial wavefront shaping has overcome the limitations imposed by incoherent diffusion. In a linear scattering system with static disorder, the mapping from the incident to the transmitted waves is deterministic, and fully described by the field transmission matrix (TM) t. The eigenvectors of $t^\dagger t$ provide the input wavefronts for a set of transmission eigenchannels. Any incoming wave can be decomposed into a linear superposition of these eigenchannels, each propagating independently through the system with a transmittance equal to the corresponding eigenvalue τ. In a lossless diffusive system of average transmittance $\langle \tau \rangle \ll 1$, the transmission eigenvalues τ range from 1 (open channels) to 0 (closed channels). Therefore, selective excitation of individual eigenchannels leads to diverse non-diffusive behaviors.

Transmission eigenchannels not only have very different transmittance but also feature distinct energy distributions inside a diffusive system. In contrast to a linear decrease in energy density with depth in a diffusive system, an open channel reaches the energy maximum near the center of depth, while a closed channel exhibits an exponential decay [222–224]. Therefore, an open channel has energy built up deep inside a diffusive system, and enhances light–matter interaction.

The depth profile of an open channel can be modified by modulating the width of a diffusive waveguide with reflecting sidewalls (figure 32(a)). This enables inverse design of an eigenchannel profile [225]. In a wide diffusive slab with open boundaries (figure 32(b)), all transmission eigenchannels are localized in the transverse direction (parallel to the slab surface), and their lateral size is much smaller than the slab width [226]. None of them expands laterally while propagating through the slab, in sharp contrast to transverse diffusion of a narrow beam with identical width but arbitrary wavefront.

Open channels exist at any frequency, although their input wavefronts are frequency-specific. Even for a broadband input light, it is possible to find an incident wavefront to enhance transmittance at all frequencies involved [227].

Current and future challenges

While there have been extensive theoretical and numerical studies on transmission eigenchannels, experimentally it is hard to observe them directly. Typical scattering samples are wide slabs with open boundaries, and it is impossible to control incident light at all angles. Such incomplete channel control greatly reduces the transmittance of open channels and their penetration depth [228].

The main challenge is to achieve complete control of incident fields in all spatial modes. To observe the internal structures of individual eigenchannels, it is necessary to probe the energy density everywhere inside a disordered system. Experimentally fluorescent beads are embedded inside three-dimensional scattering samples to extract information about internal light distribution from their fluorescence [229]. However, it is difficult to control the exact locations of these beads as well as to separate the individual fluorescence for a large number of them. Numerically it is a daunting computational task to simulate wave propagation in a three-dimensional diffusive system of practical dimensions. Finally, the ability to precisely tailor sample geometry, dimension and scattering parameters is essential to uncover their effects on the transmission eigenchannels.

The TM is specific to the disorder realization, as are its eigenchannels. In theoretical and numerical studies, the spatial profiles of transmission eigenchannels are averaged over large ensembles, whereas experiments are conducted on a single sample and the eigenchannel profile may deviate from the average. Knowledge of the extent of this realization-to-realization deviation is critical for practical applications.

Absorption is ubiquitous in optical systems, and its effect on coherent wave transport differs from that of decoherence on mesoscopic electron transport. Moreover, the spatial distribution of absorption can be homogeneous or inhomogeneous, which will impact the transmission eigenchannels in different ways [230].

Advances in science and technology to meet challenges

A unique experimental platform [231] has been built in a two-dimensional optical waveguide geometry (figure 33(a)). The waveguides, fabricated in silicon-on-insulator wafers, have highly reflecting sidewalls
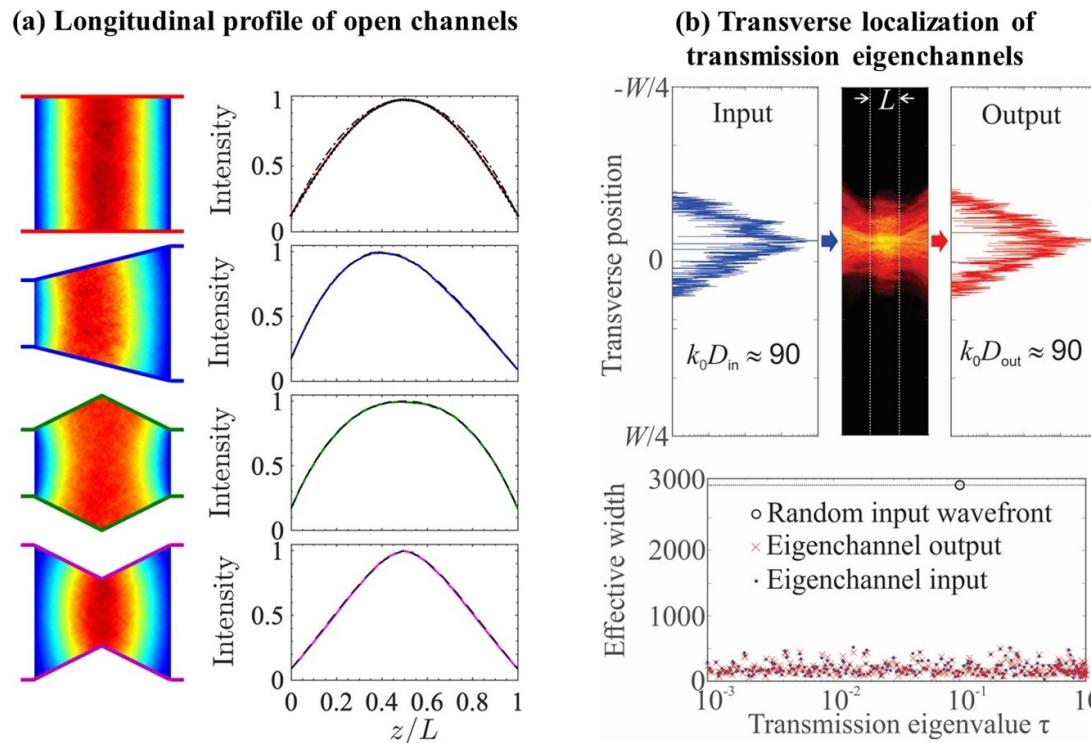
Figure 32. (a) Engineering the depth profile of open channels by modulating the width of a diffusive waveguide [225]. (b) Transverse localization of transmission eigenchannels in a wide diffusive slab [226].

composed of photonic crystal layers (figure 33(b)). Air holes are randomly distributed inside a section of the waveguide. Their size and location can be precisely controlled to tune the transport mean free path. The length of the disordered section is much larger than the transport mean free path but smaller than the localization length, to ensure diffusive transport. The waveguide width determines the number of spatial modes. A monochromatic laser beam is wavefront-shaped by a spatial light modulator (SLM), and then injected via the edge of the wafer into a ridge waveguide. The waveguide width is adiabatically tapered down to couple light into all waveguide modes incident on the disordered region. While light is predominantly scattered by air holes in the waveguide plane, a small amount is scattered out of plane. It is collected and measured with an interferometer to recover the field distribution inside the disordered region. In order to access the field incident on the disordered section of the waveguide, a weakly scattering zone (buffer) is added, and light escaping from it to the third dimension is detected.

This experimental platform enables complete channel control and measurement of the full TM *t* [230]. From *t*, transmission eigenchannels are found and individually excited by wavefront shaping. The spatial structures of both open and closed channels inside a planar waveguide are observed directly from the vertical dimension (figure 33(c)). The depth profiles of higher-transmission channels exhibit smaller fluctuations from one disorder realization to another, compared to lower-transmission eigenchannels and random input wavefronts. Realization-to-realization fluctuations of the depth profiles of different eigenchannels exhibit correlations. These correlations are weaker for higher-transmission eigenchannels, indicating that they are more isolated than lower-transmission eigenchannels (figure 33(d)). Open channels have robust depth profiles, which are consistent between disorder configurations, allowing reliable energy delivery deep inside diffusive systems. This platform also enables experimental study of energy deposition to a region of arbitrary size and shape anywhere inside the scattering system.

Concluding remarks
Experimental and numerical studies on transmission eigenchannels represent the first steps toward a physical understanding of how open and closed channels are formed inside diffusive systems, and eventually the development of a comprehensive theory. The next step is to extend these studies to wide slabs with open boundaries and to volumetric diffusive systems. Since the open channels increase the energy density inside diffusive media, they have potential applications in optogenetics and deep-tissue multiphoton imaging that aim to enhance light–matter interactions.
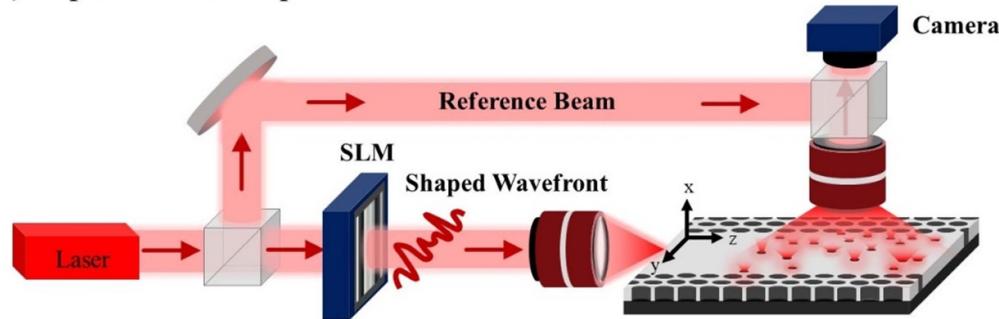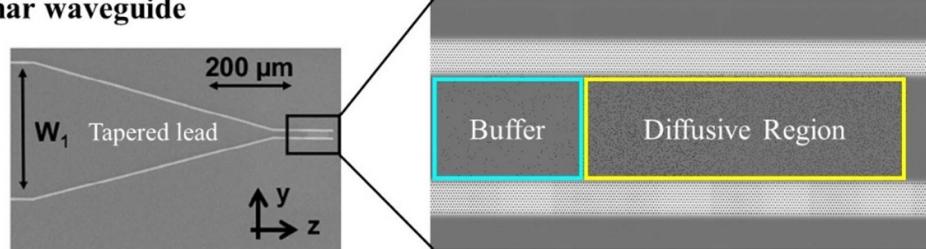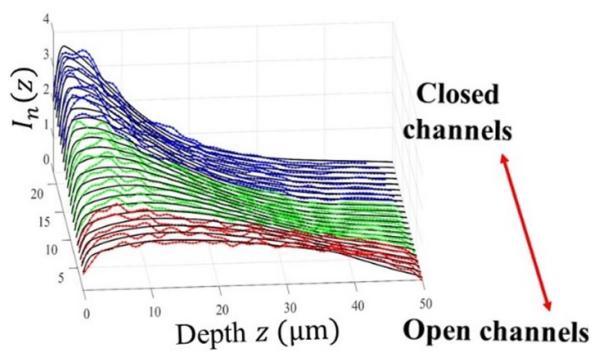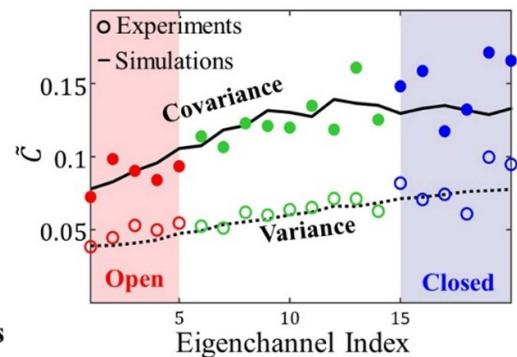
Figure 33. (a) Schematic of experimental platform for excitation and observation of individual transmission eigenchannels in a planar silicon waveguide. (b) Scanning electron micrograph showing the tapered lead (left), buffer and diffusive region (right) of the waveguide. (c) Distinct depth profiles of open and closed channels. (d) Realization-to-realization fluctuations (variance) and correlations (covariance) of eigenchannel profiles [231].

Another direction is to explore and exploit the remarkable properties of transmission eigenchannels such as, for example, the enhanced range of the angular memory effect for open channels, which is useful for imaging. Finally, it will be interesting to explore the eigenchannels of other operators, e.g. for time delay of a pulse propagating through a diffusive medium, or energy deposition deep inside a scattering system.

Acknowledgments

22. Optimal information extraction from scattering systems

Dorian Bouchet[1], *Allard P Mosk*[2] *and Stefan Rotter*[3]
[1] University Grenoble Alpes, CNRS, LIPhy, 38000 Grenoble, France
[2] Debye Institute for Nanomaterials Science, Utrecht University, Utrecht, The Netherlands
[3] Institute for Theoretical Physics, TU Wien, Vienna, Austria

Status
In free space, measuring the field scattered by an object allows one to directly estimate the values of observables characterizing this object, such as its position, size or shape. However, in the case of an object embedded in a complex scattering environment, the situation is more involved due to the influence of all absorption and scattering processes acting on the incident light. To characterize all these processes, a convenient tool is given by the system's scattering matrix, which connects incident to outgoing far-field modes (see sections 9 and 10). In the last decade, the possibility to optically measure significant fractions of scattering matrices has enabled a multitude of new approaches to image hidden objects in complex scattering environments [83].

A promising way to analyze such scattering experiments is to use tools borrowed from information theory. Notably, if the object can be described by a set of parameters, the Fisher information can be employed to quantitatively assess how well the object can be reconstructed [232]. It then turns out that, from the knowledge of the system's scattering matrix (which is now a function of these parameters), one can not only predict the achievable precision in the estimation of these parameters but also design incident coherent fields that optimally probe the system [233, 234] (figure 34(a)). These 'maximum information states' are specifically tailored to precisely characterize an object of interest within its complex environment and could thus serve to improve the quality of imaging techniques in scattering environments, such as semiconductor nanostructures or biological tissues. Remarkably, these customized light fields are not only optimal for extracting the maximum amount of Fisher information on a target but also for manipulating this target with light [235] (figure 34(b))—a feature rooted in a fundamental connection between information and measurement back-action.

Current and future challenges
Employing the Fisher information to improve imaging techniques entails describing entire images as ensembles of parameters. The large number of such parameters that need to be introduced in this case, however, easily makes a corresponding procedure prohibitively difficult. Indeed, calculating the achievable precision in the estimation of p parameters requires the inversion of a $p \times p$ Fisher information matrix, which becomes numerically expensive when p exceeds around 10 000. While the available computational power still gradually increases over the years, a suitable alternative could be to find suitable sparse representations to describe images of interest [236].

Different options are available to experimentally determine optimal input fields that maximize the Fisher information, such as brute-force optimization, iterative phase conjugation, or scattering matrix measurements. At this stage, however, all these procedures rely on a deterministic control over the parameters to be estimated, therefore strongly limiting the applicability of the approach. Developing experimental procedures to identify optimal fields without such a high level of control would thus be of great interest. Alternatively, in the case of engineered nanostructured samples, numerical models of scattering experiments could potentially be employed to determine optimal fields purely numerically [237]; it remains to be assessed, however, if such models are sufficiently accurate for these fields to be usable in actual experiments (see section 13).

In theory, one can also expect to improve the achievable precision by simultaneously taking advantage of both the spatial and quantum degrees of freedom of the incident light. In quantum metrology, general procedures already exist to identify such optimal input states that maximize the Fisher information [238]. Nevertheless, it remains unclear how such procedures can be employed in the case of complex scattering systems, as the evolution of any input state is then typically described by an unknown sub-unitary operator. Moreover, while experiments that involve spatially shaped quantum states of light start to emerge (see section 23), most quantum states remain experimentally difficult to generate, restricting the practical application of quantum metrology and imaging protocols.

Advances in science and technology to meet challenges
For experiments in which optimal input fields cannot be easily identified using information theory, the association of wavefront shaping devices with deep learning (DL) algorithms constitutes a possible alternative for the development of imaging applications based on task-specific input fields (see section 12).
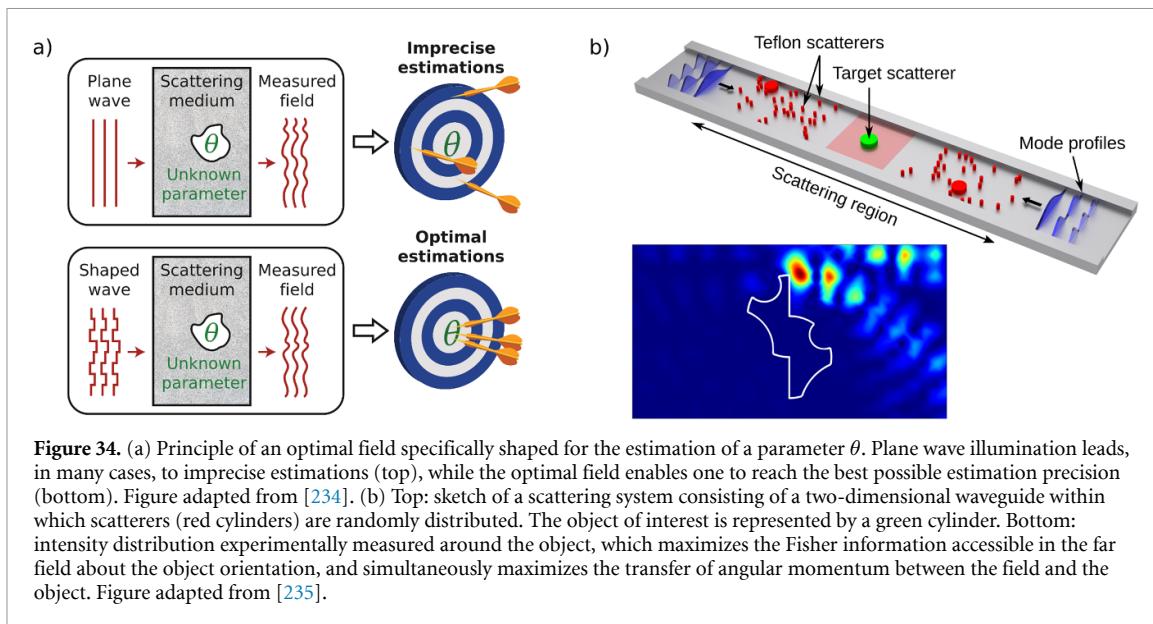
Figure 34. (a) Principle of an optimal field specifically shaped for the estimation of a parameter θ. Plane wave illumination leads, in many cases, to imprecise estimations (top), while the optimal field enables one to reach the best possible estimation precision (bottom). Figure adapted from [234]. (b) Top: sketch of a scattering system consisting of a two-dimensional waveguide within which scatterers (red cylinders) are randomly distributed. The object of interest is represented by a green cylinder. Bottom: intensity distribution experimentally measured around the object, which maximizes the Fisher information accessible in the far field about the object orientation, and simultaneously maximizes the transfer of angular momentum between the field and the object. Figure adapted from [235].

Indeed, DL algorithms offer the possibility to implicitly measure scattering matrices using training data sets. Integrating light-shaping devices (such as spatial light modulators, digital micro-mirror devices or tunable metasurfaces) as trainable layers in artificial neural networks offers a practical approach to identify input fields that are specifically tailored for a given imaging task [239], with no guarantee, however, that the true optimal solution will be reached.

It also often happens that one cannot rely on scattering matrices to describe the influence of absorption and scattering processes upon the incident light, for instance in the case of media (such as biological tissue) that feature an unknown time variation. Reconstructing an image through such media requires the use of statistical correlations—rather than deterministic relations—between fields at the detector and fields in the object plane (see section 15). Interestingly, such statistical approaches can also benefit from quantitative analyses based on information theory [240], in order to guide the experimental development of imaging techniques at large depths.

Concluding remarks

The tools of information theory offer a wide range of possibilities to quantitatively assess and optimize the capabilities of imaging techniques in scattering environments. We expect that information-driven approaches will be key to the development and refinement of new computational microscopy methods, and notably to identifying task-specific illumination schemes that optimally probe complex scattering media (see also section 17). These methods could then potentially be applied e.g. to obtain a better understanding of dynamic biological processes. In addition, an information-driven paradigm may provide us with a new level of understanding of light–matter interactions in complex systems.

Acknowledgments

23. Imaging in complex media with quantum states of light

Yaron Bromberg[1] *and Hugo Defienne*[2]
[1] Racah Institute of Physics, The Hebrew University of Jerusalem, Jerusalem, Israel
[2] School of Physics and Astronomy, University of Glasgow, United Kingdom

Status

Quantum states of light play a key role in basic research on quantum mechanics, as well as in emerging quantum technologies. Early studies on the propagation of quantum states of light in complex media focused on fundamental questions such as the survival of quantum features of light in random media [241]. Following recent rapid developments in photonic quantum technologies, it has also become critical to understand the effect of scattering of quantum states of light from a technological perspective. For example, the implementation of free-space quantum communication in real-life settings, such as ground-satellite links, requires dealing with scattering and aberrations induced by atmospheric turbulence [242]. In quantum computation, quantum supremacy was recently demonstrated by mixing squeezed states occupying 100 modes using a multiport interferometer with random mode couplings [243]. In this section, we discuss recent advancements and future challenges toward utilizing quantum resources for imaging in complex media.

Over the past few decades, researchers have considered various approaches for utilizing quantum properties of light to surpass classical bounds in optical imaging. These include enhanced sensitivity and noise rejection, utilizing anti-bunching for super-resolution imaging [244] and imaging with undetected photons [245]. Motivated by the potential of quantum imaging to lift some of these limits, in recent years we have witnessed a growing interest in going one step further, and utilizing quantum states of light for imaging through turbid media.
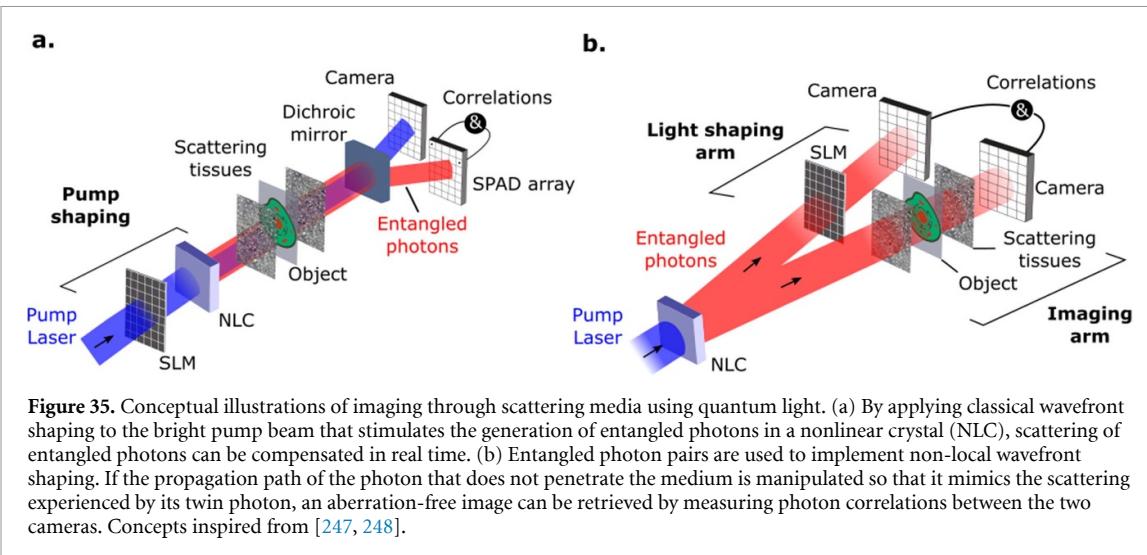
Current and future challenges

Two general approaches can be envisaged to harness quantum states for imaging in scattering media.

First, the advantages that these states provide in terms of imaging performance (e.g. resolution and sensitivity) can directly benefit existing imaging methods in scattering media. In this case, the main challenge is to adapt the corresponding optical tools, such as adaptive optics and wavefront shaping, to quantum sources. Although imaging photon pair correlations through thin static diffusers by wavefront correction was recently achieved [246], such a task remains extremely challenging in real-world situations because of the high complexity of natural scattering media and the very low intensity of quantum light sources. To advance these issues, a promising avenue is to use a hybrid approach in which quantum light is guided through scattering using an intense classical light as a beacon [247]. Figure 35(a) illustrates this concept with a beam of entangled photons that is refocused after a turbid medium by implementing real-time aberration correction using scattered light from the classical pump laser as a feedback signal. Such a hybrid approach enables the incorporation of classical wavefront correction algorithms into any quantum imaging system. Furthermore, it can lead to the development of a novel multimodal imaging framework in which quantum and classical light operate in parallel.

The second approach consists of harnessing properties that are unique to quantum light, such as entanglement, to develop new protocols for imaging inside scattering media. In this case, the main current challenge is to determine which states and specific quantum resources could potentially be used to improve such a task. In this respect, an interesting scheme was recently proposed in the context of quantum communication through multimode optical fibers [248]. Adapted to the imaging problem, its concept is illustrated in figure 35(b). One photon from an entangled pair illuminates an object hidden behind or inside a disordered medium, while its twin photon is sent toward a light shaping system (e.g. spatial light modulators). Unlike classical approaches, the shaped light does not penetrate the scattering medium and no information can be retrieved from intensity signals at the output. However, if one programs the shaping system so that it mimics the optical disorder, object information can be retrieved via intensity correlation measurements between the two distant cameras. In essence, the scattering medium is rendered transparent by carefully 'scrambling' the photons that did not enter it, rather than unscrambling the photons that did. Even though the benefits of this non-local shaping scheme compared to classical methods have not yet been established, it raises intriguing questions regarding the use of genuine quantum resources for imaging inside scattering samples, and invites us to explore them.

Interestingly, other recently developed quantum imaging approaches can indirectly contribute to advancing the problem of imaging through scattering media. For example, quantum imaging schemes with undetected photons [245] allow imaging with mid-infrared light, a wavelength range that is naturally less sensitive to scattering in biological tissues. Furthermore, quantum-dot-based super-resolution

Figure 35. Conceptual illustrations of imaging through scattering media using quantum light. (a) By applying classical wavefront shaping to the bright pump beam that stimulates the generation of entangled photons in a nonlinear crystal (NLC), scattering of entangled photons can be compensated in real time. (b) Entangled photon pairs are used to implement non-local wavefront shaping. If the propagation path of the photon that does not penetrate the medium is manipulated so that it mimics the scattering experienced by its twin photon, an aberration-free image can be retrieved by measuring photon correlations between the two cameras. Concepts inspired from [247, 248].

approaches [244] also have the potential to access deeper layers inside disordered media by using these emitters as guidestars for wavefront shaping.

Advances in science and technology to meet challenges

One of the main challenges in quantum imaging is the low light levels associated with non-classical light sources. This challenge becomes particularly severe in imaging through scattering media, as scattering spreads the photons over multiple spatial modes, making it extremely difficult to efficiently collect the scattered photons. Furthermore, to truly exploit quantum features of light, it is generally necessary to probe temporal and spatial correlations between the detected photons. This requires multi-channel detection at the single photon level, with excellent spatial and temporal resolutions. While impressive progress has been made in measuring spatial correlations using electron multiplied and intensified charge coupled device cameras [249], the inherently slow frame rates of such cameras limit the applicability for imaging in natural scattering media such as biological tissue, and prevent implementation of feedback-based wavefront shaping. The most promising technology for meeting the strict requirements for quantum imaging through scattering media is SPAD arrays, which combine the multi-channel detection of cameras with the sensitivity of single photon detectors. More importantly, they provide high-resolution timestamps for photondetection events at each pixel. Single-photon avalanche diode (SPAD) array technology has been rapidly progressing over the past decade, demonstrating megapixel sensors and photon detection efficiencies as high as 60% [250]. Yet, to meet the demanding needs of deep quantum imaging, further advancements are required in terms of the number of pixels, array fill factor, low cross-talk, efficient readout of individual pixels, and on-chip multi-channel coincidence registration.

The vast amount of spatio-temporal information made available by SPAD arrays sets new challenges in terms of data readout, transfer, processing, and management. To fully exploit the information carried by high-order correlations between multiple photon detection events, smart on-chip and field-programmable gate-array-based processing protocols will have to be developed. Efficient on-the-fly processing of the registered correlations will open the door for new deep-imaging strategies. For example, in the photon-starved regime, wavefront optimization schemes based on high-order spatio-temporal correlations may turn out to be more efficient than intensity-based schemes, as more information can be extracted per photon detection event. Similarly, the development of new algorithms based on high-order spatio-temporal photon correlations may initiate a new paradigm in computational imaging in scattering samples.

The key to the success of quantum imaging in scattering media depends on whether the quantum advantages provided by non-classical states of light can balance the cost of using weak light sources, which is reflected in low signal-to-noise ratios compared to imaging with classical light sources. The answer to this question depends on technological and scientific breakthroughs, which at this point are difficult to predict. Nonetheless, we strongly believe that research on quantum imaging through scattering media will also lead to the development of quantum-inspired imaging schemes that will utilize high-order correlations using classical bright sources.

Concluding remarks

Up to now, very few research groups have investigated the propagation of quantum optical states in scattering media, with nearly all studies focused on fundamental aspects and communication applications. Regarding

imaging in scattering media, nearly everything remains to be done. Whether it is by adapting already existing deep-tissue imaging methods to quantum imaging approaches or by truly harnessing the unique properties of quantum light to see deeper, this research field has strong potential for developing new imaging methods that can complement or even surpass classical approaches. In the coming years, this research will also benefit from the rapid development of novel imaging sensors, such as SPAD cameras, allowing detection of single photons across multiple channels in parallel at unprecedented temporal resolution and speed.

Acknowledgments

Data availability statement

No new data were created or analyzed in this study.

ORCID iDs

Sylvain Gigan ● https://orcid.org/0000-0002-9914-6231
Hilton B de Aguiar ● https://orcid.org/0000-0002-2426-0371
Emmanuel Bossy ● https://orcid.org/0000-0002-8101-8290
Dorian Bouchet ● https://orcid.org/0000-0002-9122-5170
Hui Cao ● https://orcid.org/0000-0002-5339-6892
Hugo Defienne ● https://orcid.org/0000-0002-5543-2885
Allard P Mosk ● https://orcid.org/0000-0002-1140-6626
Stefan Rotter ● https://orcid.org/0000-0002-4123-1417
Lei Tian ● https://orcid.org/0000-0002-1316-4456
Lihong Wang ● https://orcid.org/0000-0001-9783-4383
Chris Xu ● https://orcid.org/0000-0002-3493-6427
Alexey Yamilov ● https://orcid.org/0000-0002-9339-6475
Hasan Yılmaz ● https://orcid.org/0000-0003-1889-3516

References

[1] Vellekoop I M and Mosk A P 2007 Focusing coherent light through opaque strongly scattering media *Opt. Lett.* **32** 2309–11
[2] Freund I 1990 Looking through walls and around corners *Physica* A **168** 49–65
[3] Gould T J, Burke D, Bewersdorf J and Booth M J 2012 Adaptive optics enables 3D STED microscopy in aberrating specimens *Opt. Express* **20** 20998–1009
[4] Denk W and Svoboda K 1997 Photon upmanship: why multiphoton imaging is more than a gimmick *Neuron* **18** 351–7
[5] Horton N G, Wang K, Kobat D, Clark C G, Wise F W, Schaffer C B and Xu C 2013 *In vivo* three-photon microscopy of subcortical structures within an intact mouse brain *Nat. Photon.* **7** 205–9
[6] Wang M, Wu C, Sinefeld D, Li B, Xia F and Xu C 2018 Comparing the effective attenuation lengths for long wavelength *in vivo* imaging of the mouse brain *Biomed. Opt. Express* **9** 3534–43
[7] Wang T, Wu C, Ouzounov D G, Gu W, Xia F, Kim M, Yang X, Warden M R and Xu C 2020 Quantitative analysis of 1300-nm three-photon calcium imaging in the mouse brain *Elife* **9** e53205
[8] Wang T, Ouzounov D G, Wang M and Xu C 2017 Quantitative comparison of two-photon and three-photon activity imaging of GCaMP6s-labeled neurons *in vivo* in the mouse brain *Optics in the Life Sciences Congress (2017)* (Optical Society of America) p BrM4B.4
[9] Kobat D, Durst M E, Nishimura N, Wong A W, Schaffer C B and Xu C 2009 Deep tissue multiphoton microscopy using longer wavelength excitation *Opt. Express* **17** 13354–64
[10] Kou L, Labrie D and Chylek P 1993 Refractive indices of water and ice in the 0.65- to 2.5-μm spectral range *Appl. Opt.* **32** 3531–40
[11] Wang M, Kim M, Xia F and Xu C 2019 Impact of the emission wavelengths on *in vivo* multiphoton imaging of mouse brains *Biomed. Opt. Express* **10** 1905–18
[12] Theer P and Denk W 2006 On the fundamental imaging-depth limit in two-photon microscopy *J. Opt. Soc. Am.* A **23** 3139–49
[13] Wilt B A, Fitzgerald J E and Schnitzer M J 2013 Photon shot noise limits on optical detection of neuronal spikes and estimation of spike timing *Biophys. J.* **104** 51–62
[14] LaViolette A K and Xu C 2021 Shot noise limits on binary detection in multiphoton imaging *Biomed. Opt. Express* **12** 7033–48
[15] Kobat D, Horton N G and Xu C 2011 *In vivo* two-photon microscopy to 1.6-mm depth in mouse cortex *J. Biomed. Opt.* **16** 106014
[16] Cheng H, Tong S, Deng X, Liu H, Du Y, He C, Qiu P and Wang K 2019 Deep-brain 2-photon fluorescence microscopy *in vivo* excited at the 1700 nm window *Opt. Lett.* **44** 4432–5
[17] Xia F, Wu C, Sinefeld D, Li B, Qin Y and Xu C 2018 *In vivo* label-free confocal imaging of the deep mouse brain with long-wavelength illumination *Biomed. Opt. Express* **9** 6545–55
[18] Xia F, Gevers M, Fognini A, Mok A T, Li B, Akbari N, Zadeh I E, Qin-Dregely J and Xu C 2021 Short-wave infrared confocal fluorescence imaging of deep mouse brain with a superconducting nanowire single-photon detector *ACS Photonics* **8** 2800–10

[19] Weisenburger S *et al* 2019 Volumetric Ca^{2+} imaging in the mouse brain using hybrid multiplexed sculpted light microscopy *Cell* **177** 1050–66

[20] Takasaki K, Abbasi-Asl R and Waters J 2020 Superficial bound of the depth limit of two-photon imaging in mouse brain *eNeuro* **7** ENEURO.0255-19.2019

[21] Liu H *et al* 2019 *In vivo* deep-brain structural and hemodynamic multiphoton microscopy enabled by quantum dots *Nano Lett.* **19** 5260–5

[22] Wang T, Ouzounov D G, Wu C, Horton N G, Zhang B, Wu C-H, Zhang Y, Schnitzer M J and Xu C 2018 Three-photon imaging of mouse brain structure and function through the intact skull *Nat. Methods* **15** 789–92

[23] Akbari N, Rebec M R, Xia F and Xu C 2022 Imaging deeper than the transport mean free path with multiphoton microscopy *Biomed. Opt. Express* **13** 452–63

[24] Hontani Y, Xia F and Xu C 2021 Multicolor three-photon fluorescence imaging with single-wavelength excitation deep in mouse brain *Sci. Adv.* **7** eabf3531

[25] Ji N 2017 Adaptive optical fluorescence microscopy *Nat. Methods* **14** 374–80

[26] Booth M J 2014 Adaptive optical microscopy: the ongoing quest for a perfect image *Light Sci. Appl.* **3** e165

[27] Sinefeld D, Paudel H P, Ouzounov D G, Bifano T G and Xu C 2015 Adaptive optics in multiphoton microscopy: comparison of two, three and four photon fluorescence *Opt. Express* **23** 31472

[28] Streich L, Boffi J C, Wang L, Alhalaseh K, Barbieri M, Rehm R, Deivasigamani S, Gross C T, Agarwal A and Prevedel R 2021 High-resolution structural and functional deep brain imaging using adaptive optics three-photon microscopy *Nat. Methods* **18** 1253–8

[29] Li B, Wu C, Wang M, Charan K and Xu C 2020 An adaptive excitation source for high-speed multiphoton microscopy *Nat. Methods* **17** 163–6

[30] Wang K, Sun W, Richie C T, Harvey B K, Betzig E and Ji N 2015 Direct wavefront sensing for high-resolution *in vivo* imaging in scattering tissue *Nat. Commun.* **6** 7276

[31] Liu R, Li Z, Marvin J S and Kleinfeld D 2019 Direct wavefront sensing enables functional imaging of infragranular axons and spines *Nat. Methods* **16** 615–8

[32] Débarre D, Botcherby E J, Watanabe T, Srinivas S, Booth M J and Wilson T 2009 Image-based adaptive optics for two-photon microscopy *Opt. Lett.* **34** 2495–7

[33] Ji N, Milkie D E and Betzig E 2010 Adaptive optics via pupil segmentation for high-resolution imaging in biological tissues *Nat. Methods* **7** 141–7

[34] Wang C, Liu R, Milkie D E, Sun W, Tan Z, Kerlin A, Chen T-W, Kim D S and Ji N 2014 Multiplexed aberration measurement for deep tissue imaging *in vivo Nat. Methods* **11** 1037–40

[35] Papadopoulos I N, Jouhanneau J-S, Poulet J F A and Judkewitz B 2017 Scattering compensation by focus scanning holographic aberration probing (F-SHARP) *Nat. Photon.* **11** 116–23

[36] Rodríguez C *et al* 2021 An adaptive optics module for deep tissue multiphoton imaging *in vivo Nat. Methods* **18** 1259–64

[37] Sun W, Tan Z, Mensh B D and Ji N 2016 Thalamus provides layer 4 of primary visual cortex with orientation- and direction-tuned inputs *Nat. Neurosci.* **19** 308–15

[38] Shemetov A A *et al* 2021 A near-infrared genetically encoded calcium indicator for *in vivo* imaging *Nat. Biotechnol.* **39** 368–77

[39] Kong L, Tang J, Little J P, Yu Y, Lämmermann T, Lin C P, Germain R N and Cui M 2015 Continuous volumetric imaging via an optical phase-locked ultrasound lens *Nat. Methods* **12** 759–62

[40] Tang J, Germain R N and Cui M 2012 Superpenetration optical microscopy by iterative multiphoton adaptive compensation technique *Proc. Natl Acad. Sci. USA* **109** 8434–9

[41] Si K, Fiolka R and Cui M 2012 Fluorescence imaging beyond the ballistic regime by ultrasound-pulse-guided digital phase conjugation *Nat. Photon.* **6** 657–61

[42] Si K, Fiolka R and Cui M 2012 Breaking the spatial resolution barrier via iterative sound–light interaction in deep tissue microscopy *Sci. Rep.* **2** 748

[43] Wei B, Wang C, Cheng Z, Lai B, Gan W-B and Cui M 2021 Clear optically matched panoramic access channel technique (COMPACT) for large-volume deep brain imaging *Nat. Methods* **18** 959–64

[44] Cui M 2011 A high speed wavefront determination method based on spatial frequency modulations for focusing light through random scattering media *Opt. Express* **19** 2989–95

[45] Park J H, Sun W and Cui M 2015 High-resolution *in vivo* imaging of mouse brain through the intact skull *Proc. Natl Acad. Sci. USA* **112** 9236–41

[46] Park J-H, Kong L, Zhou Y and Cui M 2017 Large-field-of-view imaging by multi-pupil adaptive optics *Nat. Methods* **14** 581–3

[47] Botcherby E J, Smith C W, Kohl M M, Debarre D, Booth M J, Juskaitis R, Paulsen O and Wilson T 2012 Aberration-free three-dimensional multiphoton imaging of neuronal activity at kHz rates *Proc. Natl Acad. Sci. USA* **109** 2919–24

[48] Jiang H, Wang C, Wei B, Gan W, Cai D and Cui M 2020 Long-range remote focusing by image-plane aberration correction *Opt. Express* **28** 34008–14

[49] Leith E N and Upatnieks J 1965 Holograms: their properties and uses *Proc. SPIE* **4** 3–6

[50] Conkey D B, Caravaca-Aguirre A M and Piestun R 2012 High-speed scattering medium characterization with application to focusing light through turbid media *Opt. Express* **20** 1733–40

[51] Caravaca-Aguirre A M, Niv E, Conkey D B and Piestun R 2013 Real-time resilient focusing through a bending multimode fiber *Opt. Express* **21** 12881–7

[52] Tzang O, Niv E, Singh S, Labouesse S, Myatt G and Piestun R 2019 Wavefront shaping in complex media with a 350 kHz modulator via a 1D-to-2D transform *Nat. Photon.* **7** 788

[53] Tzang O, Caravaca-Aguirre A M, Wagner K and Piestun R 2018 Adaptive wavefront shaping for controlling nonlinear multimode interactions in optical fibres *Nat. Photon.* **12** 368

[54] Conkey D B, Caravaca-Aguirre A M, Dove J D, Ju H, Murray T W and Piestun R 2015 Super-resolution photoacoustic imaging through a scattering wall *Nat. Commun.* **6** 7902

[55] Caravaca-Aguirre A, Singh S, Labouesse S, Baratta M V, Piestun R and Bossy E 2019 Hybrid photoacoustic-fluorescence microendoscopy through a multimode fiber using speckle illumination *APL Photonics* **4** 096103

[56] Ohayon S, Caravaca-Aguirre A, Piestun R and DiCarlo J J 2018 Minimally invasive multimode optical fiber microendoscope for deep brain fluorescence imaging *Biomed. Opt. Express* **9** 1492–509

[57] Feldkhun D, Tzang O, Wagner K H and Piestun R 2019 Focusing and scanning through scattering media in microseconds *Optica* **6** 72

[58] Shalaginov M Y *et al* 2020 Design for quality: reconfigurable flat optics based on active metasurfaces *Nanophotonics* **9** 3505–34

[59] Liu Y-Z, South F A, Xu Y, Carney P S and Boppart S A 2017 Computational optical coherence tomography [Invited] *Biomed. Opt. Express* **8** 1549–74

[60] Zhou K C, Qian R, Degan S, Farsiu S and Izatt J A 2019 Optical coherence refraction tomography *Nat. Photon.* **13** 794–802

[61] Ford T N, Chu K K and Mertz J 2012 Phase-gradient microscopy in thick tissue with oblique back-illumination *Nat. Methods* **9** 12

[62] Mertz J, Gasecka A, Daradich A, Davison I and Coté D 2014 Phase-gradient contrast in thick tissue with a scanning microscope *Biomed. Opt. Express* **5** 407–16

[63] Ledwig P and Robles F E 2021 Quantitative 3D refractive index tomography of opaque samples in epi-mode *Optica* **8** 6–14

[64] Weber T D, Khetan N, Yang R and Mertz J 2021 Ultrasound differential phase contrast using backscattering and the memory effect *Appl. Phys. Lett.* **118** 124103

[65] Stähli P, Kuriakose M, Frenz M and Jaeger M 2020 Improved forward model for quantitative pulse-echo speed-of-sound imaging *Ultrasonics* **108** 106168

[66] Kadobianskyi M, Papadopoulos I N, Chaigne T, Horstmeyer R and Judkewitz B 2018 Scattering correlations of time-gated light *Optica* **5** 389–94

[67] Osnabrugge G, Horstmeyer R, Papadopoulos I N, Judkewitz B and Vellekoop I M 2017 Generalized optical memory effect *Optica* **4** 886–92

[68] Xu X, Liu H and Wang L V 2011 Time-reversed ultrasonically encoded optical focusing into scattering media *Nat. Photon.* **5** 154–7

[69] Ma C, Xu X, Liu Y and Wang L V 2014 Time-reversed adapted-perturbation (TRAP) optical focusing onto dynamic objects inside scattering media *Nat. Photon.* **8** 931–6

[70] Hsieh C-L, Pu Y, Grange R and Psaltis D 2010 Digital phase conjugation of second harmonic radiation emitted by nanoparticles in turbid media *Opt. Express* **18** 12283–90

[71] Liu Y, Lai P, Ma C, Xu X, Grabar A A and Wang L V 2015 Optical focusing deep inside dynamic scattering media with near-infrared time-reversed ultrasonically encoded (TRUE) light *Nat. Commun.* **6** 5904

[72] Vellekoop I M, Cui M and Yang C 2012 Digital optical phase conjugation of fluorescence in turbid tissue *Appl. Phys. Lett.* **101** 081108

[73] Ruan H, Haber T, Liu Y, Brake J, Kim J, Berlin J M and Yang C 2017 Focusing light inside scattering media with magnetic-particle-guided wavefront shaping *Optica* **4** 1337–43

[74] Yu Z, Huangfu J, Zhao F, Xia M, Wu X, Niu X, Li D, Lai P and Wang D 2018 Time-reversed magnetically controlled perturbation (TRMCP) optical focusing inside scattering media *Sci. Rep.* **8** 2927

[75] Ruan H, Jang M and Yang C 2015 Optical focusing inside scattering media with time-reversed ultrasound microbubble encoded light *Nat. Commun.* **6** 8968

[76] Cheng Z and Wang L V 2021 Focusing light into scattering media with ultrasound-induced field perturbation *Light Sci. Appl.* **10** 159

[77] Tao X, Azucena O, Fu M, Zuo Y, Chen D C and Kubby J 2011 Adaptive optics microscopy with direct wavefront sensing using fluorescent protein guide stars *Opt. Lett.* **36** 3389–91

[78] Papadopoulos I N, Jouhanneau J-S, Takahashi N, Kaplan D, Larkum M, Poulet J and Judkewitz B 2020 Dynamic conjugate F-SHARP microscopy *Light Sci. Appl.* **9** 110

[79] May M A, Barré N, Kummer K K, Kress M, Ritsch-Marte M and Jesacher A 2021 Fast holographic scattering compensation for deep tissue biological imaging *Nat. Commun.* **12** 4340

[80] Brake J, Jang M and Yang C 2016 Analyzing the relationship between decorrelation time and tissue thickness in acute rat brain slices using multispeckle diffusing wave spectroscopy *J. Opt. Soc. Am.* A **33** 270–5

[81] Cheng Z, Yang J and Wang L V 2020 Single-shot time-reversed optical focusing into and through scattering media *ACS Photonics* **7** 2871–7

[82] Laforest T *et al* 2013 A 4000 Hz CMOS image sensor with in-pixel processing for light measurement and modulation *2013 IEEE 11th Int. New Circuits and Systems Conf. (NEWCAS)* (Paris: IEEE) pp 1–4

[83] Rotter S and Gigan S 2017 Light fields in complex media: mesoscopic scattering meets wave control *Rev. Mod. Phys.* **89** 015005

[84] Horstmeyer R, Ruan H and Yang C 2015 Guidestar-assisted wavefront-shaping methods for focusing light into biological tissue *Nat. Photon.* **9** 563–71

[85] Berlage C, Tantirigama M, Babot M, Di Battista D, Whitmire C, Papadopoulos I N, Poulet J F A, Larkum M and Judkewitz B 2021 Deep tissue scattering compensation with three-photon F-SHARP *Optica* *bioRxiv Preprint* **8** 1613–9

[86] Boniface A, Blochet B, Dong J and Gigan S 2019 Noninvasive light focusing in scattering media using speckle variance optimization *Optica* **6** 1381–5

[87] Daniel A, Oron D and Silberberg Y 2019 Light focusing through scattering media via linear fluorescence variance maximization, and its application for fluorescence imaging *Opt. Express* **27** 21778

[88] Tian B, Rauer B, Boniface A, Han J, Gigan S and de Aguiar H B 2022 Non-invasive chemically selective energy delivery and focusing inside a scattering medium guided by Raman scattering **47** 2145–48

[89] Boniface A, Dong J and Gigan S 2020 Non-invasive focusing and imaging in scattering media with a fluorescence-based transmission matrix *Nat. Commun.* **11** 6154

[90] Zhu L, Soldevila F, Moretti C, d'Arco A, Boniface A, Shao X, de Aguiar H B and Gigan S 2022 Large field-of-view non-invasive imaging through scattering layers using fluctuating random illumination *Nat. Commun.* **13** 1447

[91] Wang D, Sahoo S K, Zhu X, Adamo G and Dang C 2021 Non-invasive super-resolution imaging through dynamic scattering media *Nat. Commun.* **12** 3150

[92] Moretti C and Gigan S 2020 Readout of fluorescence functional signals through highly scattering tissue *Nat. Photon.* **14** 361–4

[93] De Aguiar H B, Gigan S and Brasselet S 2017 Polarization recovery through scattering media *Sci. Adv.* **3** e1600743

[94] Thompson J V, Throckmorton G A, Hokr B H and Yakovlev V V 2016 Wavefront shaping enhanced Raman scattering in a turbid medium *Opt. Lett.* **41** 1769

[95] Guilbert J, Negash A, Labouesse S, Gigan S, Sentenac A and de Aguiar H B 2021 Label-free super-resolution chemical imaging of biomedical specimens *bioRxiv Preprint* (https://doi.org/10.1101/2021.05.14.444185)

[96] Kong F, Silverman R H, Liu L, Chitnis P V, Lee K K and Chen Y-C 2011 Photoacoustic-guided convergence of light through optically diffusive media *Opt. Lett.* **36** 2053–5

[97] Caravaca-Aguirre A M, Conkey D B, Dove J D, Ju H, Murray T W and Piestun R 2013 High contrast three-dimensional photoacoustic imaging through scattering media by localized optical fluence enhancement *Opt. Express* **21** 26671

[98] Chaigne T, Katz O, Boccara A C, Fink M, Bossy E and Gigan S 2013 Controlling light in scattering media non-invasively using the photoacoustic transmission matrix *Nat. Photon.* **8** 58–64

[99] Chaigne T 2016 Control of scattered coherent light and photoacoustic imaging: toward light focusing in deep tissue and enhanced, sub-acoustic resolution photoacoustic imaging (available at: https://hal.archives-ouvertes.fr/tel-01402738) (Accessed 6 June 2017)

[100] Tay J W, Liang J and Wang L V 2014 Amplitude-masked photoacoustic wavefront shaping and application in flowmetry *Opt. Lett.* **39** 5499

[101] Lai P, Wang L, Tay J W and Wang L V 2015 Photoacoustically guided wavefront shaping for enhanced optical focusing in scattering media *Nat. Photon.* **9** 126–32

[102] Deán-Ben X L, Estrada H and Razansky D 2015 Shaping volumetric light distribution through turbid media using real-time three-dimensional opto-acoustic feedback *Opt. Lett.* **40** 443

[103] Hemphill A S, Tay J W and Wang L V 2016 Hybridized wavefront shaping for high-speed, high-efficiency focusing through dynamic diffusive media *J. Biomed. Opt.* **21** 121502

[104] Inzunza-Ibarra M A, Premillieu E, Grünsteidl C, Piestun R and Murray T W 2020 Sub-acoustic resolution optical focusing through scattering using photoacoustic fluctuation guided wavefront shaping *Opt. Express* **28** 9823

[105] Chaigne T, Gateau J, Katz O, Boccara C, Gigan S and Bossy E 2014 Improving photoacoustic-guided optical focusing in scattering media by spectrally filtered detection *Opt. Lett.* **39** 6054

[106] Westerveld W J, Mahmud-Ul-Hasan M, Shnaiderman R, Ntziachristos V, Rottenberg X, Severi S and Rochus V 2021 Sensitive, small, broadband and scalable optomechanical ultrasound sensor in silicon photonics *Nat. Photon.* **15** 341–5

[107] Bossy E and Gigan S 2016 Photoacoustics with coherent light *Photoacoustics* **4** 22–35

[108] Mezil S *et al* 2020 Single-shot hybrid photoacoustic-fluorescent microendoscopy through a multi-mode fiber with wavefront shaping (arXiv:2006.10856 [physics.optics])

[109] Popoff S M, Aubry A, Lerosey G, Fink M, Boccara A C and Gigan S 2011 Exploiting the time-reversal operator for adaptive optics, selective focusing, and scattering pattern analysis *Phys. Rev. Lett.* **107** 263901

[110] Kang S, Jeong S, Choi W, Ko H, Yang T D, Joo J H, Lee J-S, Lim Y-S, Park Q-H and Choi W 2015 Imaging deep within a scattering medium using collective accumulation of single-scattered waves *Nat. Photon.* **9** 253–8

[111] Badon A, Li D, Lerosey G, Boccara A C, Fink M and Aubry A 2016 Smart optical coherence tomography for ultra-deep imaging through highly scattering media *Sci. Adv.* **2** e1600370

[112] Yoon S, Kim M, Jang M, Choi Y, Choi W, Kang S and Choi W 2020 Deep optical imaging within complex scattering media *Nat. Rev. Phys.* **2** 141–58

[113] Kang S *et al* 2017 High-resolution adaptive optical imaging within thick scattering media using closed-loop accumulation of single scattering *Nat. Commun.* **8** 2157

[114] Yoon S, Lee H, Hong J H, Lim Y-S and Choi W 2020 Laser scanning reflection-matrix microscopy for aberration-free imaging through intact mouse skull *Nat. Commun.* **11** 5721

[115] Kim M *et al* 2019 Label-free neuroimaging *in vivo* using synchronous angular scanning microscopy with single-scattering accumulation algorithm *Nat. Commun.* **10** 3152

[116] Lee H, Yoon S, Loohuis P, Hong J H, Kang S and Choi W 2021 High-throughput volumetric adaptive optical imaging using compressed time-reversal matrix (arXiv:2109.06674 [physics.optics])

[117] Choi W, Kang M, Hong J H, Katz O, Choi Y and Choi W 2020 Fourier holographic endoscopy for label-free imaging through a narrow and curved passage (arXiv:2010.11776 [physics.optics])

[118] Badon A, Barolle V, Irsch K, Boccara A, Fink M and Aubry A 2020 Distortion matrix concept for deep imaging in optical coherence microscopy *Sci. Adv.* **6** Eaay7170

[119] Skarsoulisa K, Kakkava E and Psaltis D 2021 Predicting optical transmission through complex scattering media from reflection patterns with deep neural networks *Opt. Commun.* **492** 126968

[120] Mosk A P, Lagendijk A, Lerosey G and Fink M 2012 Controlling waves in space and time for imaging and focusing in complex media *Nat. Photon.* **6** 283–92

[121] Jang M, Ruan H, Vellekoop I M, Judkewitz B, Chung E and Yang C 2015 Relation between speckle decorrelation and optical phase conjugation (OPC)-based turbidity suppression through dynamic scattering media: a study on *in vivo* mouse skin *Biomed. Opt. Express* **6** 72–85

[122] Ambichl P, Brandstötter A, Böhm J, Kühmayer M, Kuhl U and Rotter S 2017 Focusing inside disordered media with the generalized Wigner–Smith operator *Phys. Rev. Lett.* **119** 033903

[123] Matthès M W, Bromberg Y, de Rosny J and Popoff S M 2021 Model-based wavefront shaping microscopy *Phys. Rev.* X **11** 021060

[124] Thendiyammal A, Osnabrugge G, Knop T and Vellekoop I M 2020 Model-based wavefront shaping microscopy *Opt. Lett.* **45** 5101–4

[125] Zhu L, de Monvel J B, Berto P, Brasselet S, Gigan S and Guillon M 2020 Chromato-axial memory effect through a forward-scattering slab *Optica* **7** 338–45

[126] Mounaix M, Ta D M and Gigan S 2018 Transmission matrix approaches for nonlinear fluorescence excitation through multiple scattering media *Opt. Lett.* **43** 2831

[127] Mounaix M, de Aguiar H B and Gigan S 2017 Temporal recompression through a scattering medium via a broadband transmission matrix *Optica* **4** 1289

[128] Hofer M, Shivkumar S, El Waly B and Brasselet S 2020 Coherent anti-Stokes Raman scattering through thick biological tissues by single-wavefront shaping *Phys. Rev. Appl.* **14** 024019

[129] Badon A, Barolle V, Irsch K, Claude Boccara A, Fink M and Aubry A 2020 Distortion matrix concept for deep optical imaging in scattering media *Sci. Adv.* **6** 7170–92

[130] Barbastathis G, Ozcan A and Situ G 2019 On the use of deep learning for computational imaging *Optica* **6** 921–43

[131] Li S, Deng M, Lee J, Sinha A and Barbastathis G 2018 Imaging through glass diffusers using densely connected convolutional networks *Optica* **5** 803–13

[132] Li Y, Xue Y and Tian L 2018 Deep speckle correlation: a deep learning approach toward scalable imaging through scattering media *Optica* **5** 1181–90

[133] Li Y, Cheng S, Xue Y and Tian L 2021 Displacement-agnostic coherent imaging through scatter with an interpretable deep neural network *Opt. Express* **29** 2244

[134] Zheng S, Wang H, Dong S, Wang F and Situ G 2021 Incoherent imaging through highly nonstatic and optically thick turbid media based on neural network *Photon. Res.* **9** B220–8

[135] Metzler C A, Heide F, Rangarajan P, Balaji M M, Viswanath A, Veeraraghavan A and Baraniuk R G 2020 Deep-inverse correlography: towards real-time high-resolution non-line-of-sight imaging *Optica* **7** 63–71

[136] Matlock A and Tian L 2021 Physical model simulator-trained neural network for computational 3D phase imaging of multiple-scattering samples (arXiv:2103.15795 [eess.IV])

[137] Tahir W, Wang H and Tian L 2022 Adaptive 3D descattering with a dynamic synthesis network *Light Sci. Appl.* **11** 1

[138] Vellekoop I M, van Putten E G, Lagendijk A and Mosk A P 2008 Demixing light paths inside disordered metamaterials *Opt. Express* **16** 67

[139] Vellekoop I M and Aegerter C M 2010 Scattered light fluorescence microscopy: imaging through turbid layers. *Opt. Lett.* **35** 1245–7

[140] van Putten E G, Akbulut D, Bertolotti J, Vos W L, Lagendijk A and Mosk A P 2011 Scattering lens resolves sub-100 nm structures with visible light *Phys. Rev. Lett.* **106** 193905

[141] Feng S, Kane C, Lee P A and Stone A D 1988 Correlations and fluctuations of coherent wave transmission through disordered media *Phys. Rev. Lett.* **61** 834–7

[142] Salter P S, Baum M, Alexeev I, Schmidt M and Booth M J 2014 Exploring the depth range for three-dimensional laser machining with aberration correction *Opt. Express* **22** 17644–56

[143] Plöschner M, Tyc T and Čižmár T 2015 Seeing through chaos in multimode fibres *Nat. Photon.* **9** 529–35

[144] Kamilov U S, Papadopoulos I N, Shoreh M H, Goy A, Vonesch C, Unser M and Psaltis D 2015 Learning approach to optical tomography *Optica* **2** 517–22

[145] Chowdhury S, Chen M, Eckert R, Ren D, Wu F, Repina N and Waller L 2019 High-resolution 3D refractive index microscopy of multiple-scattering samples from intensity images *Optica* **6** 1211–9

[146] Osnabrugge G, Benedictus M and Vellekoop I M 2021 Ultra-thin boundary layer for high-accuracy simulations of light propagation *Opt. Express* **29** 1649–58

[147] Jang M, Ruan H, Zhou H, Judkewitz B and Yang C 2014 Method for auto-alignment of digital optical phase conjugation systems based on digital propagation *Opt. Express* **22** 14054–71

[148] Katz O, Small E and Silberberg Y 2012 Looking around corners and through thin turbid layers in real time with scattered incoherent light *Nat. Photon.* **6** 549–53

[149] Katz O, Small E, Guan Y and Silberberg Y 2014 Noninvasive nonlinear focusing and imaging through strongly scattering turbid layers *Optica* **1** 170–4

[150] Yeminy T and Katz O 2021 Guidestar-free image-guided wavefront shaping *Sci. Adv.* **7** eabf5364

[151] Porat A, Andresen E R, Rigneault H, Oron D, Gigan S and Katz O 2016 Widefield lensless imaging through a fiber bundle via speckle correlations *Opt. Express* **24** 16835–55

[152] Bertolotti J, van Putten E G, Blum C, Lagendijk A, Vos W L and Mosk A P 2012 Non-invasive imaging through opaque scattering layers *Nature* **491** 232–4

[153] Labeyrie A 1970 Attainment of diffraction limited resolution in large telescopes by Fourier analysing speckle patterns in star images *Astron. Astrophys.* **6** 85–7

[154] Katz O, Heidmann P, Fink M and Gigan S 2014 Non-invasive single-shot imaging through scattering layers and around corners via speckle correlations *Nat. Photon.* **8** 784–90

[155] Rosenfeld M, Weinberg G, Doktofsky D, Li Y, Tian L and Katz O 2021 Acousto-optic ptychography *Optica* **8** 936–43

[156] Wu T, Katz O, Shao X and Gigan S 2016 Single-shot diffraction-limited imaging through scattering layers via bispectrum analysis *Opt. Lett.* **41** 5003–6

[157] Popoff S M, Lerosey G, Carminati R, Fink M, Boccara A C and Gigan S 2010 Measuring the transmission matrix in optics: an approach to the study and control of light propagation in disordered media *Phys. Rev. Lett.* **104** 100601

[158] Freund I, Rosenbluh M and Feng S 1988 Memory effects in propagation of optical waves through disordered media *Phys. Rev. Lett.* **61** 2328

[159] Akkermans E and Montambeaux G 2007 *Mesoscopic Physics of Electrons and Photons* (Cambridge: Cambridge University Press)

[160] Bartelt H, Lohmann A W and Wirnitzer B 1984 Phase and amplitude recovery from bispectra *Appl. Opt.* **23** 3121

[161] Judkewitz B, Horstmeyer R, Vellekoop I M, Papadopoulos I N and Yang C 2015 Translation correlations in anisotropically scattering media *Nat. Phys.* **11** 684–9

[162] Starshynov I, Paniagua-Diaz A M, Fayard N, Goetschy A, Pierrat R, Carminati R and Bertolotti J 2018 Non-Gaussian correlations between reflected and transmitted intensity patterns emerging from opaque disordered media *Phys. Rev.* X **8** 021041

[163] Schott S, Bertolotti J, Léger J-F, Bourdieu L and Gigan S 2015 Characterization of the angular memory effect of scattered light in biological tissues *Opt. Express* **23** 13505

[164] Mait J, Euliss G and Athale R 2018 Computational imaging *Adv. Opt. Photonics* **10** 409–83

[165] Ables G 1968 Fourier transform photography: a new method for x-ray astronomy *Proc. Astron. Soc. Aust.* **1** 172–3

[166] Baraniuk R 2007 Compressive sensing *IEEE Signal Process. Mag.* **24** 118–21

[167] Potuluri P, Xu M and Brady D 2003 Imaging with random 3D reference structures *Opt. Express* **11** 2134–41

[168] Popoff S, Lerosey G, Fink M, Boccara A and Gigan S 2010 Image transmission through an opaque material *Nat. Commun.* **1** 81

[169] Horisaki R, Takagi R and Tanida J 2016 Learning-based imaging through scattering media *Opt. Express* **24** 13738–43

[170] Horisaki R, Takagi R and Tanida J 2017 Learning-based focusing through scattering media *Appl. Opt.* **56** 4358–62

[171] Horisaki R, Okamoto Y and Tanida J 2019 Single-shot noninvasive three-dimensional imaging through scattering media *Opt. Lett.* **44** 4032–5

[172] Ehira K, Horisaki R, Nishizaki Y, Naruse M and Tanida J 2021 Spectral speckle-correlation imaging *Appl. Opt.* **60** 2388–92

[173] Parot V J, Sing-Long C, Adam Y, Böhm U L, Fan L Z, Farhi S L and Cohen A E 2019 Compressed hadamard microscopy for high-speed optically sectioned neuronal activity recordings *J. Phys. D: Appl. Phys.* **52** 144001

[174] Curtis V R, Caira N W, Xu J, Sata A G and Pégard N C 2021 DCGH: dynamic computer generated holography for speckle-free, high fidelity 3D displays *2021 IEEE Virtual Reality and 3D User Interfaces (VR)* pp 1–9

[175] Schedl D C and Bimber O 2017 Compressive volumetric light-field excitation *Sci. Rep.* **7** 13981

[176] Peng Y, Choi S, Padmanaban N and Wetzstein G 2020 Neural holography with camera-in-the-loop training *ACM Trans. Graph.* **39** 185

[177] Ersumo N T, Yalcin C, Antipa N, Pégard N, Waller L, Lopez D and Muller R 2020 A micromirror array with annular partitioning for high-speed random-access axial focusing *Light Sci. Appl.* **9** 183

[178] Pinkard H *et al* 2021 Learned adaptive multiphoton illumination microscopy for large-scale immune response imaging *Nat. Commun.* **12** 1916

[179] Eybposh M, Caira N, Atisa M, Chakravarthula P and Pegard N 2020 DeepCGH: 3D computer-generated holography using deep learning *Opt. Express* **28** 26636–50
[180] Spitz E and Werts A 1967 Transmission des images à travers une fibre optique *C. R. Hebd. Seances Acad. Sci.* B **264** 1015
[181] Mounaix M, Fontaine N K, Neilson D T, Ryf R, Chen H, Alvarado-Zacarias J C and Carpenter J 2020 Time reversed optical waves by arbitrary vector spatiotemporal field generation *Nat. Commun.* **11** 5813
[182] Turtaev S, Leite I T, Altwegg-Boussac T, Pakan J M, Rochefort N L and Čižmár T 2018 High-fidelity multi-mode fibre-based endoscopy for deep brain *in vivo* imaging *Light Sci. Appl.* **7** 92
[183] Stellinga D, Phillips D B, Mekhail S Peter, Selyem A, Turtaev S, Čižmár T and Padgett M J 2021 Time-of-flight 3D imaging through multimode optical fibers *Science* **374** 1395–9
[184] Li S, Saunders C, Lum D J, Murray-Bruce J, Goyal V K, Čižmár T and Phillips D B 2021 Compressively sampling the optical transmission matrix of a multimode fibre *Light Sci. Appl.* **10** 88
[185] Li S, Horsley S A, Tyc T, Čižmár T and Phillips D B 2021 Memory effect assisted imaging through multimode optical fibres *Nat. Commun.* **12** 3715
[186] Fontaine N K, Ryf R, Chen H, Neilson D T, Kim K and Carpenter J 2019 Laguerre-Gaussian mode sorter *Nat. Commun.* **10** 1865
[187] Čižmár T and Dholakia K 2012 Exploiting multimode waveguides for pure fibre-based imaging *Nat. Commun.* **3** 1027
[188] Kim G, Nagarajan N, Pastuzyn E, Jenks K, Capecchi M, Shepherd J and Menon R 2017 Deep-brain imaging via epi-fluorescence computational cannula microscopy *Sci. Rep.* **7** 44791
[189] Čižmár T and Dholakia K 2011 Shaping the light transmission through a multimode optical fibre: complex transformation analysis and applications in biophotonics *Opt. Express* **19** 18871–84
[190] Thompson A J, Paterson C, Neil M A A, Dunsby C and French P M W 2011 Adaptive phase compensation for ultracompact laser scanning endomicroscopy *Opt. Lett.* **36** 1707–9
[191] Vasquez-Lopez S A, Turcotte R, Koren V, Plöschner M, Padamsey Z, Booth M J, Čižmár T and Emptage N J 2018 Subcellular spatial resolution achieved for deep-brain imaging *in vivo* using a minimally invasive multimode fiber *Light Sci. Appl.* **7** 110
[192] Andresen E R, Bouwmans G, Monneret S and Rigneault H 2013 Toward endoscopes with no distal optics: video-rate scanning microscopy through a fiber bundle *Opt. Lett.* **38** 609–11
[193] Andresen E R, Bouwmans G, Monneret S and Rigneault H 2013 Two-photon lensless endoscope *Opt. Express* **21** 20713–21
[194] Sivankutty S, Tsvirkun V, Vanvincq O, Bouwmans G, Andresen E R and Rigneault H 2018 Nonlinear imaging through a Fermat golden spiral multicore fiber *Opt. Lett.* **43** 3638–41
[195] Sivankutty S, Tsvirkun V, Bouwmans G, Kogan D, Oron D, Andresen E R and Rigneault H 2016 Extended field-of-view in a lensless endoscope using an aperiodic multicore fiber *Opt. Lett.* **41** 3531–4
[196] El Moussawi F, Bouwmans G, Vanvincq O and Andresen E R 2021 Numerical study of a multi-mode fiber with three-diemensionally structured index profile *Presented at the Optique Dijon 2021* (*Dijon, France*)
[197] Tsvirkun V, Sivankutty S, Baudelle K, Habert R, Bouwmans G, Vanvincq O, Andresen E R and Rigneault H 2019 Flexible lensless endoscope with a conformationally invariant multi-core fiber *Optica* **6** 1185–9
[198] Warren S C, Kim Y, Stone J M, Mitchell C, Knight J C, Neil M A A, Paterson C, French P M W and Dunsby C 2016 Adaptive multiphoton endomicroscopy through a dynamically deformed multicore optical fiber using proximal detection *Opt. Express* **24** 21474–84
[199] Gissibl T, Thiele S, Herkommer A and Giessen H 2016 Two-photon direct laser writing of ultracompact multi-lens objectives *Nat. Photon.* **10** 554–60
[200] Sivankutty S, Bertoncini A, Tsvirkun V, Gajendra Kumar N, Brevalle G, Bouwmans G, Andresen E R, Liberale C and Rigneault H 2021 Miniature 120-beam coherent combiner with 3D printed optics for multicore fiber based endoscopy *Opt. Lett.* **46** 4968–71
[201] Kim Y, Parada G A, Liu S and Zhao X 2019 Ferromagnetic soft continuum robots *Sci. Robot.* **4** eaax7329
[202] Rahmani B, Loterie D, Konstantinou G, Psaltis D and Moser C 2018 Multimode optical fiber transmission with a deep learning network *Light Sci. Appl.* **7** 69
[203] Borhani N, Kakkava E, Moser C and Psaltis D 2018 Learning to see through multimode fibers *Optica* **5** 960–6
[204] Kakkava E, Rahmani B, Borhani N, Teğin U, Loterie D, Konstantinou G, Moser C and Psaltis D 2019 Imaging through multimode fibers using deep learning: the effects of intensity versus holographic recording of the speckle pattern *Opt. Fiber Technol.* **52** 101985
[205] Caramazza P, Moran O, Murray-Smith R and Faccio D 2019 Transmission of natural scene images through a multimode fibre *Nat. Commun.* **10** 2029
[206] Zhu C, Chan E A, Wang Y, Peng W, Guo R, Zhang B, Soci C and Chong Y 2021 Image reconstruction through a multimode fiber with a simple neural network architecture *Sci. Rep.* **11** 896
[207] Rahmani B, Loterie D, Kakkava E, Borhani N, Teğin U, Psaltis D and Moser C 2020 Actor neural networks for the robust control of partially measured nonlinear systems showcased for image propagation through diffuse media *Nat. Mach. Intell.* **2** 403–10
[208] Turpin A, Vishniakou I and Seelig J D 2018 Light scattering control in transmission and reflection with neural networks *Opt. Express* **26** 30911–29
[209] Kakkava E, Borhani N, Rahmani B, Teğin U, Moser C and Psaltis D 2020 Deep learning-based image classification through a multimode fiber in the presence of wavelength drift *Appl. Sci.* **10** 3816
[210] Kakkava E, Borhani N, Rahmani B, Teğin U, Moser C and Psaltis D 2019 Wavelength independent image classification through a multimode fiber using deep neural networks *The European Conf. on Lasers and Electro-Optics* p ci_2_1
[211] Kakkava E, Borhani N, Rahmani B, Tegin U, Moser C and Psaltis D 2019 Efficient image classification through a multimode fiber using deep neural networks in presence of wavelength drifting *Computational Optical Sensing and Imaging* p CW1A.4
[212] Fan P, Zhao T and Su L 2019 Deep learning the high variability and randomness inside multimode fibers *Opt. Express* **27** 20241–58
[213] Resisi S, Popoff S M and Bromberg Y 2020 Image transmission through a flexible multimode fiber by deep learning (arXiv:2011.05144 [eess.IV])
[214] Zhao J *et al* 2021 High-fidelity imaging through multimode fibers via deep learning *J. Phys. Photon.* **3** 015003
[215] Luo Y, Yan S, Li H, Lai P and Zheng Y 2021 Towards smart optical focusing: deep learning-empowered dynamic wavefront shaping through nonstationary scattering media *Photon. Res.* **9** B262–78
[216] Wei M, Tang G, Liu J, Zhu L, Liu J, Huang C, Zhang J, Shen L and Yu S 2021 Neural network based perturbation-location fiber specklegram sensing system towards applications with limited number of training samples *J. Lightwave Technol.* **39** 6315–26
[217] Liu Y, Li G, Qin Q, Tan Z, Wang M and Yan F 2020 Bending recognition based on the analysis of fiber specklegrams using deep learning *Opt. Laser Technol.* **131** 106424

[218] Xiong W, Redding B, Gertler S, Bromberg Y, Tagare H D and Cao H 2020 Deep learning of ultrafast pulses with a multimode fiber *APL Photonics* **5** 096106

[219] Salmela L, Tsipinakis N, Foi A, Billet C, Dudley J M and Genty G 2021 Predicting ultrafast nonlinear dynamics in fibre optics with a recurrent neural network *Nat. Mach. Intell.* **3** 344–54

[220] Teğin U, Rahmani B, Kakkava E, Borhani N, Moser C and Psaltis D 2020 Controlling spatiotemporal nonlinearities in multimode fibers with deep neural networks *APL Photonics* **5** 030804

[221] Salmela L, Lapre C, Dudley J M and Genty G 2020 Supercontinuum spectral evolution prediction by recurrent neural network *2020 Conf. on Lasers and Electro-Optics (CLEO)* pp 1–2

[222] Choi W, Mosk A P, Park Q-H and Choi W 2011 Transmission eigenchannels in a disordered medium *Phys. Rev. B* **83** 134207

[223] Davy M, Shi Z, Park J, Tian C and Genack A Z 2015 Universal structure of transmission eigenchannels inside opaque media *Nat. Commun.* **6** 6893

[224] Sarma R, Yamilov A G, Petrenko S, Bromberg Y and Cao H 2016 Control of energy density inside a disordered medium by coupling to open or closed channels *Phys. Rev. Lett.* **117** 086803

[225] Koirala M, Sarma R, Cao H and Yamilov A 2017 Inverse design of perfectly transmitting eigenchannels in scattering media *Phys. Rev. B* **96** 054209

[226] Yılmaz H, Hsu C W, Yamilov A and Cao H 2019 Transverse localization of transmission eigenchannels *Nat. Photon.* **13** 352–8

[227] Hsu C W, Goetschy A, Bromberg Y, Stone A D and Cao H 2015 Broadband coherent enhancement of transmission and absorption in disordered media *Phys. Rev. Lett.* **115** 223901

[228] Popoff S M, Goetschy A, Liew S F, Stone A D and Cao H 2014 Coherent control of total transmission of light through disordered media *Phys. Rev. Lett.* **112** 133903

[229] Ojambati O S, Yılmaz H, Lagendijk A, Mosk A P and Vos W L 2016 Coupling of energy into the fundamental diffusion mode of a complex nanophotonic medium *New J. Phys.* **18** 043032

[230] Sarma R, Yamilov A and Cao H 2017 Enhancing light transmission through a disordered waveguide with inhomogeneous scattering and loss *Appl. Phys. Lett.* **110** 021103

[231] Bender N, Yamilov A, Yılmaz H and Cao H 2020 Fluctuations and correlations of transmission eigenchannels in diffusive media *Phys. Rev. Lett.* **125** 165901

[232] Barrett H H and Myers K J 2013 *Foundations of Image Science* (New York: Wiley)

[233] Bouchet D, Carminati R and Mosk A P 2020 Influence of the local scattering environment on the localization precision of single particles *Phys. Rev. Lett.* **124** 133903

[234] Bouchet D, Rotter S and Mosk A P 2021 Maximum information states for coherent scattering measurements *Nat. Phys.* **17** 564–8

[235] Horodynski M, Kühmayer M, Brandstötter A, Pichler K, Fyodorov Y V, Kuhl U and Rotter S 2020 Optimal wave fields for micromanipulation in complex scattering environments *Nat. Photon.* **14** 149–53

[236] Szameit A *et al* 2012 Sparsity-based single-shot subwavelength coherent diffractive imaging *Nat. Mater.* **11** 455–9

[237] Bouchet D, Seifert J and Mosk A P 2021 Optimizing illumination for precise multi-parameter estimations in coherent diffractive imaging *Opt. Lett.* **46** 254–7

[238] Giovannetti V, Lloyd S and Maccone L 2006 Quantum Metrology *Phys. Rev. Lett.* **96** 010401

[239] Del Hougne P, Imani M F, Diebold A V, Horstmeyer R and Smith D R 2020 Learned integrated sensing pipeline: reconfigurable metasurface transceivers as trainable physical layer in an artificial neural network *Adv. Sci.* **7** 1901913

[240] Fayard N, Goetschy A, Pierrat R and Carminati R 2018 Mutual information between reflected and transmitted speckle images *Phys. Rev. Lett.* **120** 073901

[241] Smolka S, Huck A, Andersen U L, Lagendijk A and Lodahl P 2009 Observation of spatial quantum correlations induced by multiple scattering of nonclassical light *Phys. Rev. Lett.* **102** 193901

[242] Cao Y *et al* 2020 Long-distance free-space measurement-device-independent quantum key distribution *Phys. Rev. Lett.* **125** 260503

[243] Zhong H-S *et al* 2020 Quantum computational advantage using photons *Science* **370** 1460–3

[244] Tenne R, Rossman U, Rephael B, Israel Y, Krupinski-Ptaszek A, Lapkiewicz R, Silberberg Y and Oron D 2019 Super-resolution enhancement by quantum image scanning microscopy *Nat. Photon.* **13** 116–22

[245] Lemos G B, Borish V, Cole G D, Ramelow S, Lapkiewicz R and Zeilinger A 2014 Quantum imaging with undetected photons *Nature* **512** 409–12

[246] Defienne H, Reichert M and Fleischer J W 2018 Adaptive quantum optics with spatially entangled photon pairs *Phys. Rev. Lett.* **121** 233601

[247] Lib O, Hasson G and Bromberg Y 2020 Real-time shaping of entangled photons by classical control and feedback *Sci. Adv.* **6** eabb6298

[248] Valencia N H, Goel S, McCutcheon W, Defienne H and Malik M 2020 Unscrambling entanglement through a complex medium *Nat. Phys.* **16** 1112–6

[249] Moreau P-A, Toninelli E, Gregory T and Padgett M J 2019 Imaging with quantum states of light *Nat. Rev. Phys.* **1** 367–80

[250] Madonini F, Severini F, Zappa F and Villa F 2021 Single photon avalanche diode arrays for quantum imaging and microscopy *Adv. Quantum Technol.* **4** 2100005